

Developing Novel Therapeutics for Chronic Kidney Disease

by

Shayna Toyan Joy Bradford

A dissertation submitted in partial fulfillment
of the requirements for the degree of
Doctor of Philosophy
(Molecular and Cellular Pathology)
in the University of Michigan
2019

Doctoral Committee:

Professor Gregory R. Dressler, Chair
Associate Professor Jorge Iñiguez-Lluhí
Professor Andrew P. Lieberman
Associate Professor Zaneta Nikolovska-Coleska

Shayna Toyan Joy Bradford

bradforz@umich.edu

ORCID iD: 0000-0003-4049-7384

© Shayna Toyan Joy Bradford 2019

Dedication

This dissertation is dedicated to my adored 9-year-old son, extraordinary parents, and the best big brother a little sister could ever have. As well as, my loving extended family members and close friends that have been true blessings in my life. I am forever grateful for your endless support, cheerfulness, and patience while I traveled this journey.

Acknowledgements

I must first thank my mentor, Dr. Gregory Dressler, for creating a rich and safe environment for me to grow and develop as a young scientist. On a daily basis while working in the Dressler lab I was given space to explore, ask questions (any question), and seek help. From the very first day in Dr. Dressler's lab there was zero doubt in my mind that he had a genuine interest in and wanted to support my academic growth. He has since served as a highly trusted advisor on both professional and personal matters. I have been truly fortunate to be advised by Dr. Dressler as he has a wealth of hard-earned knowledge and knew how to deliver it effectively. He always knew just what to say to encourage my work and never killed my young spirit of scientific curiosity and potential. Instead, in a professional and affable way, he helped to mold and refine it. I admire his mentoring style. Dr. Dressler was always approachable and engaged scientifically which made working in his lab exciting. I can never thank him enough for agreeing to mentor me and for ALL of the effort he poured into my development on a regular basis. In all, I am eternally grateful for the opportunity he gave me to study kidney disease and development through the lens of drug discovery in his lab.

I would also like to especially thank the former and current members of the Dressler lab: (former members) Dr. Edward Grimley, Dr. Atsuko Higashi, Dr. Egon Ranghini, (current members) Dr. Abdul Soofi, Dr. Sanjeevkumar Patel, and Dr. Ann Laszczyk. They all welcomed me and helped to bring me up to speed on experimental assays and procedures. Surrounded by such amazing people I was able to learn at an exponential rate as they were all very knowledgeable

and willing to help me. They have been my role models and I appreciate their efforts that contributed to my development.

The members of my dissertation committee: Dr. Gregory Dressler, Dr. Jorge Iñiguez-Lluhí, Dr. Andrew Lieberman, and Dr. Zaneta Nikolovska-Coleska were like a dream team! With deep gratitude I thank them for accepting the request to serve on my committee. For each committee meeting they all brought their sharp scientific minds to help advance my thesis project. I was always excited after each committee meeting to get back in the lab as they provided great feedback and suggestions. It was an amazing experience working with such brilliant yet gracious scientists. My committee members were all fair in their assessments of me and met me where I was in my development. Nevertheless, they all challenged me to grow through reasonable requests. Additionally, my committee members all took precious time to individually mentor me prior to serving on my committee, which provided me with even more positive experiences in graduate school. I must again especially thank Dr. Zaneta Nikolovska-Coleska who also serves as the Director of the MCP program. Dr. Zaneta Nikolovska-Coleska advocated for me during a very challenging period of my graduate career before joining the Dressler lab and I am forever grateful to her for her dedication to my success in the MCP program.

To my extraordinary parents, Mr. and Mrs. Bradford, thank you for supporting me in anything and everything I've ever wanted to do. I admire you two too! You both have showered me with pure love and encouragement throughout my life. During graduate school in particular you both always wanted to hear about what I was working on in the lab and we would talk for hours. It was always a joy and a blessing to be able to come home and share my experiences in graduate school with you two. To my inspiring brother, Will Bradford, thank you for pouring all you have learned about life into me. You are not only my brother but also my close friend and our

relationship was a strong source of support during my time in graduate school. It is a phenomenal blessing to be your little sister.

To my amazing and adored son, Moses Chambers, thank you for being my #1 supporter! We started this journey when you were almost 3 and you have witnessed each day of it. You have supported me by being an excellent student and athlete in school, helping around our home, and cheering for mommy to complete this journey. Thank you so much for letting mommy do her science and I only hope that I have inspired you and made you so proud.

To my treasured friends, Eboni Taylor, Kelley Grice, Shakir Edwards, Casta Guillaume, Dr. Pinsky, Dr. Ferrer-Torres, Dr. Luciana Aenasoaie, and Dr. Sarah Trinh. I cannot thank you enough for your friendship especially during my time in graduate school. You all cared so much for me, helped celebrate milestones, and eased the difficult phases. Simply, you all helped make this journey much more enjoyable because I knew I wasn't on it alone. To my extended family and additional long-time friends (aka the FAM), I sincerely appreciate your meaningful words of support and for simply believing in me.

Table of Contents

Dedication.....	ii
Acknowledgements.....	iii
List of Tables	viii
List of Figures.....	ix
Abstract.....	x
Chapter 1 – Introduction to Chronic Kidney Disease and its evolving therapeutic landscape.....	1
Abstract.....	1
Overview of Chronic Kidney Disease epidemiology and pathophysiology.....	3
Current therapeutic landscape for Chronic Kidney Disease management.....	7
Evolving landscape of therapeutics to treat Chronic Kidney Disease.....	8
Stimulation of Bone Morphogenetic Protein signaling to treat fibrotic kidneys.....	27
Reactivation of the nephrogenic regulator, Pax2, in kidney cancer.....	33
Pax2 transactivation in cystic kidney epithelial cells.....	36
Chapter 1 Summary and Conclusion	37
Bibliography.....	39
Chapter 2 – Kidney Fibrosis: HTS for small-molecule agonists of BMP signaling	52
Abstract.....	52
Introduction.....	53
Results.....	62
Discussion.....	64
Figures.....	65
Materials and Methods.....	69
Bibliography.....	73
Acknowledgements.....	78
Chapter 3 – Characterization of BMP signaling agonists identified using HTS	79
Abstract.....	79

Introduction.....	80
Results.....	83
Discussion.....	91
Figures.....	94
Materials and Methods.....	103
Bibliography.....	107
Acknowledgements.....	110
Chapter 4 – Proliferative renal diseases: Re-mining screens for Pax2 inhibitors.....	111
Abstract.....	111
Introduction.....	113
Results.....	119
Discussion.....	122
Figures.....	124
Materials and Methods.....	130
Bibliography.....	133
Acknowledgements.....	136
Chapter 5 – Conclusion and Future Directions.....	137
TGF- β and BMP signaling are implicated in the progression and reversal of CKD.....	137
Future investigations to further develop the identified BMP signaling agonists.....	141
Future investigations to further develop the identified Pax2 inhibitors.....	145
Bibliography.....	147

List of Tables

Table 1.1 Compounds that directly or indirectly target the TGF- β system for inhibition.....	25
Table 1.2 Antibodies that directly or indirectly target the TGF- β system for inhibition.....	26
Table 4.1 Comparison of CRC activities between original and fresh powder compounds	125
Table 4.2 Initial SAR analysis of a set of 35 CRC active compounds	127

List of Figures

Figure 1.1 Schematic of the canonical and non-canonical TGF- β signaling pathways.....	10
Figure 1.2 Schematic of the canonical BMP signaling pathway.	29
Figure 2.1 Characterization and validation of BRE-Luc cells for HTS.....	65
Figure 2.2 Assessment of TGF- β effectors p-SMAD-2 and p-SMAD-3 in BRE-Luc cells.	66
Figure 2.3 High-Throughput Screening strategy in BRE-Luc cells.	67
Figure 2.4 Dose-response curves of the top twelve potential BMP signaling agonists.....	68
Figure 3.1 Activation of p-SMAD-1/5/9 by HTS small-molecules.....	94
Figure 3.2 Evaluation of the top twelve agonists in non-canonical BMP signaling activation. ...	95
Figure 3.3 Assessment of the top twelve agonists in TGF- β signaling effector induction.....	96
Figure 3.4 Activation of p-SMAD-1/5/9 by sb4 in PRECs.	97
Figure 3.5 Effects of endogenous and chemical BMP inhibitors on sb4 activity.....	98
Figure 3.6 BMP signaling agonists enhance the efficacy of BMPs.....	99
Figure 3.7 Sb4 activates endogenous BMP4 target genes.	100
Figure 3.8 Initial Structure Activity Relationships (SAR) among 11 sb4-like compounds.	101
Figure 3.9 Profile of sb4 and key mechanistic insights gained.....	102
Figure 4.1 Re-mining strategy to test additional small-molecules in PRS4-Luc cells.	124
Figure 4.2 Fresh powder dose-response curves of emerging lead series of Pax2 inhibitors.	126

Abstract

Chronic Kidney Disease (CKD) is a major global health burden. In the United States alone, roughly 30 million Americans have CKD. Each year in the United States, thousands of CKD patients progress toward the most severe form of CKD, End-Stage Renal Disease (ESRD). Once patients reach ESRD, costly renal replacement therapy is needed to sustain life. Striking disparities also exist within the CKD patient population. In fact, Native Americans, Americans of African descent, Native Hawaiians, and Asians are several times more likely to advance to ESRD relative to Americans of European descent. To decrease the burden of CKD, effective early interventions and accessible therapeutics are desperately needed.

Bone Morphogenetic Protein (BMP) signaling is critical in renal development and disease. In animal models of CKD or kidney fibrosis, re-activation of BMP signaling is reported to be protective by promoting renal repair and regeneration. Clinical use of recombinant BMPs, however, requires high and harmful doses to achieve efficacy. BMPs are also expensive therapeutic agents to use clinically due to the complexity of their synthesis. Consequently, alternative strategies are needed to harness the beneficial properties of BMP signaling in fibrotic kidneys. The first aim of the work in this dissertation was to identify simpler to synthesize small-molecules that could potentially be developed further to treat kidney disease. Therefore, current and powerful high-throughput screening (HTS) methodologies used for drug discovery were implemented to assess approximately 64,000 small-molecules in human kidney cells. These cells have a genomically integrated BRE-Luc reporter making them highly responsive to BMPs. The

HTS campaign identified twelve small-molecules that activated the BRE-Luc reporter in a dose-dependent manner. Of these compounds, sb4, displayed the lowest EC₅₀ (74 nM) and further investigations revealed its capacity to induce key downstream BMP signaling events. For instance, in the presence of sb4 levels of key second messengers in BMP signaling, p-SMADs-1/5/9, rapidly increased. Additional studies suggested that the increase in p-SMADs-1/5/9 was likely due to stabilization by sb4, which resulted in activation of BMP target genes, ID1 and ID3. These results are significant as they demonstrate the feasibility of identifying small-molecules using HTS that mimic key downstream BMP signaling events. Accordingly, compounds like sb4 could prove useful in clinically treating fibrosis by activating the BMP signaling pathway. Furthermore, sb4 also resists inhibition by endogenous BMP inhibitors, such as Noggin. This mechanistic feature may prove advantageous in clinical settings where BMPs alone are ineffective due to elevated levels of Noggin, which suppress BMP signaling.

Proliferative kidney diseases such as cystic kidney disease and kidney cancer are subtypes of CKD. Pax2, a critical transcription factor required for kidney development is generally undetectable in mature nephrons. However, Pax2 is reactivated in proliferative kidney diseases and correlates with disease progression. Inhibiting Pax2 arrests cystogenesis and decelerates kidney cancer, which makes Pax2 a potential therapeutic target. Thus, the second aim of this dissertation was to identify small-molecule inhibitors of Pax2. Re-mining efforts lead to the discovery of an emerging lead series of promising Pax2 inhibitors. These Pax2 inhibitors can potentially be further developed into therapeutics that could reverse kidney disease or manage it with less side effects than current FDA-approved agents. Ultimately, the BMP signaling agonists and Pax2 inhibitors identified can be further enhanced and used as tools to advance biomedical knowledge of pathophysiological processes of various forms of CKD.

Chapter 1 – Introduction to Chronic Kidney Disease and its evolving therapeutic landscape

Abstract

Chronic Kidney Disease (CKD) is deemed a silent killer as it typically progresses over long periods of time without noticeable symptoms. Ultimately, CKD advances toward End-Stage Renal Disease (ESRD) and can be deadly if left untreated. Diabetes and hypertension are the leading risk factors for developing ESRD. As such, to slow the progression of kidney disease it is necessary to strictly control diabetes and hypertension. However, even with carefully managed diabetes and hypertension patients can still progress toward ESRD. Presumably, this is because the underlying drivers of kidney disease progression are not directly targeted by these treatments. Once patients reach ESRD, renal replacement therapy is required to sustain life. Two clinical options for managing ESRD exist and include chronic dialysis treatment or kidney transplantation. Though these clinical options help sustain life, they are costly and burdensome to the patients receiving these treatments. Consequently, many patients succumb to disease while undergoing dialysis or while waiting for a kidney transplant.

Therefore, alternative therapeutics are needed to manage and potentially reverse chronic kidney disease. TGF- β and BMP signaling are both implicated in CKD. Longstanding studies have demonstrated that TGF- β contributes to driving the progression of CKD. Whereas, BMP signaling has been reported by numerous studies to reverse CKD. Various drug development programs for the treatment of CKD have been heavily centered and designed around targeting pathological levels of TGF- β . However, futile results were recently reported for clinical trials aimed at

suppressing pathological levels of TGF- β 1 with monoclonal antibodies. Another strategy to modulate TGF- β signaling is to activate BMP signaling, which counters the disease-causing effects of TGF- β . Chapter 1 provides an overview of the various strategies that have been employed to develop novel agents that target the TGF- β system for the treatment of CKD. Additionally, studies that have provided evidence of renoprotection by BMPs in the pathological context of CKD/fibrosis are also reviewed.

Lastly, Chapter 1 provides an overview of proliferative diseases of the kidney such as polycystic kidney disease and clear cell renal cell carcinoma. Current treatment strategies for these proliferative renal diseases and potential targets for therapeutic intervention are also discussed.

Overview of Chronic Kidney Disease epidemiology and pathophysiology

Chronic Kidney Disease (CKD) develops as an injurious and gradual loss of kidney function over several decades of life without noticeable symptoms. Patients with CKD can progress to having 10% of kidney function or End-Stage Renal Disease (ESRD) before experiencing any symptoms. Globally, some 720 million people have CKD [1]. Equally concerning, the prevalence of ESRD, the most severe type of CKD, is steadily rising; especially, in the United States where ESRD has risen 86% since 2000 [2]. Nearly 30 million Americans are afflicted with CKD and at least 100,000 of these patients progress towards ESRD each year [2]. There are currently over 700,000 prevalent cases of ESRD in the United States [2].

Marked disease disparities complicate the burden of CKD in the United States. Native Americans, Americans of African descent, Native Hawaiians, and Asians are several times more likely to reach ESRD relative to Americans of European descent [2]. Causes that contribute to CKD disparities included behavioral, socioeconomic, and environmental determinants. Genetic factors such as variants in the apolipoprotein L1 (APOL1) gene have also emerged to account for the excess risk in CKD disparity among Americans of African descent [3]. Similar to sickle cell anemia genes that are protective from malaria, APOL1 risk alleles are protective from African sleeping sickness, which although rare is endemic in parts of sub-Saharan Africa [4]. However, and alarmingly, patients with two APOL1 risk alleles are 3-100 times more likely to develop CKD compared to those lacking the risk alleles [5, 6].

Diabetes, hypertension, glomerulonephritis, and cystic kidney disease are the leading risk factors for developing ESRD [2]. Another risk factor for developing ESRD is kidney cancer specifically, the clear-cell renal cell carcinoma (ccRCC) subtype [7]. Of note, the risk for developing kidney cancer or kidney failure functions bidirectionally, with CKD patients being at

an increased risk for developing ccRCC and vice versa [7]. For example, type II diabetes induced CKD also puts patients at risk for developing kidney cancer [7, 8]. More risk factors for developing ESRD include chronic use of NSAIDs and a family history of CKD. As the causes of CKD are varied and complex, long-term management is economically burdensome. In 2016, nearly \$114 billion of the Medicare budget or 23% was allocated to kidney disease patients, with over \$79 billion spent on CKD treatment and \$35 billion spent on ESRD treatment [9].

As outlined above, the etiology of CKD can vary. Regardless of the underlying cause, CKD ultimately progresses to total kidney failure. No cures or targeted molecular therapies for CKD are available. The current therapeutic options for ESRD are limited to either chronic dialysis treatment or kidney transplantation. Chronic dialysis treatment is costly with per capita treatment per year at \$90,971 for hemodialysis and \$76,177 for peritoneal dialysis [9]. Strikingly, chronic dialysis treatment only restores roughly 15% of kidney function. This is reflected by the shortened patient life expectancy after starting dialysis treatment. In 2016, a patient on chronic dialysis between the ages of 50-54 years old could expect to live approximately 8 years after starting treatment [10]. With a kidney transplantation, which costs \$34,780, the same 50-54 year old patient could expect to live at least 20 years [9, 10]. At least 90,000 candidates are currently on the waitlist for a kidney transplantation and wait times vary widely between less than 30 days to more than 5 years [11]. Regrettably, many patients succumb to disease while waiting for a kidney donation. Neither chronic dialysis treatment nor kidney transplantation are a cure for ESRD. As such, individuals 50-54 years old in the general United States population still have a greater life expectancy (27-31 years) compared to dialysis or transplant patients [10].

Fibrosis is the principal histopathological finding in patients with CKD. At the molecular level, fibrogenesis is primarily driven by the cytokine TGF- β . Under normal physiological conditions, TGF- β is transiently released in response to injury in order to initiate and later terminate the process of tissue repair [12]. However, under pathophysiological conditions or sustained injury, TGF- β release persists and feeds into an injurious cycle of excessive extracellular matrix (ECM) tissue deposition. Excessive ECM deposition damages complex functional compartments of the kidney such as the vasculature, glomerulus, and tubulointerstitium [13].

Along with its normal physiological role of shaping tissue structure to support tissue function, the ECM is also important for tissue repair and regeneration [14]. Therefore, in tissues with disturbed ECM homeostasis compromised by overactive TGF- β , tissue loss can ensue (excessive ECM degradation) or tissue fibrosis and scarring can occur (excessive ECM accumulation) [14]. Fibrotic kidneys, therefore, at the histological level exhibit an excessive deposition of TGF- β induced extracellular matrix particles, which primarily consists of fibrous proteins such as collagens and hydrogel forming proteoglycans such as perlecan [15]. These particles can cause the glomerulus (capillaries) to become sclerotic and/or, the kidney interstitial space which typically consists of physiological levels of extracellular matrix, fluid, and multiple cellular constituents such as fibroblasts can become fibrotic [16, 17]. Continued damage of these functional structures by ECM overtime leads to the development of CKD which later culminates as ESRD.

While TGF- β drives fibrogenesis at the molecular level [18, 19], at the cellular level, myofibroblasts promote the fibrogenic scarring process. Under normal physiological conditions interstitial fibroblasts are quiescent and few in number. However, overactive TGF- β stimulates the abnormal proliferation and accumulation of interstitial fibroblasts. These activated fibroblasts,

termed myofibroblast, secrete excessive levels of ECM such as collagens and α -smooth muscle actin and thereby, at the cellular level drive fibrogenesis [13, 20-22].

Current therapeutic landscape for Chronic Kidney Disease management

As previously mentioned, no cures or targeted molecular therapies for CKD exist. However, since diabetes and hypertension are the leading primary causes of CKD, strict control of these ailments help slow CKD to ESRD progression [23-26]. Therefore, modulation of kidney hemodynamics is the standard of care for slowing the progression of CKD in patients. This is achieved by targeting the Renin-Angiotensin-Aldosterone system (RAAS) with renin enzyme inhibitors, angiotensin converting enzyme inhibitors (ACEi), angiotensin receptor blockers (ARBs), or mineralocorticoid antagonists to target aldosterone [5].

Renin enzyme inhibitors such as Aliskiren inhibit the first step of the RAAS cascade, while ACEi and ARBs work further downstream. ACEi, such as captopril, block the conversion of angiotensin I to angiotensin II. Angiotensin II is induced upon sensing low blood pressure and when released acts directly on smooth muscle cells to induce vasoconstriction, which increases intraglomerular filtration pressure [5, 27]. Inhibiting the process of converting angiotensin I into angiotensin II results in vasodilation and reduced hyperfiltration and proteinuria, which slows the progression of CKD to ESRD. ARBs work by competing for the type I angiotensin II receptor.

Still, patients with controlled diabetes and/or hypertension and modulated kidney hemodynamics remain at risk for developing ESRD. These strategies do not stop the progression of CKD to ESRD. In these treatment scenarios, it is likely that the underlying cause for CKD is not addressed and damage is still ongoing. Ultimately, novel medications that promote renal repair and regeneration are urgently needed and must be practical to synthesize and cost-effective for patient accessibility.

Evolving landscape of therapeutics to treat Chronic Kidney Disease

A breadth of aberrant aspects and molecular targets of CKD have been identified which has allowed research, evaluation, and development of novel clinical therapeutics. The evolving therapeutic landscape for CKD is largely tailored around diabetes and hypertension treatment. For example, in the clinical case of diabetic nephropathy one strategy to slow disease progression includes mitigating high levels of systemic glucose via inhibition of the sodium-glucose co-transporter 2 (SGLT2). The SGLT2 is chiefly responsible for roughly 90% of glucose reabsorption in the kidney whereas SGLT1 is responsible for 10% [28]. Due to these transporters, nearly all glucose is reabsorbed in the kidneys and therefore virtually untraceable in excreted urine. However, in diabetic patients, pathological amounts of glucose in urine are characteristic of this disease. High glucose levels overburden the transporters and cause excretion of glucose into the urine. SGLT2 inhibitors therefore further promote the process of glucose excretion in the urine and are used as a method to lower high blood glucose levels. Additional effects of SGLT2 inhibition involves regulating kidney hemodynamics specifically, at the level of the afferent arterioles [5]. These agents may also have beneficial effects similar to ACEi and ARB in that they lower glomerular filtration pressure and thus stabilize CKD [5].

Targeting the TGF- β system and its pathological effects for the treatment of CKD

The evolving landscape of novel therapies to treat organ damage caused by fibrosis has also been strategically designed around and intensely focused on modulating aberrant transforming growth factor- β (TGF- β) activity. TGF- β proteins are multifunctional signaling cytokines with essential roles in organ development, homeostasis, and disease. TGF- β s are extremely potent and their activity is heavily safeguarded within a large latency complex which consists of latency-associated proteins (LAPs) and latent-TGF- β -binding proteins (LTBP) [29]. The large latency complex sequesters and quarantines TGF- β to the ECM to diffuse its activity (**figure 1.1**). A variety of molecules, on the other hand, are responsible for liberating TGF- β from the large latency complex such as, integrin- $\alpha\beta$ receptors. LAPs of the large latency complex are a substrate for integrin- $\alpha\beta$ receptors and upon binding a conformational change in LAPs invokes liberation of bound TGF- β from LAP sequestration.

Liberation of TGF- β can be triggered by a plethora of stimuli that disturb ECM homeostasis including inflammation and would repair [29]. Upon release from the extracellular matrix dimerized TGF- β proteins bind to a heterotetramer comprised of type I and type II TGF- β receptors (**figure 1.1**). The constitutively active type II TGF- β receptors phosphorylate the glycine-serine domain of the type I TGF- β receptors. In turn, the TGF- β receptors phosphorylate and activate receptor activated SMADs (R-SMADs) (**figure 1.1**). Specifically, TGF- β signaling is transduced through R-SMAD-2 and R-SMAD-3 effectors, which form a heteromeric complex with common-SMAD4 (co-SMAD4) (**figure 1.1**). This heteromeric complex drives the expression of target genes such as α -smooth muscle actin and collagens which are particularly important molecules in fibrogenesis.

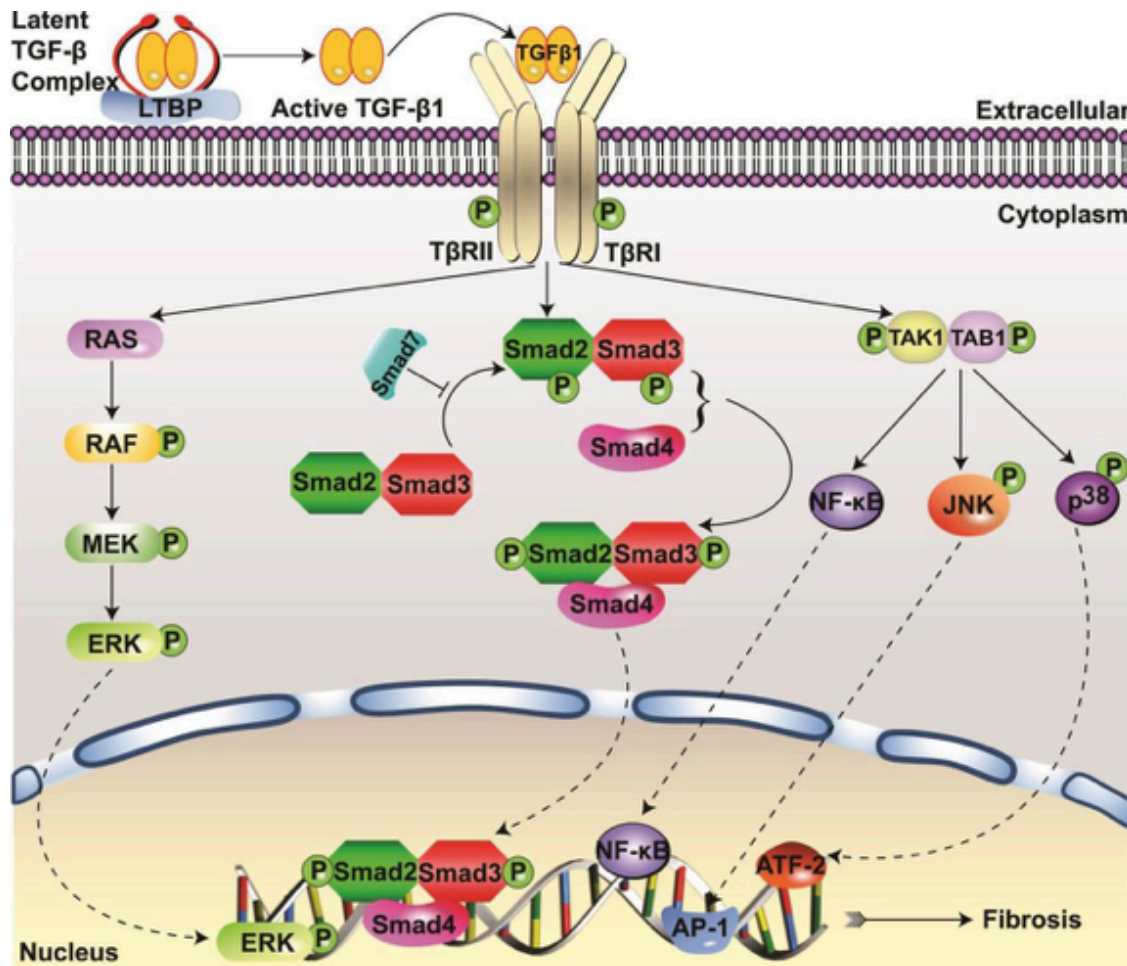


Figure 1.1 Schematic of the canonical and non-canonical TGF- β signaling pathways.

Many drug discovery programs have been designed around inhibiting components of both the canonical and non-canonical TGF- β signaling pathways. In the TGF- β signaling pathway a large latency complex sequesters and quarantines TGF- β to the ECM. Integrin- $\alpha\beta$ receptors help liberate TGF- β s from the ECM. Upon release from the ECM, dimerized TGF- β ligands bind to a heterotetramer comprised of type I and type II TGF- β receptors. The constitutively active type II TGF- β receptors phosphorylate the glycine-serine domain of the type I TGF- β receptors. In turn, the type I TGF- β receptors phosphorylate and activate the TGF- β effectors SMAD-2 and SMAD-3. SMADs-2/3 then form a heteromeric complex with co-SMAD4. This heteromeric complex then translocates to the nucleus where it drives the expression of target genes such as α -smooth muscle actin and collagens which are important in fibrogenesis. Binding of TGF- β ligands to TGF- β receptors also activates non-canonical TGF- β signaling pathways such as ERK. This figure appears in—Sureshababu, A., S. A. Muhsin and M. E. Choi (2016). "TGF-beta signaling in the kidney: profibrotic and protective effects." *Am J Physiol Renal Physiol*. PMID: 26739888 [30].

The role of TGF- β in inflammation, ECM homeostasis, and its proliferative and anti-proliferative actions on different cell types has been extensively studied. For instance, experimental animal models with ablated TGF- β 1 have uncontrolled inflammation and die within 2-3 weeks [31]. These TGF- β 1 heterozygous animals generated by Shull and colleagues exhibit significant lesions in the heart and stomach due to infiltration of inflammatory cells such as lymphocytes and neutrophils; and, tissues such as the liver and lung are riddled with pro-inflammatory cytokines (interferon- γ , MIP-1 α , and TNF- α) [31]. Similarly, TGF- β 1 null animals generated by Kulkarni and colleagues exhibit inflammatory lesions in the heart and lungs and die 3-4 weeks after birth due to cardiopulmonary disease [32]. Furthermore, integrin- β ₆^{-/-} animals, which lack the ability to convert latent TGF- β to maturity, also develop uncontrolled inflammation. However, fibrogenesis is suppressed in these animals after bleomycin induced pulmonary fibrosis [33]. Additional lines of experimental evidence also confirm that TGF- β functions across several organs as a driver of fibrogenesis [34]. These organs include: the kidneys, lungs, heart, liver, skin, intestine, and bone marrow [35-40].

Pirfenidone suppresses the TGF- β system through unknown mechanisms

Concerted efforts by academic laboratories and pharmaceutical companies have fostered the development of a catalog of small-molecules and biologics aimed at inhibiting the TGF- β system at multiple levels (**table 1.1 and table 1.2**). Pirfenidone (Esbriet[®]), is an FDA approved synthetic small-molecule for the treatment of mild-to-moderate Idiopathic Pulmonary Fibrosis (IPF). It has been speculated that Pirfenidone may exert its anti-fibrotic effects through TGF- β promoter inhibition, which may result in arrested TGF- β protein synthesis and secretion [41, 42].

However, the complete mechanism of action of Pirfenidone is not completely understood. Generally, Pirfenidone acts to preserve and protect lung function from the damaging actions of overactive TGF- β such as its excessive stimulation of procollagens I and III. However, even under Pirfenidone therapy IPF may persist as it only slows disease progression. Animal models of and patients with kidney disease have also been treated with Pirfenidone and demonstrated better kidney function as assessed by improved estimated glomerular filtration rate (eGFR) [43, 44]. F-351 is a Pirfenidone analog (10 times more potent) currently being evaluated for safety and efficacy for the treatment of chronic viral hepatitis B induced liver fibrosis in a Phase II clinical trial sponsored by Shanghai Genomics, Incorporated [45].

BG00011 (STX-100) and VPI-2690B inhibit integrin- $\alpha\beta$ receptors

Neutralization of integrin- $\alpha\beta$ receptors is another strategy to target overactive TGF- β activity. In particular, BG00011 (STX-100) is a humanized monoclonal antibody in the Biogen Inc. pipeline that selectively targets and deactivates integrin- $\alpha_v\beta_6$ receptors [46]. BG00011 has been tested in Phase IIa dosage studies and is currently under investigation in Phase IIb efficacy studies in patients with IPF (estimated completion date 2021) [47, 48]. Vascular Pharmaceuticals, Incorporated have also developed VPI-2690B, a monoclonal antibody that selectively inhibits integrin- $\alpha_v\beta_3$ receptors. Phase II clinical studies testing the efficacy of VPI-2690B in patients with type I and II diabetic kidney disease were completed in March 2017 [49].

TGF- β 1 is selectively targeted with LY2382770

Pathological levels of TGF- β s can also be targeted with neutralizing antibodies. Based on data from pre-clinical studies in animals with kidney disease, Eli Lilly and Company developed LY2382770 (humanized monoclonal antibody) which selectively targets TGF- β 1. However, in Phase II dosing studies using patients with type I and type II diabetes receiving RAS inhibition therapy, efficacy measures (changes in serum creatinine and eGFR) were not reached and the studies were terminated 4 months early (initial 12 month study design) [50]. Voelker and colleagues proposed several reasons for lack of efficacy and posited that treating diabetic nephropathy patients with anti-TGF- β 1 at a less severe stage and/or more frequent administration may provide additional strategies to fully inhibit TGF- β 1 [50]. Although, effects from prolonged and/or over-suppression of TGF- β 1 could lead to harmful side effects such as systemic inflammatory lesions [31, 32].

Fresolimumab neutralizes TGF- β 1, β 2, and β 3 ligands

In addition to selective antibodies that neutralize TGF- β 1, pan-anti-TGF- β antibodies have also been developed and evaluated in fibrotic diseases. Specifically, Fresolimumab, a humanized monoclonal antibody in the Sanofi portfolio, neutralizes all three isoforms of TGF- β (TGF- β 1, β 2, and β 3). Fresolimumab has been evaluated in Phase I and Phase II clinical trials in patients with steroid-resistant primary focal segmental glomerulosclerosis (SR-FSGS) where TGF- β is reported to be increased in patient biopsies [51]. In both Phase I and II studies, tested doses of Fresolimumab were determined to be safe and tolerable; however, primary and secondary efficacy measures of decreased proteinuria and eGFR respectively were not reached [52, 53]. Interestingly, a small subset of FSGS patients (Americans of African descent) showed a significant reduction in

proteinuria after just one-single infusion of Fresolimumab in Phase I clinical trials [52]. In Phase II clinical trials a similar beneficial effect in Americans of African descent was also observed [53].

GW788388 inhibits both type I and type II TGF- β kinase receptors

Pre-clinical investigations in animal models of renal fibrosis have also explored the utility of targeting TGF- β receptors to ameliorate the pro-fibrotic effects of TGF- β . In particular, GW788388 inhibits both type I and type II TGF- β kinase receptors which results in suppression of key pathological events observed in both *in vitro* and *in vivo* experimental conditions [54]. Semi-quantitative RT-PCR reaction analysis revealed attenuated TGF- β signaling as assessed by a reduction in TGF- β target genes (SNAIL, E-cadherin, fibronectin) after GW788388 treatment in cells stimulated for 48hr with 5 ngml⁻¹ TGF- β 3 [54]. While, a significant reduction in collagen, as assessed by immunohistochemical staining, was observed in six-month-old mouse models of advanced diabetes-induced renal fibrosis receiving daily oral treatments of GW788388 at 2 mg⁻¹kg¹ for five weeks [54]. Additionally, TGF- β target genes that drive the deposition of excessive extracellular matrix such as PAI-1, collagen α 1(I), and collagen α 1(III) were also significantly suppressed in these GW788388 treated type II diabetic animals [54].

IN-1130 and SB-525334 inhibit type I TGF- β kinase receptors

In a rat model of renal fibrosis, unilateral ureteral obstruction (UUO), the type I TGF- β receptor inhibitor, IN-1130, was evaluated and demonstrated anti-fibrotic properties. Particularly, IN-1130 (intraperitoneally injected at 10 or 20 mg/kg/day for 7 or 14 days, which constituted early and late states of fibrogenesis) reduced striking pathological manifestations such as tubular loss, atrophy, and dilation; while, these diseased morphological changes persisted in

vehicle treated animals [55]. Further, the phosphorylation of TGF- β effector SMAD-2 in rat UUO kidneys was significantly downregulated in a dose-dependent manner after 14 days of IN-1130 treatment compared to UUO vehicle treated groups [55]. Although p-SMAD-2 levels didn't return to basal levels seen in sham operated animals at the doses tested and time points examined (10 and 20 mg/kg for 14 days) [55]. Similarly, at 14 days or later stages of fibrogenesis, IN-1130 was not as efficacious at reducing α -smooth muscle actin (α -SMA) when compared to earlier stages of disease [55]. This highlights the possibility that progressive fibrogenesis may be driven by both dependent and independent TGF- β pathways [55]. If such is the case, full recovery from fibrotic lesions may only be achieved through a combination of therapeutic agents and carefully designed treatment regimens.

Full suppression of fibrotic events was also not achieved with oral administration of the type I TGF- β receptor inhibitor, SB-525334. In puromycin induced renal fibrosis in rats, SB-525334, significantly suppressed proteinuria relative to untreated animals at 10 mg/kg/day [56]. However, proteinuria in these animals still remained at concerning levels of approximately 50% of the untreated puromycin induced fibrotic animals (still a sign of damaged kidneys) [56]. Likewise, PAI-1 mRNA levels were significantly increased 7.5-fold above control animals and although each dose tested (1, 3, 10 mg/kg) significantly reduced PAI-1, levels hovered around 3-4-fold higher than control levels in control animals, which again suggests additional pathways at play in driving fibrogenesis [56]. Procollagen α 1(I), and Procollagen α 1(III) mRNA expression in puromycin induced fibrotic animals was significantly decreased relative to untreated animals with significance reached at the 10 mg/kg/day dose [56]. Procollagen α 1(I) mRNA levels persisted at nearly 1-fold above control animals and Procollagen α 1(III) expression leveling near control baseline. Interestingly, TGF- β mRNA was not regulated by SB-525334 in the puromycin model

of fibrosis whereas, IN-1130 caused a dose-dependent decrease in TGF- β ligand mRNA in UUO induced fibrosis [55, 56].

SIS-3 inhibits the TGF- β effector SMAD-3

TGF- β signaling effectors SMAD-2 and SMAD-3 can also be targeted to modulate overactive TGF- β . SMAD-3 in particular is reported to execute the majority of fibrotic effects instigated by TGF- β . Several experimental animal models illustrate ablation of SMAD-3 as a potential mechanism to achieve protection from fibrotic lesions. For example, conditional SMAD-3 knock-out animals are protected from UUO and STZ induced tubulointerstitial fibrosis [57-59]. Additionally, reduced collagen IV and fibronectin expression in the tubulointerstitium and glomeruli of STZ-induced diabetic mice was observed after treatment with a specific inhibitor of SMAD-3 (SIS-3) [60]. Furthermore, confocal microscopy analysis revealed a decrease in the total number of α -SMA⁺ cells in the renal interstitium after SIS-3 treatment in STZ-induced diabetic mice [60]. And, although SIS-3 was unable to reduce proteinuria in these animals, levels of serum creatine were significantly reduced in SIS-3 treated STZ-induced diabetic mice [60].

Pentoxifylline diminishes TGF- β /SMAD-3/4 signaling

Pre-clinical and clinical studies evaluating the nonselective phosphodiesterase inhibitor, Pentoxifylline (PTX), have also demonstrated encouraging results on mitigating the pro-fibrotic effects caused by overactive TGF- β . Specifically, by targeting TGF- β /SMAD-3/4 signaling, PTX diminished connective tissue growth factor (CTGF) promoter activity and subsequently collagen I (α 1) expression induced by CTGF in rat kidney fibroblasts [61]. Additionally, PTX reduced α -SMA expression induced by CTGF in rat kidney proximal tubular epithelial cells [61]. These

CTGF events are regulated upstream by TGF- β /SMAD-3/4 signaling. Furthermore, interstitial fibroblasts stimulated with 1 μ M of angiotensin II for 4 hours increased both TGF- β 1 and CTGF gene expression [62]. However, PTX diminished CTGF gene levels but not TGF- β 1 gene levels, which demonstrated the selective inhibition of PTX towards CTGF [62]. Moreover, rat kidney interstitial fibroblasts stimulated with 5 ng/ml of TGF- β 1 and treated with PTX at increasing concentrations showed a dose-dependent reduction of CTGF at each concentration tested (0, 0.1, 0.3, 1 millimolar) [62]. Notably, PTX was also able to slow the proliferation of rat interstitial fibroblasts in a dose-dependent manner during a 48hr time course experiment [62].

In vivo evaluation of PTX in two different models of kidney disease, 5/6 subtotal nephrectomy (5/6 Nx) and unilateral ureteral obstruction (UUO), demonstrated beneficial effects in lessening disease severity and slowing disease progression [61, 62]. Alongside glomerulosclerosis and interstitial fibrotic and inflammatory lesions, 5/6 Nx rats develop proteinuria and increased plasma creatinine levels [62]. In each of the aforementioned markers of disease progression assessed, PTX significantly decreased each by 40-60% [62]. Furthermore, compared to sham operated rats, 5/6 Nx rats develop significant levels of hypertension that PTX was unable to positively regulate [62]. Notably, when PTX was combined with Cilazapril (an ACEi), not only was uncontrollable hypertension in 5/6 Nx resolved, levels of proteinuria were reduced to levels matching those of sham operated animals [62].

Animals that have undergone uretic ligation/UUO rapidly develop tubulointerstitial fibrosis compared to sham operated animals. Interstitial macrophage infiltration and an expansion of α -SMA positive myofibroblasts play key roles in fibrogenesis in UUO animals. PTX treatment in UUO rats exhibited anti-fibrotic effects by decreasing accumulation of ED-1 positive macrophages and α -SMA positive myofibroblasts which remain elevated in UUO rats [61].

Compared to UUO rats PTX also diminished interstitial damage, as well as, interstitial collagen deposition, which were assessed by PAS and Masson trichrome staining respectfully [61]. Moreover, in UUO/PTX rat kidneys, CTGF and collagen I (α 1) gene expression were also reduced relative to levels in untreated UUO rats [61].

The renoprotective/anti-proteinuria effects of PTX have also been demonstrated in several clinical studies in patients with type I and II diabetes [63-66]. Particularly, in a randomized trial using 40 type II diabetic patients treated for 16-weeks with 400 mg of PTX daily, microalbuminuria decreased significantly from 8.4 ± 4.9 mg/mmol urine creatinine to 2.2 ± 2.6 mg/mmol urine creatinine by the end of the treatment period [66]. Whereas, microalbuminuria decreased slightly from 8.5 ± 4.9 mg/mmol urine creatinine to 7.9 ± 4.7 mg/mmol urine creatinine in placebo treated patients, which did not reach significance [66]. These patients were non-hypertensive and therefore not on ACEi or ARBs. In 2010, a phase IV clinical trial was initiated to investigate the renoprotective effects of PTX coupled with angiotensin receptor blockade using Valsartan, this study is expected to be completed in December 2018 [67]. Primary and secondary outcome measurements for this clinical trial include: doubling of serum creatinine or development of ESRD (primary) or changes in microalbuminuria/proteinuria, or the development of heart failure or stroke (secondary) [67].

The Tranilast analog FT011/SHP-627 reduces TGF- β induced ERK1/2 activity

As previously outlined, TGF- β signaling is transduced canonically via SMADs. However, branches of the mitogen activated kinase (MAPK) signaling pathway are also activated by TGF- β signaling. In particular, TGF- β can exert its effects through the activation of the extracellular signal-regulated kinase 1/2 (ERK1/2) branch of MAPK signaling [68]. Hence, another strategy to

attenuate the damaging effects of overactive TGF- β can be achieved through targeting TGF- β induced ERK1/2 activation. Tranilast which is proposed to inhibit TGF- β activity and is used for the treatment of allergies and fibrotic skin disorders such as keloids has also demonstrated anti-fibrotic activity in other tissue types [69]. Chemical synthesis of the Tranilast analog, FT011/SHP-627, however, was prompted due to the high doses of Tranilast needed to exhibit anti-fibrotic effects, which ultimately compromised kidney and liver function [70, 71]. In comparison to Tranilast, FT011/SHP-627 demonstrated superior anti-fibrotic actions with improved *in vivo* activity and an attractive metabolic profile [70, 72].

FT011/SHP-627 has been evaluated in heart and kidney cells and tissues. Following overnight serum starvation in 0.5% fetal bovine serum, primary rat cardiac fibroblasts pre-treated with increasing doses of FT011/SHP-627 (10, 30, 100 μ M) for 4 hours and later stimulated with 10^{-7} ng/ml of angiotensin II for 15 minutes, displayed a dose-dependent decrease in levels of phosphorylated-ERK1/2 [72]. Additionally, primary rat cardiac fibroblasts pre-treated for 4 hours with 30 μ M FT011/SHP-627 (also following overnight serum starvation in 0.5% fetal bovine serum) were significantly protected from high levels collagen type III expression after being stimulated with 10 ng/ml TGF- β 1 for 5 minutes [72]. Cardiomyocytes from streptozotocin-induced diabetes in Ren-2 rats treated with FT011/SHP-627 (200 mg/kg/day for 6 weeks) demonstrated significantly reduced nuclear staining of p-SMAD-2 and p-ERK1/2 relative to vehicle treated diabetic Ren-2 rats [72].

FT011/SHP-627 is postulated, therefore, to exert its actions further downstream via inhibition of the phosphorylation of TGF- β induced SMADs and TGF- β induced ERK1/2 which attenuates fibrosis in animal models of diabetic cardiomyopathy/diabetes-associated cardiac fibrosis [72, 73]. In rat mesangial cells, FT011/SHP-627 has been demonstrated to not only block

the actions of TGF- β and its downstream effectors SMAD2 and ERK1/2 but, FT011/SHP-627 is also able to block platelet-derived growth factor (PDGF) activity as well [74]. This is a useful observation as PDGF is reported to contribute along with TGF- β to the development of the profibrotic milieu in renal tissues [75, 76]. In a 16-week assessment of FT011/SHP-627 in diabetic rats, albuminuria was significantly decreased at each time-point tested [74]. Likewise, FT011/SHP-627 assessment in STNx rats improved GFR rates and blood pressure as well as reduced urinary proteins [74]. Furthermore, FT011/SHP-627 completely absolved Armani-Ebstein lesions in diabetic Ren-2 rat kidneys which are caused by a significant abnormal accumulation of glycogen protein [77].

Using both healthy and type II diabetic nephropathy patients the safety, tolerability, and pharmacokinetics of FT011/SHP-627 was tested in a three-part Phase I clinical trial conducted in Australia by Fibrotech Therapeutics which was acquired by Shire in 2014 [78]. In the first phase, 5 different cohorts of healthy patients received single doses of FT011/SHP-627 ranging between 10-1000 mg, the patients were followed for 7 days. The second phase observed the effect of food on 100 mg doses of FT011/SHP-627 while, the third phase tested the effects of increasing doses of FT011/SHP-627 on healthy and diabetic patients for two weeks. The pharmacokinetic profile of FT011/SHP-627 in these human Phase I trials included an approximately 12-hour half-life and clearance over 24 hours, therefore, FT011/SHP-627 would be amenable to evaluation in Phase II clinical trials. Additionally, FT011/SHP-627 is also being considered for evaluation in treating focal segmental glomerulosclerosis; Phase I formulation and dose studies and Phase II studies were expected to commence in 2016 and 2017, respectively [79].

Simtuzumab/AB0023 neutralizes LOXL2 activity

Novel therapeutics that target excessive ECM accumulation have also been identified and evaluated in both *in vitro* and *in vivo* studies. For instance, Simtuzumab (a humanized monoclonal antibody; AB0023) neutralizes lysyl-oxidase like protein 2 (LOXL2) activity. LOXL2 is an important target in the treatment of fibrosis because it catalyzes covalent bond formation between collagen monomers [5, 14]. Further, relative to healthy controls, pathological levels of insoluble collagen are observed in fibrotic tissues along with increased levels of LOXL2 expression [80]. In particular, LOXL2 expression has been detected in liver fibrosis induced by hepatitis C infection or steatohepatitis in humans [80]. Evidence from preclinical studies show that LOXL2 neutralization confers protection against the development of fibrotic and cancerous lesions. For instance, compared to untreated mice with liver fibrosis (carbon tetrachloride induced) a significant reduction in p-SMAD-3 signaling was observed after Simtuzumab/AB0023 therapy (30 mg kg⁻¹ twice per week during a 22-day treatment window) [80]. Furthermore, TGF- β 1 and other mediators such as endothelin-1, CXCL12, and LOXL2 implicated in fibrogenesis decreased with Simtuzumab/AB0023 therapy in animal models of bleomycin induced lung fibrosis [80]. Bleomycin induced fibrotic lungs after Simtuzumab/AB0023 therapy also show a reduction in the abnormal abundance of cross-linked collagenous matrix [80].

Likewise, Simtuzumab/AB0023 inhibited the production of cross-linked collagenous matrix in the stroma of animals with tumors (MDA-MB-435 induced). As well as, significantly reduced the pathological abundance of growth factors such as TGF- β , VEGF-A, CXCL12, and CTGF in the stroma of these tumors [80]. Gilead Sciences, Incorporated funded a Phase II clinical trial to assess the efficacy and safety of Simtuzumab/AB0023 in patients with IPF diagnosed at least 3 years prior to screening (IPF average survival rate is 2-3 years) [81]. Baseline levels of

serum LOXL2, forced vital capacity (FVC), and pirfenidone or nintedanib therapy were used to stratify treatment groups and 125 mg/ml of Simtuzumab/AB0023 was given subcutaneously once a week to IPF patients over an event driven treatment timespan [81]. The clinical trial was ultimately terminated early due to failure to meet primary outcome efficacy measures (progression-free survival) [81, 82]. Reasons posited for lack of efficacy include LOXL family members, as well as, other cross-linking enzymes (e.g. Transglutaminase 2) that are not sensitive to Simtuzumab/AB0023 neutralization. Lack of efficacy was also attributed to insufficient drug exposure and/or drug delivery across fibrotic lung tissues [81]. Additional therapies to block the synthesis of collagen and its conversion from procollagen are also being tested for application towards treating fibrotic disease. An example of this strategy is UK-421,045 which targets Bone Morphogenetic Protein 1, a metalloproteinase, that catalyzes the conversion of soluble procollagen to insoluble collagen [14].

ROCK and FAK inhibitors target the damaging effects of TGF- β

Agents that target TGF- β induced myofibroblast proliferation or that target activation of fibroblasts are essential in the anti-fibrotic therapeutic toolkit. ROCK (Rho-associated coiled-coil forming protein kinase) and FAK (focal adhesion kinase) inhibitors that block the cellular signaling required for α -SMA expression have been tested preclinically as a strategy to impede fibroblast to myofibroblast differentiation [14]. Of note, ROCK ablated mice subjected to pressure-overload cardiac hypertrophy are protected from the development of perivascular and interstitial fibrosis [83]. Additionally, in the unilateral ureteral obstruction (UUO) animal model of fibrosis, the ROCK specific inhibitor, Y-27632, exhibited efficacy in significantly decreasing pathological levels of α -SMA, TGF- β , and collagen α 1(I) gene expression 10 days after UUO surgery [84].

Suppression of α -SMA by Y-27632 was similar *in vitro*, however, suppression of TGF- β and collagen α 1(I) were not significantly suppressed *in vitro* [84]. Furthermore, Y-27632 treated UUO animals upon histological examination revealed significantly decreased levels of α -SMA [84]. Moreover, *in vitro* experimentation revealed that Y-27632 was ineffective at inhibiting mouse renal fibroblast proliferation although macrophage migration upon histological examination was diminished [84]. Lastly, Y-27632 significantly reduced interstitial expansion in UUO animals which was assessed by Masson's Trichrome staining 10 days after surgery [84].

It has been reported that in order to incite a successful fibroblast to myofibroblast transdifferentiation program in fibrotic tissues, overactive TGF- β requires FAK activation [85, 86]. Immunohistochemical analysis of biopsies from patients with IPF or connective tissue disease-associated lung fibrosis revealed upregulated expression of FAK in myofibroblast foci and in remodeled arteries in fibrotic lungs [87]. Additionally, compared to embryonic fibroblast isolated from wild-type mice, FAK ablated mouse embryos exhibit resistance to endothelin-1 induced FAK activation and fibrosis [87]. More specifically, FAK ablated cells were unresponsive to endothelin-1 induced expression of type I collagen and α -SMA which thereby impaired the myofibroblast differentiation program [87]. Preclinical studies in animals with bleomycin induced lung fibrosis revealed attenuated fibrogenesis in animals undergoing twice daily FAK inhibitor/PF-562271 therapy at 15 mg/kg for three weeks [87].

Several strategies aimed at targeting the TGF- β system either directly or indirectly have been outlined in this section. The preclinical and clinical results from these studies have been detailed as well. Through these studies, significant advances in the understanding of the molecular and cellular events that drive fibrogenesis have been realized, which yielded innovative medical breakthroughs for the treatment of pulmonary fibrosis. Yet and still, a dearth of precise treatment

options for patients with organ fibrosis such as kidney fibrosis exists. It should also be noted that many of the drugs discussed in this section possess complex mechanisms of action and likely have targets beyond the TGF- β system. In support of this reality, the currently approved medications for the treatment of pulmonary fibrosis, Pirfenidone (Esbriet[®]; Genentech) and Nintedanib (OFEV[®]; Boehringer Ingelheim Pharmaceuticals), are insufficient at completely halting the progression of pulmonary fibrosis; for example, Nintedanib can only slow disease progression for up to 3-years [88-90]. These outcomes likely highlight the complex nature and unknown mechanisms of action of these drugs. Therefore, additional strategies and novel agents with direct targets are needed to bolster the repertoire of anti-fibrotic therapeutics for fibrosis of the kidney and other organs such as the lungs and heart.

Table 1.1 Compounds that directly or indirectly target the TGF- β system for inhibition.

Compound	Proposed Target of Inhibition	Compound	Proposed Target of Inhibition
<p>Pirfenidone (Esbriet[®])</p>	unknown target	<p>Pentoxifylline</p>	TGF- β /SMAD-3/4 signaling
<p>F-351 (Pirfenidone analog)</p>	unknown target	<p>Tranilast</p>	unknown target
<p>GW788388</p>	Type I and Type II TGF- β receptors	<p>FT011/SHP-627 (Tranilast analog)</p>	unknown target
<p>IN-1130</p>	Type I TGF- β receptors	<p>Y-27632</p>	ROCK (Y-27632 indirectly suppresses the TGF- β system)
<p>SB-525334</p>	Type I TGF- β receptors	<p>PF-562271</p>	FAK (PF-562271 indirectly suppresses the TGF- β system)
<p>SIS-3</p>	SMAD-3		

Table 1.2 Antibodies that directly or indirectly target the TGF- β system for inhibition.

Monoclonal Antibodies (mAbs)	Target of Neutralization
BG00011 (STX-100)	Integrin- $\alpha_v\beta_6$ receptors
VPI-2690B	Integrin- $\alpha_v\beta_3$ receptors
LY2382770	TGF- β 1 ligand
Fresolimumab (GC1008)	TGF- β 1, β 2, and β 3 ligands
Simtuzumab (AB0023)	LOXL2 (Simtuzumab indirectly suppresses the TGF- β system)

Stimulation of Bone Morphogenetic Protein signaling to treat fibrotic kidneys

Another strategy emerging to potentially treat fibrotic diseases is stimulation of Bone Morphogenetic Protein (BMP) signaling. Critical investigations have uncovered the functional capacity of BMP signaling to antagonize the pro-fibrotic activity of TGF- β in several cellular contexts [91, 92]. Intriguingly, BMPs are a subfamily of the TGF- β superfamily of growth factor cytokines and a variety of tissue types depend on BMP signaling for proper development. Animals with genetically excised components of the BMP signaling pathway display severe developmental defects or die soon after birth. For instance, neonatal kidneys with genetically excised BMP7 nearly lack glomeruli due to failed mesenchymal cell differentiation [93]. BMP7 excised embryonic kidneys also show abnormalities in the expression of key markers of nephrogenesis such as Pax2 and Wnt4 at 12.5- and 14.5-days post coitum [93]. This evidence revealed the key role of BMP7 in kidney development and more precisely its crucial role as an early inducer of glomeruli maturation [93]. BMP10, on the other hand, is essential for maintaining the proliferative capacity of cardiomyocytes [94]. Fittingly, embryonic BMP10 ablated cardiac tissues harbor excessive levels of the negative cell cycle regulator, p57^{kip2} [94]. As a result, BMP10 deletion in animals stalls cardiac tissue maturation which is embryonically lethal [94]. Deficient expression levels of key cardiogenic transcriptional factors involved in patterning, NKX2.5 and MEF2C, are also apparent in BMP10 ablated cardiac tissues [94]. Proper lung tissue development is also compromised upon deletion of SMAD-1, a key component of the BMP signaling pathway [95]. SMAD-1 conditionally ablated lung epithelial cells display differentiation and proliferation defects [95]. Furthermore, conditionally ablated SMAD-1 mice also exhibit arrested lung branching and ultimately succumb to neonatal lung failure a few hours after birth [95].

Over 30 BMP ligands have been identified in humans along with an array of type I (Alk1/2/3/6) and type II (BMP2, ACVR2A/B, AMHR2) BMP receptors (**figure 1.2**) [96]. BMP transmembrane signal transduction once initiated is carried out by critical molecular events. First, BMPs are secreted and cleaved before forming hetero or homo dimers. Next, the dimerized ligand engages with a heterotetramer of two type I BMP receptors and two type II BMP receptors (**figure 1.2**). Type II BMP receptors then phosphorylate the glycine/serine-rich domains of the type I BMP receptors (**figure 1.2**). Once the type I BMP receptor is activated, it phosphorylates SMADs-1/5/8/9 (**figure 1.2**). SMADs are key intracellular transducers of canonical BMP signaling. Activated SMADs form a complex with a common-SMAD4 (co-SMAD4) which gains the capacity to translocate to the nucleus and complex with tissue specific transcription factors that subsequently drives target gene transcription (**figure 1.2**).

The intensity and duration of BMP signaling can be fine-tuned by both intracellular and extracellular molecular mechanisms and regulators. Intracellularly, inhibitory-SMADs (I-SMADs-6/7) compete with co-SMAD4 for access to activated SMADs-1/5/8/9 which subsequently suppresses BMP signaling (**figure 1.2**). Similarly, secreted proteins such as Noggin and Chordin negatively regulate BMP signaling using an extracellular mechanism of BMP ligand binding sequestration to ultimately quell BMP signaling (**figure 1.2**) [97, 98]. In contrast, secreted Kielin/Chordin-like proteins (KCP) enhance BMP signaling via stabilization of ligand:receptor interactions (**figure 1.2**) [99].

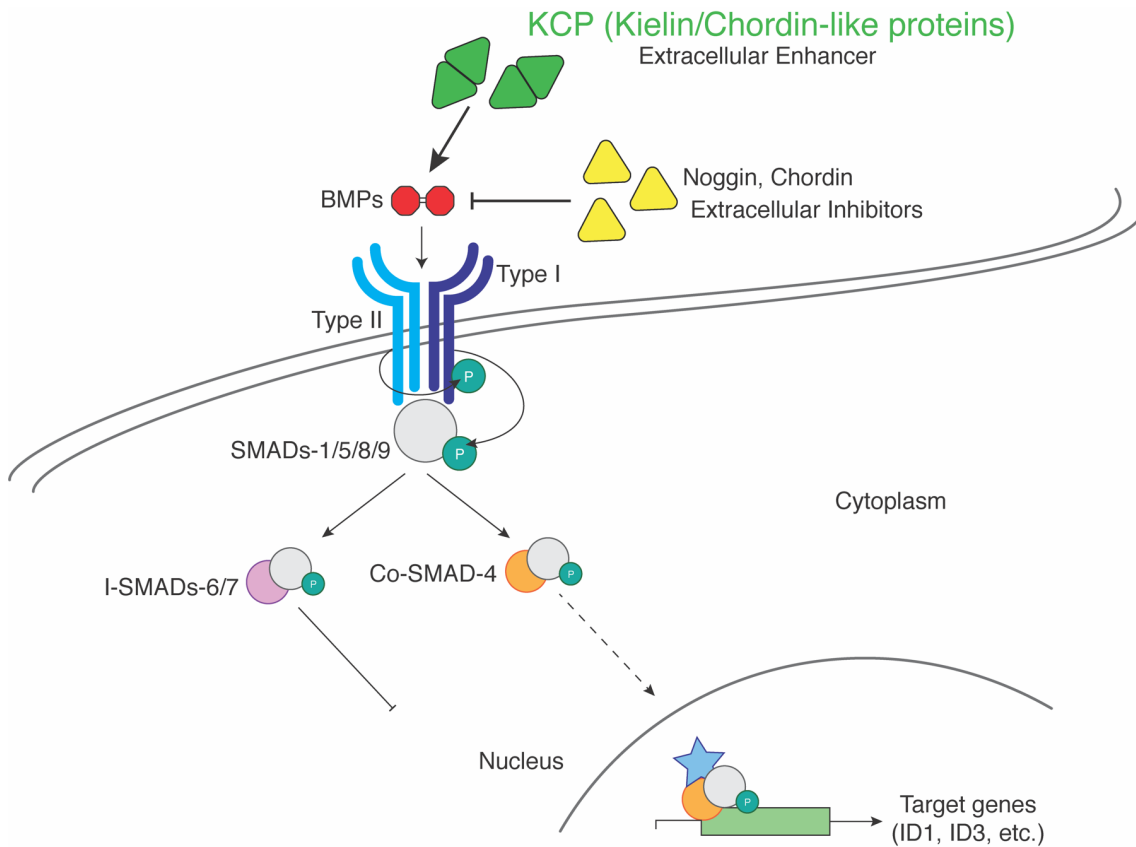


Figure 1.2 Schematic of the canonical BMP signaling pathway.

Cleaved and dimerized BMP ligands initiate the canonical BMP signaling cascade by engaging with a heterotetramer comprised of two type I BMP receptors and two type II BMP receptors. Once the heterotetramer is liganded, the type II BMP receptors phosphorylate the glycine/serine-rich domains of the type I BMP receptors. Activated, the type I BMP receptor phosphorylates SMADs-1/5/8/9, which are key intracellular transducers of canonical BMP signaling. Key aspects of the BMP signaling pathway are regulated by both extracellular and intracellular molecules. Secreted proteins like Noggin and Chordin inhibit BMP activity whereas, Kielin/Chordin-like proteins (KCP) enhance BMP activity. Intracellular proteins such as I-SMADs-6/7 compete with co-SMAD-4 for access to receptor activated SMADs-1/5/9, which suppresses BMP signaling.

Extensive studies have been undertaken to demonstrate the beneficial effects of BMP signaling activation in animal models of kidney disease [91, 100-102]. Complete understanding of the mechanisms underlying the beneficial actions of BMP signaling in the fibrotic kidney however, still remains elusive [103, 104]. Recombinant BMP2 and BMP7 are currently FDA approved for clinical use in bone disorders [96]. However, harmful doses of BMPs are needed to achieve efficacy and recombinant BMPs are both complex and expensive to synthesize with a single therapeutic dose costing \$5,000 [105-107].

KCP proteins, as highlighted above, promote enhanced BMP signaling and exhibit beneficial effects in fibrotic kidney tissues. Contralateral and UUO kidneys harvested at 1, 2, or 4 weeks from transgenic KCP expressing mice, exhibit strong levels of p-SMAD-1 expression as detected by immunoblotting [99]. Conversely, contralateral and obstructed kidneys harvested at the timepoints stated above from KCP deficient animals exhibit suppressed BMP signaling as assessed by a marked reduction in p-SMAD-1 expression [99]. In these same studies, α -SMA assessed interstitial fibrosis and collagen deposition were far more pronounced in KCP deficient animals compared to wild-type UUO kidneys [99]. Pathological expansion of activated fibroblasts was also 2-fold higher in UUO kidneys from KCP deficient mice at 7 and 13 days after obstruction compared to wild-type UUO kidneys harvested at comparable stages [99]. Inversely, studies in transgenic animals overexpressing KCP revealed a less severe response to acute and chronic kidney injury compared to wild-type animals [108]. Notably, overexpressed KCP has similar protective effects in animal models of non-alcoholic fatty liver disease and diet-induced obesity [109, 110]. KCP proteins contain 1,254 amino-acids and 18-cysteine rich domains. Thus, large scale synthesis of KCP for clinical anti-fibrotic use is precluded by its size and complexity [99]. Small-molecules, however, that are easier to synthesize and more cost-effective to produce may

provide an alternative strategy to exogenously enhance BMP signaling relative to large scale production of BMP and KCP recombinant proteins.

To employ the beneficial effects of BMP activity in several disease contexts, identifying novel small-molecules that stimulate BMP signaling is of interest. Bone disease investigators have identified small-molecules that have the capacity to enhance BMP signaling and induce osteoblast activity and differentiation [111-114]. Likewise, for potential application towards medulloblastoma treatment, researchers have also identified several molecules that activate BMP signaling as assessed by: increased levels of p-SMAD-1/5/8 signaling, ventralized zebrafish embryos, activation of direct BMP4 gene targets, and osteoblast differentiation from myoblasts [115, 116]. Even more, application of FK506 for the treatment of pulmonary hypertension has been explored and found to enhance BMP signaling as assessed by activated SMAD-1/5 and ID1, as well as, MAPK (non-canonical BMP signaling) [117]. Chemical sensitizers of BMP signaling to achieve directed stem cell differentiation have also been described. Reports show these BMP sensitizers are able to induce human embryonic stem cells towards mesoderm or cytotrophoblast lineages, as well as, osteoblast lineages [118, 119].

Identification of a small-molecule that induce heterotetramerization and activation of type I and type II BMP receptors exactly as BMP ligands has not been reported. Although the immunosuppressants, Sirolimus (Rapamycin) and Tacrolimus (FK506), have been identified as agents with the capacity to activate type I BMP receptors by liberating the glycine/serine-rich domains of type I BMP receptors from FKBP12 inhibition [117, 119]. Importantly, potent and selective small-molecule inhibitors of BMP signaling have also been identified and include: dorsomorphin [120], dorsomorphin homolog 1 (DMH1) [121], and LDN-193189 [122]. These

inhibitors block the kinase domain of type I BMP receptors and prevent ATP-pocket binding which results in suppressed BMP signaling.

Reactivation of the nephrogenic regulator, Pax2, in kidney cancer

Kidney cancer is another major contributor to ESRD. In the United States, an estimated 73,820 new kidney cancer patients will need treatment and 14,770 patients will succumb to kidney cancer in 2019 [123]. Worldwide, 403,262 new kidney cancer cases along with 175,098 patient deaths were documented in 2018 [124]. Between 1975-2012 mortality rates for kidney and renal pelvis cancer remained steady [125]. Incidence rates from 1975-2008, on the other hand, *initially* spiked but, have plateaued over the last decade [125-127]. Key risk factors for kidney and renal pelvis cancer include obesity, hypertension or its treatment, chronic use of NSAIDs, smoking, and environmental/work related factors [125, 128]. The 5-year relative survival rate for localized kidney and renal pelvis cancer is 73% [125]. Unfortunately, however, the 5-year relative survival rate for metastasized kidney and renal pelvis cancer is at a dismally low 11.6% [125].

Clear-cell Renal Cell Carcinomas (ccRCC) are the most common type of adult kidney cancer and 90% of kidney cancer patients are diagnosed with this subtype [129]. ccRCC develops in the nephrons of the kidneys, which are the key filtration units that ensure proper cleansing of systemic blood. The nephrons consist of a glomerulus and its associated proximal and distal tubules. ccRCC develops in the proximal tubule epithelial cells the most abundant cell type in the kidney. The majority of ccRCC have von-Hippel-Lindau (VHL) gene inactivating mutations, which can be inherited or sporadic [7, 130, 131]. VHL is part of a complex that harbors E3 ubiquitin ligase functional activity. Normoxia promotes tight VHL regulation of hypoxia-inducible factor-1 α (HIF-1 α) which is upregulated in response to hypoxic or ischemic conditions [132]. Mutated VHL, therefore, lacks the functional capacity to ubiquitinate HIF-1 α which prevents targeting of HIF-1 α to the proteasome for degradation. Deregulated and stabilized HIF-1 α is therefore able to translocate into the nucleus and dimerize with constitutively active HIF-1 β . The

aberrantly functional HIF-1 α β transcriptional complex consequently activates an abundance of HIF-1 α β target genes, which become pro-oncogenic under the deregulated HIF-1 α signaling cascade. Important mediators driving malignant behavior include HIF-1 α gene targets vascular endothelial growth factor (VEGF) and mechanistic target of rapamycin (mTOR).

The paired-homeobox 2 (Pax2) protein is reported to be negatively regulated by VHL and a significant correlation between Pax2 and HIF-1 α in ccRCC has been demonstrated in patient tumors [133]. Immunohistochemical analysis revealed that of 294 Pax2-positive patient tumors, 222 also expressed HIF-1 α [133]. Nearly all ccRCC possess reactivated Pax2 that is required to sustain proliferative and malignant tumor behavior [134]. Expression of Pax2 is also observed in Wilms' tumor and often in ovarian cancer [135]. Pax2 is a critical transcription factor upregulated during and required for normal kidney development and the female reproductive tract [136]. As such, homozygous Pax2 deficient animals lack kidneys while animals with overactive Pax2 acquire dysfunctional renal epithelial tissues [136, 137].

Upregulated Pax2 during development is required for the crucial step needed to convert mesenchymal cells into epithelial cells in emerging nephrons. However, Pax2 repression is needed as emerging nephrons are maturing to achieve fully differentiated and functional renal epithelium [137, 138]. Therefore, once nephrogenesis is fulfilled, mature nephrons terminate Pax2 expression in each of its epithelial lined compartments (i.e. glomerulus and its associated proximal and distal tubules) [133, 139]. Pax2 reactivation has been observed in both kidney injury and ccRCC [134, 140]. Downregulation of Pax2 expression by antisense oligonucleotides, however, arrested growth and proliferation of kidney tumor cells [134].

Current treatment strategies for ccRCC include total or partial nephrectomy. However, roughly 30% of these patients will still develop metastatic spread of cancerous cells [129]. At the

time of nephrectomy, patients with low-, intermediate-, and high-risk metastatic renal cell carcinoma have 5-year survival rates of 41%, 18%, and 8% respectively [141]. Moreover, partial nephrectomy treatment can lead to ESRD which requires dialysis or kidney transplantation. A significant panel of first- and second-line targeted therapeutics exist to treat metastatic ccRCC, such as VEGF mTOR inhibitors [127]. However, resistance continues to be an obstacle in achieving effective long-term therapy and increasing survival rates [142]. Therefore, the development of novel therapeutics and treatment strategies are warranted.

As stated previously, Pax2 is a transcription factor that is ectopically expressed in ccRCC and Pax2 can be identified in metastasized tumors [143]. Thus, small-molecule inhibitors of Pax2 transcription activity could provide novel treatments for ccRCC patients. Nuclear transcription factors such as Pax2 lack a ligand binding pocket which deemed Pax2 an *undruggable* target. However, using *in silico* methods to identify small-molecules with the capacity to inhibit Pax2 DNA binding activity and follow-up analog assays, an encouraging study identified a small-molecule, EG1, that inhibits Pax2 activity [144]. This study demonstrated an up to 75% reduction of Pax2 mediated branching morphogenesis in cultured kidney rudiments harvested at e11.5 and treated for 2 days with 50 μ M EG1. Incomplete aggregation of Pax2⁺ cells at ureter tip buds was also observed in EG1 treated cultured kidney rudiments [144]. A Pax2⁺ renal cell carcinoma cell line (RCC111) also displayed decreased cell proliferation and viability after treatment with EG1 [144]. Furthermore, a 3-hit mouse model to study renal cell carcinoma was also recently developed and these animals and their cells can be used to test small-molecules like EG1 that inhibit Pax2 transactivation [131].

Pax2 transactivation in cystic kidney epithelial cells

Dysregulated Pax2 activity is also documented in Polycystic Kidney Disease (PKD) [145]. In PKD, epithelial cells lining the renal tubules become cystic and progressively dilate which leads to enlarged kidneys or nephromegaly, and eventual ESRD [146]. PKD is the fourth leading known primary causes of ESRD in the United States and can be inherited in either an autosomal dominant or autosomal recessive manner [147, 148]. PKD development via de novo mutations is also reported at considerable rates [147]. Mutated genes that cause autosomal dominant PKD include polycystins (PC1 or PC2) whereas mutations in polycystin kidney and hepatic disease I (PKHD1) cause autosomal recessive PKD [147]. Autosomal dominant PKD is the most common monogenic disorder among adults, approximately 1/400-1/1000 cases are reported each year while, 1/10,000-40,000 cases are reported for the much rarer autosomal recessive form of PKD [147, 149].

In both mice and humans, cystic epithelial cells of the renal tubules harbor ectopic Pax2 expression [137, 145, 150]. In cystic animal kidneys that possess only one Pax2 allele, arrested cystogenesis is observed and animals survive for 4-6 weeks after birth [151]. Notably, increased apoptotic events are observed in kidneys with reduced Pax2 expression during normal kidney development in both mice and humans [151]. In contrast, kidneys in diseased animals harboring two Pax2 alleles have large cysts and animals die within 3 weeks of birth [151].

No curative therapies for PKD exist, however, the current standard of care is management of hypertension with ACEi or ARBs as a first line therapy [147]. Therefore, novel-small molecules with the functional capacity to inhibit Pax2 activity specifically in renal tubular epithelial cells could potentially slow disease progression. Preclinical testing of small-molecule inhibitors of Pax2 in animal models of PKD including human xenograft animal models of PKD will aid in the identification of novel therapeutics for PKD.

Chapter 1 Summary and Conclusion

Chronic Kidney Disease constitutes a serious global health burden where reported cases are steadily rising and encompass fibrosis, cancer, and cystic disease of the kidney. Kidney fibrosis manifests as loss of epithelial tissues and vascular supply. Whereas, kidney cancer results in increased proliferation of epithelial tissues and increased vascular supply. Cystic kidney disease also presents with an increased proliferation of cystic epithelial cells. Given the array of factors that can cause CKD and lead to ESRD, limited therapeutic options exist although multiple novel agents are being explored. Overall, developing effective and targeted therapeutics that will aid in the repair and regeneration of damaged and diseased tissues will help reduce the global health burden of CKD.

Embryological tissues designated as the intermediate mesoderm generate the ureteric bud and mesenchyme tissues that ultimately form adult kidneys. Key in the development of adult kidneys is the critical process of mesenchymal cell differentiation into epithelial cells from which nephrons arise. Dysregulation of developmental molecules that coordinate the induction of mesenchymal-to-epithelial transition are implicated in pathological processes that drive kidney disease. As highlighted in this chapter, bone morphogenetic proteins have essential roles in normal kidney development. Animals deficient in BMP7 essentially fail to generate glomeruli due to unsuccessful mesenchymal cell differentiation and abnormal expression patterns of key markers of nephrogenesis such as Pax2 and Wnt4 are apparent [93].

Activation of BMP signaling has been reported to be protective in animal models of fibrosis or chronic kidney disease by promoting repair and regeneration of damaged kidney tissues. In contrast, TGF- β drives fibrogenesis and the TGF- β signaling system can be targeted for inhibition at multiple levels (i.e. mature ligands, receptors, etc.). Hence, combinatorial molecular tools that

aim to suppress TGF- β signaling while simultaneously activating BMP signaling may provide new therapeutic strategies to treat chronic kidney disease.

As with BMPs, Pax transcription factors have an absolutely essential role in kidney development. Homozygous Pax2 deficient animals lack kidneys as Pax2 is required for renal mesenchymal-to-epithelial transition [136]. Mature kidney epithelial tissues silence Pax2 gene activity. However, in mice and humans, ectopically expressed Pax2 expression is observed and correlates with kidney cancer and cystogenesis progression. Reduction of Pax2 activity in animal models slows the progression of renal cell carcinoma and cystic kidney disease.

This dissertation describes experimental efforts toward identifying novel small-molecules that stimulate Bone Morphogenic Protein signaling, As well as, efforts that attempt to identify small-molecules that inhibit the transcriptional activity of Pax2. The purpose of these efforts are to ultimately test the potential efficacy of these small-molecules in animal models of various subtypes of chronic kidney disease, which include fibrosis and proliferative disorders such as cancer and cystic kidney disease.

Bibliography

1. Hill, N.R., et al., *Global Prevalence of Chronic Kidney Disease - A Systematic Review and Meta-Analysis*. PLoS One, 2016. **11**(7): p. e0158765.
2. *United States Renal Data System: Incidence, Prevalence, Patient Characteristics, and Treatment Modalities In: 2018 USRDS Annual Data Report: Epidemiology of Kidney Disease in the United States*. 2018; Available from: <https://www.usrds.org>.
3. Genovese, G., et al., *Association of trypanolytic ApoL1 variants with kidney disease in African Americans*. Science, 2010. **329**(5993): p. 841-5.
4. Buscher, P., et al., *Human African trypanosomiasis*. Lancet, 2017. **390**(10110): p. 2397-2409.
5. Breyer, M.D. and K. Susztak, *The next generation of therapeutics for chronic kidney disease*. Nat Rev Drug Discov, 2016. **15**(8): p. 568-88.
6. Parsa, A., et al., *APOLI risk variants, race, and progression of chronic kidney disease*. N Engl J Med, 2013. **369**(23): p. 2183-96.
7. Perazella, M.A., R. Dreicer, and M.H. Rosner, *Renal cell carcinoma for the nephrologist*. Kidney Int, 2018. **94**(3): p. 471-483.
8. Hartmann, A., T. Jenssen, and H. Holdaas, *Diabetes, chronic kidney disease and cancer risk*. Nephrol Dial Transplant, 2012. **27**(8): p. 3018-20.
9. *United States Renal Data System: Healthcare Expenditures for Persons with ESRD In: 2018 USRDS Annual Data Report: Epidemiology of Kidney Disease in the United States*. 2018; Available from: <https://www.usrds.org/>.
10. *United States Renal Data System: Mortality, Expected Remaining Lifetime: Comparison of ESRD Patients to the General U.S. Population: In: 2018 USRDS Annual Data Report: Epidemiology of Kidney Disease in the United States*. 2018; Available from: <https://www.usrds.org/>.
11. *Organ Procurement and Transplantation Network: Organ by Waiting Time*. 2019; Available from: <https://optn.transplant.hrsa.gov/data/view-data-reports/national-data/>.

12. Border, W.A. and N.A. Noble, *Transforming growth factor beta in tissue fibrosis*. N Engl J Med, 1994. **331**(19): p. 1286-92.
13. Hewitson, T.D., *Fibrosis in the kidney: is a problem shared a problem halved?* Fibrogenesis Tissue Repair, 2012. **5**(Suppl 1): p. S14.
14. Nanthakumar, C.B., et al., *Dissecting fibrosis: therapeutic insights from the small-molecule toolbox*. Nat Rev Drug Discov, 2015. **14**(10): p. 693-720.
15. Frantz, C., K.M. Stewart, and V.M. Weaver, *The extracellular matrix at a glance*. J Cell Sci, 2010. **123**(Pt 24): p. 4195-200.
16. Zeisberg, M. and R. Kalluri, *Physiology of the Renal Interstitium*. Clin J Am Soc Nephrol, 2015. **10**(10): p. 1831-40.
17. Lemley, K.V. and W. Kriz, *Anatomy of the renal interstitium*. Kidney Int, 1991. **39**(3): p. 370-81.
18. Border, W.A. and E. Ruoslahti, *Transforming growth factor-beta 1 induces extracellular matrix formation in glomerulonephritis*. Cell Differ Dev, 1990. **32**(3): p. 425-31.
19. Border, W.A., et al., *Suppression of experimental glomerulonephritis by antiserum against transforming growth factor beta 1*. Nature, 1990. **346**(6282): p. 371-4.
20. Zeisberg, M., F. Strutz, and G.A. Muller, *Role of fibroblast activation in inducing interstitial fibrosis*. J Nephrol, 2000. **13** Suppl 3: p. S111-20.
21. Groma, V., *Demonstration of collagen type VI and alpha-smooth muscle actin in renal fibrotic injury in man*. Nephrol Dial Transplant, 1998. **13**(2): p. 305-12.
22. Hewitson, T.D., S.G. Holt, and E.R. Smith, *Progression of Tubulointerstitial Fibrosis and the Chronic Kidney Disease Phenotype - Role of Risk Factors and Epigenetics*. Front Pharmacol, 2017. **8**: p. 520.
23. *Chapter 1: Incidence, Prevalence, Patient Characteristics, and Treatment Modalities*. American Journal of Kidney Diseases, 2018. **71**(3, Supplement 1): p. S247-S276.

24. Wong, M.G., et al., *Long-term Benefits of Intensive Glucose Control for Preventing End-Stage Kidney Disease: ADVANCE-ON*. Diabetes Care, 2016. **39**(5): p. 694-700.
25. MacIsaac, R.J., G. Jerums, and E.I. Ekinci, *Glycemic Control as Primary Prevention for Diabetic Kidney Disease*. Advances in Chronic Kidney Disease, 2018. **25**(2): p. 141-148.
26. *K/DOQI clinical practice guidelines on hypertension and antihypertensive agents in chronic kidney disease*. Am J Kidney Dis, 2004. **43**(5 Suppl 1): p. S65-73.
27. Weir, M.R. and V.J. Dzau, *The renin-angiotensin-aldosterone system: a specific target for hypertension management*. Am J Hypertens, 1999. **12**(12 Pt 3): p. 205S-213S.
28. Chao, E.C. and R.R. Henry, *SGLT2 inhibition--a novel strategy for diabetes treatment*. Nat Rev Drug Discov, 2010. **9**(7): p. 551-9.
29. Annes, J.P., J.S. Munger, and D.B. Rifkin, *Making sense of latent TGFbeta activation*. J Cell Sci, 2003. **116**(Pt 2): p. 217-24.
30. Sureshababu, A., S.A. Muhsin, and M.E. Choi, *TGF-beta signaling in the kidney: profibrotic and protective effects*. Am J Physiol Renal Physiol, 2016. **310**(7): p. F596-F606.
31. Shull, M.M., et al., *Targeted disruption of the mouse transforming growth factor-beta 1 gene results in multifocal inflammatory disease*. Nature, 1992. **359**(6397): p. 693-9.
32. Kulkarni, A.B., et al., *Transforming growth factor beta 1 null mutation in mice causes excessive inflammatory response and early death*. Proc Natl Acad Sci U S A, 1993. **90**(2): p. 770-4.
33. Munger, J.S., et al., *The integrin alpha v beta 6 binds and activates latent TGF beta 1: a mechanism for regulating pulmonary inflammation and fibrosis*. Cell, 1999. **96**(3): p. 319-28.
34. Pohlers, D., et al., *TGF-beta and fibrosis in different organs - molecular pathway imprints*. Biochim Biophys Acta, 2009. **1792**(8): p. 746-56.
35. Ziyadeh, F.N., M. Isono, and S. Chen, *Involvement of the transforming growth factor-beta system in the pathogenesis of diabetic nephropathy*. Clin Exp Nephrol, 2002. **6**(3): p. 125-9.

36. Tatler, A.L. and G. Jenkins, *TGF-beta activation and lung fibrosis*. Proc Am Thorac Soc, 2012. **9**(3): p. 130-6.
37. Bujak, M. and N.G. Frangogiannis, *The role of TGF-beta signaling in myocardial infarction and cardiac remodeling*. Cardiovasc Res, 2007. **74**(2): p. 184-95.
38. Dooley, S. and P. ten Dijke, *TGF-beta in progression of liver disease*. Cell Tissue Res, 2012. **347**(1): p. 245-56.
39. Vallance, B.A., et al., *TGF-beta1 gene transfer to the mouse colon leads to intestinal fibrosis*. Am J Physiol Gastrointest Liver Physiol, 2005. **289**(1): p. G116-28.
40. Agarwal, A., et al., *Bone marrow fibrosis in primary myelofibrosis: pathogenic mechanisms and the role of TGF-beta*. Stem Cell Investig, 2016. **3**: p. 5.
41. Tampe, D. and M. Zeisberg, *Potential approaches to reverse or repair renal fibrosis*. Nat Rev Nephrol, 2014. **10**(4): p. 226-37.
42. Iyer, S.N., G. Gurujeyalakshmi, and S.N. Giri, *Effects of pirfenidone on transforming growth factor-beta gene expression at the transcriptional level in bleomycin hamster model of lung fibrosis*. J Pharmacol Exp Ther, 1999. **291**(1): p. 367-73.
43. Sharma, K., et al., *Pirfenidone for diabetic nephropathy*. J Am Soc Nephrol, 2011. **22**(6): p. 1144-51.
44. Shihab, F.S., et al., *Pirfenidone treatment decreases transforming growth factor-beta1 and matrix proteins and ameliorates fibrosis in chronic cyclosporine nephrotoxicity*. Am J Transplant, 2002. **2**(2): p. 111-9.
45. *A Phase II Clinical Trial of Hydronidone Capsules(F351) in Patients With Liver Fibrosis Induced by HBV Chronic Hepatitis*. 2015; Available from: <https://ClinicalTrials.gov/show/NCT02499562>.
46. Lo, D.J., et al., *Inhibition of alphavbeta6 promotes acute renal allograft rejection in nonhuman primates*. Am J Transplant, 2013. **13**(12): p. 3085-93.
47. *STX-100 in Patients With Idiopathic Pulmonary Fibrosis (IPF)*. 2012; Available from: <https://ClinicalTrials.gov/show/NCT01371305>.

48. *An Efficacy and Safety Study of BG00011 in Participants With Idiopathic Pulmonary Fibrosis (SPIRIT)*. 2018; Available from: <https://ClinicalTrials.gov/show/NCT03573505>.
49. *Phase 2 Study to Evaluate Safety & Efficacy of VPI-2690B in Diabetic Nephropathy Patients*. 2014; Available from: <https://ClinicalTrials.gov/show/NCT02251067>.
50. Voelker, J., et al., *Anti-TGF-beta1 Antibody Therapy in Patients with Diabetic Nephropathy*. *J Am Soc Nephrol*, 2017. **28**(3): p. 953-962.
51. Kim, J.H., et al., *Activation of the TGF-beta/Smad signaling pathway in focal segmental glomerulosclerosis*. *Kidney Int*, 2003. **64**(5): p. 1715-21.
52. Trachtman, H., et al., *A phase I, single-dose study of fresolimumab, an anti-TGF-beta antibody, in treatment-resistant primary focal segmental glomerulosclerosis*. *Kidney Int*, 2011. **79**(11): p. 1236-43.
53. Vincenti, F., et al., *A Phase 2, Double-Blind, Placebo-Controlled, Randomized Study of Fresolimumab in Patients With Steroid-Resistant Primary Focal Segmental Glomerulosclerosis*. *Kidney Int Rep*, 2017. **2**(5): p. 800-810.
54. Petersen, M., et al., *Oral administration of GW788388, an inhibitor of TGF-beta type I and II receptor kinases, decreases renal fibrosis*. *Kidney Int*, 2008. **73**(6): p. 705-15.
55. Moon, J.A., et al., *IN-1130, a novel transforming growth factor-beta type I receptor kinase (ALK5) inhibitor, suppresses renal fibrosis in obstructive nephropathy*. *Kidney Int*, 2006. **70**(7): p. 1234-43.
56. Grygielko, E.T., et al., *Inhibition of gene markers of fibrosis with a novel inhibitor of transforming growth factor-beta type I receptor kinase in puromycin-induced nephritis*. *J Pharmacol Exp Ther*, 2005. **313**(3): p. 943-51.
57. Sato, M., et al., *Targeted disruption of TGF-beta1/Smad3 signaling protects against renal tubulointerstitial fibrosis induced by unilateral ureteral obstruction*. *J Clin Invest*, 2003. **112**(10): p. 1486-94.
58. Fujimoto, M., et al., *Mice lacking Smad3 are protected against streptozotocin-induced diabetic glomerulopathy*. *Biochem Biophys Res Commun*, 2003. **305**(4): p. 1002-7.

59. Zhang, Y., et al., *The preventive and therapeutic implication for renal fibrosis by targetting TGF-beta/Smad3 signaling*. Clin Sci (Lond), 2018. **132**(13): p. 1403-1415.
60. Li, J., et al., *Blockade of endothelial-mesenchymal transition by a Smad3 inhibitor delays the early development of streptozotocin-induced diabetic nephropathy*. Diabetes, 2010. **59**(10): p. 2612-24.
61. Lin, S.L., et al., *Pentoxifylline attenuates tubulointerstitial fibrosis by blocking Smad3/4-activated transcription and profibrogenic effects of connective tissue growth factor*. J Am Soc Nephrol, 2005. **16**(9): p. 2702-13.
62. Lin, S.L., et al., *Pentoxifylline attenuated the renal disease progression in rats with remnant kidney*. J Am Soc Nephrol, 2002. **13**(12): p. 2916-29.
63. Gorson, D.M., *Reduction of macroalbuminuria with pentoxifylline in diabetic nephropathy. Report of three cases*. Diabetes Care, 1998. **21**(12): p. 2190-1.
64. Navarro, J.F. and C. Mora, *Antiproteinuric effect of pentoxifylline in patients with diabetic nephropathy*. Diabetes Care, 1999. **22**(6): p. 1006-8.
65. Navarro, J.F., et al., *Effects of pentoxifylline administration on urinary N-acetyl-beta-glucosaminidase excretion in type 2 diabetic patients: a short-term, prospective, randomized study*. Am J Kidney Dis, 2003. **42**(2): p. 264-70.
66. Rodriguez-Moran, M., et al., *Effects of pentoxifylline on the urinary protein excretion profile of type 2 diabetic patients with microproteinuria: a double-blind, placebo-controlled randomized trial*. Clin Nephrol, 2006. **66**(1): p. 3-10.
67. *Renoprotection by Pentoxifylline and Angiotensin Receptor Blocker in Chronic Kidney Disease (CKD)*. 2011; Available from: <https://ClinicalTrials.gov/show/NCT01377285>.
68. Zhang, Y.E., *Non-Smad Signaling Pathways of the TGF-beta Family*. Cold Spring Harb Perspect Biol, 2017. **9**(2).
69. Darakhshan, S. and A.B. Pour, *Tranilast: a review of its therapeutic applications*. Pharmacol Res, 2015. **91**: p. 15-28.

70. Zammit, S.C., et al., *Evaluation and optimization of antifibrotic activity of cinnamoyl anthranilates*. *Bioorg Med Chem Lett*, 2009. **19**(24): p. 7003-6.
71. Holmes, D.R., Jr., et al., *Results of Prevention of REStenosis with Tranilast and its Outcomes (PRESTO) trial*. *Circulation*, 2002. **106**(10): p. 1243-50.
72. Zhang, Y., et al., *FT011, a new anti-fibrotic drug, attenuates fibrosis and chronic heart failure in experimental diabetic cardiomyopathy*. *Eur J Heart Fail*, 2012. **14**(5): p. 549-62.
73. Russo, I. and N.G. Frangogiannis, *Diabetes-associated cardiac fibrosis: Cellular effectors, molecular mechanisms and therapeutic opportunities*. *J Mol Cell Cardiol*, 2016. **90**: p. 84-93.
74. Gilbert, R.E., et al., *A purpose-synthesised anti-fibrotic agent attenuates experimental kidney diseases in the rat*. *PLoS One*, 2012. **7**(10): p. e47160.
75. Floege, J. and R.J. Johnson, *Multiple roles for platelet-derived growth factor in renal disease*. *Miner Electrolyte Metab*, 1995. **21**(4-5): p. 271-82.
76. Floege, J., F. Eitner, and C.E. Alpers, *A new look at platelet-derived growth factor in renal disease*. *J Am Soc Nephrol*, 2008. **19**(1): p. 12-23.
77. Lau, X., et al., *Attenuation of Armani-Ebstein lesions in a rat model of diabetes by a new anti-fibrotic, anti-inflammatory agent, FT011*. *Diabetologia*, 2013. **56**(3): p. 675-9.
78. *Safety, tolerability, food effect and pharmacokinetics of FT011 in healthy volunteers and patients with Type 2 diabetes-associated diabetic nephropathy*. 2013; Available from: <https://www.anzctr.org.au/Trial/Registration/TrialReview.aspx?ACTRN=12613000386730>.
79. *Shire Plc quarterly report pursuant to section 13 or 15(d) of the securities exchange act of 1934 for the quarterly period ended September 30, 2015*.; Available from: https://www.sec.gov/Archives/edgar/data/936402/000095010315008508/dp60717_10q.htm.
80. Barry-Hamilton, V., et al., *Allosteric inhibition of lysyl oxidase-like-2 impedes the development of a pathologic microenvironment*. *Nat Med*, 2010. **16**(9): p. 1009-17.

81. Raghu, G., et al., *Efficacy of simtuzumab versus placebo in patients with idiopathic pulmonary fibrosis: a randomised, double-blind, controlled, phase 2 trial*. *Lancet Respir Med*, 2017. **5**(1): p. 22-32.
82. *Study to Assess the Efficacy and Safety of Simtuzumab (GS-6624) in Adults With Idiopathic Pulmonary Fibrosis (IPF)*. Available from: <https://ClinicalTrials.gov/show/NCT01769196>.
83. Zhang, Y.M., et al., *Targeted deletion of ROCK1 protects the heart against pressure overload by inhibiting reactive fibrosis*. *FASEB J*, 2006. **20**(7): p. 916-25.
84. Nagatoya, K., et al., *Y-27632 prevents tubulointerstitial fibrosis in mouse kidneys with unilateral ureteral obstruction*. *Kidney Int*, 2002. **61**(5): p. 1684-95.
85. Liu, S., et al., *FAK is required for TGFbeta-induced JNK phosphorylation in fibroblasts: implications for acquisition of a matrix-remodeling phenotype*. *Mol Biol Cell*, 2007. **18**(6): p. 2169-78.
86. Kinoshita, K., et al., *Antifibrotic effects of focal adhesion kinase inhibitor in bleomycin-induced pulmonary fibrosis in mice*. *Am J Respir Cell Mol Biol*, 2013. **49**(4): p. 536-43.
87. Lagares, D., et al., *Inhibition of focal adhesion kinase prevents experimental lung fibrosis and myofibroblast formation*. *Arthritis Rheum*, 2012. **64**(5): p. 1653-64.
88. Richeldi, L., et al., *Efficacy and safety of nintedanib in idiopathic pulmonary fibrosis*. *N Engl J Med*, 2014. **370**(22): p. 2071-82.
89. Rodriguez-Portal, J.A., *Efficacy and Safety of Nintedanib for the Treatment of Idiopathic Pulmonary Fibrosis: An Update*. *Drugs R D*, 2018. **18**(1): p. 19-25.
90. King, T.E., Jr., et al., *A phase 3 trial of pirfenidone in patients with idiopathic pulmonary fibrosis*. *N Engl J Med*, 2014. **370**(22): p. 2083-92.
91. Zeisberg, M., et al., *BMP-7 counteracts TGF-beta1-induced epithelial-to-mesenchymal transition and reverses chronic renal injury*. *Nat Med*, 2003. **9**(7): p. 964-8.
92. Wang, S. and R. Hirschberg, *BMP7 antagonizes TGF-beta -dependent fibrogenesis in mesangial cells*. *Am J Physiol Renal Physiol*, 2003. **284**(5): p. F1006-13.

93. Luo, G., et al., *BMP-7 is an inducer of nephrogenesis, and is also required for eye development and skeletal patterning*. *Genes Dev*, 1995. **9**(22): p. 2808-20.
94. Chen, H., et al., *BMP10 is essential for maintaining cardiac growth during murine cardiogenesis*. *Development*, 2004. **131**(9): p. 2219-31.
95. Xu, B., et al., *Smad1 and its target gene Wif1 coordinate BMP and Wnt signaling activities to regulate fetal lung development*. *Development*, 2011. **138**(5): p. 925-35.
96. Salazar, V.S., L.W. Gamer, and V. Rosen, *BMP signalling in skeletal development, disease and repair*. *Nat Rev Endocrinol*, 2016. **12**(4): p. 203-21.
97. Zimmerman, L.B., J.M. DeJesusEscobar, and R.M. Harland, *The Spemann organizer signal noggin binds and inactivates bone morphogenetic protein 4*. *Cell*, 1996. **86**(4): p. 599-606.
98. Piccolo, S., et al., *Dorsoventral patterning in Xenopus: inhibition of ventral signals by direct binding of chordin to BMP-4*. *Cell*, 1996. **86**(4): p. 589-98.
99. Lin, J., et al., *Kielin/chordin-like protein, a novel enhancer of BMP signaling, attenuates renal fibrotic disease*. *Nat Med*, 2005. **11**(4): p. 387-93.
100. Morrissey, J., et al., *Bone morphogenetic protein-7 improves renal fibrosis and accelerates the return of renal function*. *J Am Soc Nephrol*, 2002. **13 Suppl 1**: p. S14-21.
101. Wang, S., et al., *Bone morphogenic protein-7 (BMP-7), a novel therapy for diabetic nephropathy*. *Kidney Int*, 2003. **63**(6): p. 2037-49.
102. Zeisberg, M., et al., *Bone morphogenic protein-7 inhibits progression of chronic renal fibrosis associated with two genetic mouse models*. *Am J Physiol Renal Physiol*, 2003. **285**(6): p. F1060-7.
103. Nakamura, J. and M. Yanagita, *Bmp modulators in kidney disease*. *Discov Med*, 2012. **13**(68): p. 57-63.
104. Zeisberg, M., *Bone morphogenic protein-7 and the kidney: current concepts and open questions*. *Nephrol Dial Transplant*, 2006. **21**(3): p. 568-73.

105. Nauth, A., et al., *Bone morphogenetic proteins in open fractures: past, present, and future*. Injury, 2009. **40 Suppl 3**: p. S27-31.
106. A, A.I.H. and B.D. P, *Bone morphogenetic proteins and their antagonists: current and emerging clinical uses*. British Journal of Pharmacology, 2014. **171**(15): p. 3620-3632.
107. Carragee, E.J., E.L. Hurwitz, and B.K. Weiner, *A critical review of recombinant human bone morphogenetic protein-2 trials in spinal surgery: emerging safety concerns and lessons learned*. Spine J, 2011. **11**(6): p. 471-91.
108. Soofi, A., P. Zhang, and G.R. Dressler, *Kielin/chordin-like protein attenuates both acute and chronic renal injury*. J Am Soc Nephrol, 2013. **24**(6): p. 897-905.
109. Soofi, A., et al., *The kielin/chordin-like protein KCP attenuates nonalcoholic fatty liver disease in mice*. Am J Physiol Gastrointest Liver Physiol, 2016. **311**(4): p. G587-G598.
110. Soofi, A., et al., *The kielin/chordin-like protein (KCP) attenuates high-fat diet-induced obesity and metabolic syndrome in mice*. J Biol Chem, 2017. **292**(22): p. 9051-9062.
111. Okada, M., et al., *Development and optimization of a cell-based assay for the selection of synthetic compounds that potentiate bone morphogenetic protein-2 activity*. Cell Biochem Funct, 2009. **27**(8): p. 526-34.
112. Kato, S., et al., *A synthetic compound that potentiates bone morphogenetic protein-2-induced transdifferentiation of myoblasts into the osteoblastic phenotype*. Mol Cell Biochem, 2011. **349**(1-2): p. 97-106.
113. Baek, S.H., et al., *Quinoline compound KMI1073 enhances BMP-2-dependent osteogenic differentiation of C2C12 cells via activation of p38 signaling and exhibits in vivo bone forming activity*. PLoS One, 2015. **10**(3): p. e0120150.
114. Cao, Y., et al., *Selective small molecule compounds increase BMP-2 responsiveness by inhibiting Smurf1-mediated Smad1/5 degradation*. Sci Rep, 2014. **4**: p. 4965.
115. Vrijens, K., et al., *Identification of small molecule activators of BMP signaling*. PLoS One, 2013. **8**(3): p. e59045.

116. Genthe, J.R., et al., *Ventromorphins: A New Class of Small Molecule Activators of the Canonical BMP Signaling Pathway*. ACS Chem Biol, 2017. **12**(9): p. 2436-2447.
117. Spiekerkoetter, E., et al., *FK506 activates BMPR2, rescues endothelial dysfunction, and reverses pulmonary hypertension*. J Clin Invest, 2013. **123**(8): p. 3600-13.
118. Feng, L., et al., *Discovery of a Small-Molecule BMP Sensitizer for Human Embryonic Stem Cell Differentiation*. Cell Rep, 2016. **15**(9): p. 2063-75.
119. Lee, K.W., et al., *Rapamycin promotes the osteoblastic differentiation of human embryonic stem cells by blocking the mTOR pathway and stimulating the BMP/Smad pathway*. Stem Cells Dev, 2010. **19**(4): p. 557-68.
120. Yu, P.B., et al., *Dorsomorphin inhibits BMP signals required for embryogenesis and iron metabolism*. Nat Chem Biol, 2008. **4**(1): p. 33-41.
121. Hao, J., et al., *In vivo structure-activity relationship study of dorsomorphin analogues identifies selective VEGF and BMP inhibitors*. ACS Chem Biol, 2010. **5**(2): p. 245-53.
122. Cuny, G.D., et al., *Structure-activity relationship study of bone morphogenetic protein (BMP) signaling inhibitors*. Bioorg Med Chem Lett, 2008. **18**(15): p. 4388-92.
123. Siegel, R.L., K.D. Miller, and A. Jemal, *Cancer statistics, 2019*. CA Cancer J Clin, 2019. **69**(1): p. 7-34.
124. Bray, F., et al., *Global cancer statistics 2018: GLOBOCAN estimates of incidence and mortality worldwide for 36 cancers in 185 countries*. CA Cancer J Clin, 2018. **68**(6): p. 394-424.
125. *SEER Cancer Stat Facts: Kidney and Renal Pelvis Cancer*. [cited 2019; Available from: <https://seer.cancer.gov/statfacts/html/kidrp.html>].
126. Saad, A.M., et al., *Trends in Renal-Cell Carcinoma Incidence and Mortality in the United States in the Last 2 Decades: A SEER-Based Study*. Clin Genitourin Cancer, 2018.
127. Choueiri, T.K. and R.J. Motzer, *Systemic Therapy for Metastatic Renal-Cell Carcinoma*. N Engl J Med, 2017. **376**(4): p. 354-366.

128. Capitanio, U., et al., *Epidemiology of Renal Cell Carcinoma*. Eur Urol, 2019. **75**(1): p. 74-84.
129. Hsieh, J.J., et al., *Renal cell carcinoma*. Nat Rev Dis Primers, 2017. **3**: p. 17009.
130. Nickerson, M.L., et al., *Improved identification of von Hippel-Lindau gene alterations in clear cell renal tumors*. Clin Cancer Res, 2008. **14**(15): p. 4726-34.
131. Harlander, S., et al., *Combined mutation in Vhl, Trp53 and Rb1 causes clear cell renal cell carcinoma in mice*. Nat Med, 2017. **23**(7): p. 869-877.
132. Ke, Q. and M. Costa, *Hypoxia-inducible factor-1 (HIF-1)*. Mol Pharmacol, 2006. **70**(5): p. 1469-80.
133. Luu, V.D., et al., *Loss of VHL and hypoxia provokes PAX2 up-regulation in clear cell renal cell carcinoma*. Clin Cancer Res, 2009. **15**(10): p. 3297-304.
134. Gnarra, J.R. and G.R. Dressler, *Expression of Pax-2 in human renal cell carcinoma and growth inhibition by antisense oligonucleotides*. Cancer Res, 1995. **55**(18): p. 4092-8.
135. Robson, E.J., S.J. He, and M.R. Eccles, *A PANorama of PAX genes in cancer and development*. Nat Rev Cancer, 2006. **6**(1): p. 52-62.
136. Torres, M., et al., *Pax-2 controls multiple steps of urogenital development*. Development, 1995. **121**(12): p. 4057-65.
137. Dressler, G.R., et al., *Deregulation of Pax-2 expression in transgenic mice generates severe kidney abnormalities*. Nature, 1993. **362**(6415): p. 65-7.
138. Rothenpieler, U.W. and G.R. Dressler, *Pax-2 is required for mesenchyme-to-epithelium conversion during kidney development*. Development, 1993. **119**(3): p. 711-20.
139. Dressler, G.R., et al., *Pax2, a new murine paired-box-containing gene and its expression in the developing excretory system*. Development, 1990. **109**(4): p. 787-95.
140. Lindoso, R.S., K.S. Verdoorn, and M. Einicker-Lamas, *Renal recovery after injury: the role of Pax-2*. Nephrol Dial Transplant, 2009. **24**(9): p. 2628-33.

141. Belldegrün, A.S., et al., *Cancer-specific survival outcomes among patients treated during the cytokine era of kidney cancer (1989-2005): a benchmark for emerging targeted cancer therapies*. *Cancer*, 2008. **113**(9): p. 2457-63.
142. Grimley, E. and G.R. Dressler, *Are Pax proteins potential therapeutic targets in kidney disease and cancer?* *Kidney Int*, 2018. **94**(2): p. 259-267.
143. Gokden, N., et al., *The utility of PAX-2 in distinguishing metastatic clear cell renal cell carcinoma from its morphologic mimics: an immunohistochemical study with comparison to renal cell carcinoma marker*. *Am J Surg Pathol*, 2008. **32**(10): p. 1462-7.
144. Grimley, E., et al., *Inhibition of Pax2 Transcription Activation with a Small Molecule that Targets the DNA Binding Domain*. *ACS Chem Biol*, 2017. **12**(3): p. 724-734.
145. Winyard, P.J., et al., *The PAX2 transcription factor is expressed in cystic and hyperproliferative dysplastic epithelia in human kidney malformations*. *J Clin Invest*, 1996. **98**(2): p. 451-9.
146. Igarashi, P. and S. Somlo, *Polycystic kidney disease*. *J Am Soc Nephrol*, 2007. **18**(5): p. 1371-3.
147. Bergmann, C., et al., *Polycystic kidney disease*. *Nat Rev Dis Primers*, 2018. **4**(1): p. 50.
148. *United States Renal Data System: Incidence, Prevalence, Patient Characteristics, and Treatment Modalities In: 2016 USRDS Annual Data Report: Epidemiology of Kidney Disease in the United States*. 2016; Available from: <https://www.usrds.org>.
149. Sweeney, W.E. and E.D. Avner, *Polycystic Kidney Disease, Autosomal Recessive*, in *GeneReviews((R))*, M.P. Adam, et al., Editors. 1993-2019: University of Washington, Seattle. Available from: <https://www.ncbi.nlm.nih.gov/books/NBK1326/>.
150. Stayner, C., et al., *Pax2 gene dosage influences cystogenesis in autosomal dominant polycystic kidney disease*. *Hum Mol Genet*, 2006. **15**(24): p. 3520-8.
151. Ostrom, L., et al., *Reduced Pax2 gene dosage increases apoptosis and slows the progression of renal cystic disease*. *Dev Biol*, 2000. **219**(2): p. 250-8.

Chapter 2 – Kidney Fibrosis: HTS for small-molecule agonists of BMP signaling

Abstract

High-throughput screening (HTS) is a common methodology utilized in industry and academic settings to carry out drug discovery programs. Millions of diverse chemical structures can be rapidly screened to yield drug/lead-like compounds that can be optimized for pre-clinical studies and clinical trials. Cell-based HTS assays in particular offer the advantage of screening compounds in an intact cellular environment. This feature of cell-based HTS aids in discovering chemical structures with not only potential extracellular activity but also possible intracellular activity due to their capacity to penetrate cellular membranes. This is in contrast to biochemical HTS assays that may not yield a drug/lead-like compound that is biologically active in an intact cellular environment. Cell-based HTS methods can be applied toward meeting the unmet clinical need for targeted therapeutics to treat chronic kidney disease or kidney fibrosis. To launch any drug discovery project the first step is to identify a drug target or pathway implicated in the disease. At least two decades of research have pointed toward the renoprotective benefits of BMP signaling in animal models of acute and chronic kidney disease. This chapter will discuss academic drug discovery efforts to identify small-molecules that activate BMP signaling in renal cells using HTS methodologies.

Introduction

A key methodology in the quest for novel drugs to treat disease is the use of high-throughput screening (HTS). HTS allows up to millions of drug/lead-like small-molecules to be screened for biological activity in a relatively short period of time and is the most widely used technology to identify drug/lead-like molecules [1, 2]. Cell-based HTS assays, in particular, offer the advantage of testing potential drugs in an intact cellular environment. Therefore, cell-based HTS improves the prospects of identifying biologically relevant drug/lead-like compounds [1]. Whereas biochemical HTS assays, where the target is isolated, may prove futile in this regard. A disadvantage of cell-based HTS, however, is that the direct binding target of the compound identified is unknown. In contrast, this is a powerful aspect of mechanism-based biochemical assays. Therefore, additional experimentation would be necessary in order to identify direct binding targets of small-molecules identified in cell-based HTS. Follow-up optimization of biological activity and minimization of off-target effects of the compound would be feasible by such efforts.

Reporter gene systems are heavily used in cell-based HTS assays and monitor the expression of pathway genes linked to enzymes such as luciferase [1]. Luciferase-based reporter assays in particular offer sensitivity and a sizeable dynamic range, as well as rapid results [1]. Several disadvantages of luciferase-based HTS however, have been described. Some of these disadvantages are inherent to the process of screening large chemical libraries with diverse structures of small-molecules. In particular, many libraries contain small-molecules that interfere with the luciferase assay because they are structurally similar to the natural substrate of firefly luciferase, D-luciferin [3, 4]. Reports have described a phenomenon by which such small-molecules stabilize the firefly luciferase protein and prevent its degradation which ultimately leads

to increased luminescence detection [3-5]. Some chemical series that have been reported to behave in this way include: quinolines, 1,2,4-oxadiazoles, benzthiazoles, benzimidazoles, and benzoxazoles [3, 4]. However, it is important to note that some small-molecules that inhibit an enzymatic reporter such as luciferase may still possess relevant biological activity, such as resveratrol [3, 6]. Moreover, several compounds that are currently being marketed possess a benzoxazole core moiety such as: funoxaprofen, benoxaprofen (nonsteroidal anti-inflammatory drugs), calcimycin (antibiotic), boxazomycin B (antibacterial), and chloroxazone (muscle relaxant) [7].

HTS technology can be applied towards discovering medicines that can alleviate chronic kidney disease or renal fibrosis. Cell-based HTS assays in particular can be used to identify small-molecules with novel mechanisms of action that can potentially activate pathways that play a role in tissue regeneration and repair such as BMP signaling. Furthermore, development of small-molecules for clinical use offers many advantages and include: low cost, relatively long shelf-life, reversible and rapid activity, as well as, spatial and temporal control [8].

Histologically, chronic kidney disease manifests as kidney fibrosis [9]. Meaning, injured functional structures and compartments of the kidney such as the nephron, its surrounding capillary supply, and the tubulointerstitium are overcome with excessive ECM deposition [10]. Under fibrotic conditions, TGF- β provokes interstitial fibroblasts to proliferate, turn contractile, and deposit excessive ECM in the renal parenchyma [11]. Early on in renal fibrosis, pro-apoptotic stimuli such as ischemia triggers hypoperfusion and peritubular capillary rarefaction, which is worsened later by an expanding ECM filled renal parenchyma [12-14]. Tubules of nephrons once tightly pack together with narrow interstitial spacing and few fibroblasts surrounding them atrophy due to apoptosis and/or necrosis [15]. Furthermore, excessive ECM deposition contributes to the

expansion of nonfunctional tissue in the renal interstitium [16]. Moreover, inflammatory lesions are additional key features of diseased renal tissues in the fibrotic milieu [17].

While extensive evidence has implicated overactive TGF- β 1 as the principle molecular driver of fibrogenesis in the kidney in both mouse and man. Pre-clinical and clinical studies have also highlighted dysregulated BMP7 signaling as another key characteristic of fibrotic kidneys. Specifically, animals with ischemic acute renal failure [18], unilateral ureteral obstruction [19], diabetic nephropathy [20, 21], or genetic forms of chronic kidney disease [22], exhibit significantly decreased levels of BMP7 relative to the 0.1-0.5 ng/ml of normal circulating levels of BMP7 in healthy animals [18]. However, in human proximal tubular epithelial cells from patients with proteinuric nephropathies, BMP7 is upregulated approximately 4 fold compared to controls [23]. Other studies in human diabetic nephropathy noted decreased expression of BMP7 and BMP signaling in the glomerular compartment, specifically, in podocytes, which maintain the filtration barrier [24, 25].

Reinduction of suppressed BMP signaling has been demonstrated to be protective in animal models of acute and chronic kidney injury. Acute kidney injury is a risk factor of chronic kidney disease and ischemia is a common primary cause of acute kidney injury in adults [26-28]. Several damaging changes in the kidneys occur following ischemia and reperfusion injury. In particular, ischemia and reperfusion induced injury to the kidneys include: tubular apoptosis and necrosis, inflammatory lesions, as well as, abnormal levels of blood urea nitrogen and serum creatinine.

In rat kidneys injured by bilateral artery occlusion for 60 minutes, systemic administration of 250 μ g/kg BMP7 was shown to stimulate the proliferation of damaged tubular epithelial cells of the nephron after reperfusion [18]. This observation led to the suggestion that BMP7 promotes renal repair and regeneration through mechanisms that it employs during kidney development [18].

Since, during kidney development, BMP7 acts as a survival factor for the metanephric mesenchyme [29]. Specifically, BMP7 maintains and expands nephron progenitor cells by inhibiting apoptosis and differentiation [29]. Simultaneously, however, BMP7 stimulates the proliferation of nephron progenitor cells [29]. Additionally, BMP7 deficient neonatal kidneys have low glomeruli and nephron numbers [29]. Inflammation was also suppressed in BMP7 treated animals with ischemic injury, which was demonstrated by downregulated levels of ICAM-1 (intracellular adhesion molecule-1) expression and a significant reduction in neutrophil accumulation [18]. Creatinine and blood urea nitrogen levels were also 8-10 times lower in BMP7 treated animals compared to vehicle treated animals that underwent bilateral artery occlusion [18].

BMP7 also demonstrates several renoprotective effects in animals subjected to unilateral ureteral obstruction (UUO). UUO surgery in animals is a model of progressive renal fibrosis [15]. Albeit common in children, UUO is an unusual primary cause of adult human renal failure [15, 30]. Nevertheless, in UUO subjected animals, upregulated TGF- β is found within 10 hours after surgery, which is stimulated by overactive angiotensin II [31-33]. Vasoconstriction of afferent renal arterioles is also induced by overactive angiotensin II in UUO animals [30, 34]. Additionally, within 24 hours, reduced blood flow and decreased rates of glomerular filtration are apparent in UUO animals [15, 34]. A few days later, hydronephrosis, macrophage induced inflammatory lesions in the interstitium, and demise of tubular structures from apoptosis and necrosis also occur [15]. Furthermore, UUO causes fibrotic lesions in the interstitium which is mediated by transdifferentiated renal cells into myofibroblasts which lay down excessive levels of extracellular matrix proteins such as collagen (I, III, IV) and fibronectin [15].

Systemic therapy of both 100 and 300 $\mu\text{g}/\text{kg}$ of BMP7, given at the time of UUO followed by once daily doses of BMP7 every other day, significantly reduced atrophic renal tubules induced

by 5 days of unilateral obstruction in rats [19]. This evidence suggested that BMP7, in a dose-dependent manner, exerts its renoprotective effects through maintaining the integrity of the tubular epithelium. Importantly, the ACE inhibitor, enalapril (25 mg/kg, high dose), lacked the capacity to preserve tubular integrity in UUO animals [19]. Use of ACE inhibitors is a common clinical therapeutic strategy for patients with CKD to slow disease progression, however, many patients still advance to ESRD [35].

BMP7 therapy at the initiation of UUO abated fibrotic lesions as assessed by α -SMA positive myofibroblasts and collagen IV [19]. Of note, BMP7 therapy at the doses tested, was unable to return α -SMA positive myofibroblast accumulation and collagen IV expression to baseline levels observed in the contralateral kidneys treated with either vehicle or BMP7. This may underscore the need for combinatorial strategies that simultaneously suppress pro-fibrotic TGF- β activity, as well as, stimulate BMP7 signaling to maintain tubular epithelial integrity in diseased kidneys for optimal therapy. Additionally, inflammatory lesions, as assessed by macrophage interstitium infiltration, were significantly attenuated in a dose-dependent manner in animals undergoing BMP7 therapy [19]. The renoprotective effects of BMP7 in UUO animals were also accompanied by preserved renal blood flow which is typically decreased within 24 hours of surgery [19, 34].

As demonstrated in the two seminal studies outlined above, loss of BMP7 in the tubular epithelium leads to cellular apoptosis and ultimately tubular atrophy in animal models of acute and chronic kidney disease. Loss of BMP7 is also evident in animals subjected to experimental doses of STZ, which models key aspects of type I diabetes induced nephropathy in humans [20, 21]. These animals typically develop albuminuria, glomerulosclerosis, and tubulointerstitial fibrosis; however, some renal histopathological changes are species, strain, and dosing regimen specific

[36-39]. In rats with diabetic syndrome induced by one 62 mg/kg dose of STZ, considerable glomerular hypertrophy at 16-weeks post STZ injection was observed in vehicle treated animals [21]. Twice weekly doses of 10, 30, or 100 µg/kg of BMP7 therapy commenced at week 16 post STZ injection and continuing until week 32, however, partially reversed this histopathological finding [21]. Segmental glomerulosclerosis and the accumulation of early interstitial matrix accumulation (assessed by collagen staining) was also reduced by BMP7 therapy in a dose-dependent manner [21].

As with animal models of inducible forms of acute and chronic kidney disease, BMP7 therapy is also beneficial in protecting animals from genetic causes of kidney failure. Within 4 weeks, MRL lupus mice exhibit early signs of increased interstitial volume and tubular atrophy, BMP7 therapy reverses these fibrosis-associated changes [22]. Glomerulosclerosis and glomerular hypercellularity was reduced in MRL lupus mice under 300 µg/kg BMP7 therapy [22]. Additionally, type I collagen levels in these mice were also decreased under BMP7 treatment [22]. In mice with deficient type IV collagen- $\alpha 3$ gene (*Col4A3^{-/-}*), tubulointerstitial fibrosis and tubular atrophy were also diminished with 300 µg/kg BMP7 treatment [22]. Renal function in *Col4A3^{-/-}* mice was also improved under BMP7 therapy as assessed by improvements in serum creatinine, blood urea nitrogen levels, and urine protein [22].

The therapeutic effects of BMP7 in the fibrotic kidney have been demonstrated in numerous studies using different animal models of acute and chronic kidney disease. BMP2 and BMP7 are currently FDA approved for clinical use in bone repair procedures. However, several barriers exist in translating this therapy into clinical settings for renal disease. One barrier in the clinical application of BMPs is the 1.5 mg/ml doses required to achieve efficacy in human bone repair procedures [40]. The high therapeutic dose of BMP needed in humans is in stark contrast to

the potency displayed and efficacy yielded using significantly lower doses of BMPs in both cell culture and animal studies. In renal studies for instance, 10 and 100 ng/ml of recombinant BMP7 sufficiently displayed a dose-dependent reduction in the synthesis of type I collagen and fibronectin in activated human fibroblast (TK-173) [22]. Additionally, 30-300 µg/ml of recombinant BMP7 was sufficient to observe dose-dependent reversal of fibrosis associated changes in animals with acute and chronic kidney injury [18, 19, 22]. Humans treated with supra-physiological doses of BMPs have consequently experienced harmful side effects such as inflammation and ectopic bone growth [41-43].

Another barrier in translating recombinant BMPs into clinical use is the high manufacturing costs associated with the complex structure of BMPs. BMPs have a distinctive cysteine-knot fold tertiary structure formed by six conserved cysteine residues that form three intrapeptide disulfide bonds [29]. Additionally, BMPs have multiple proteolytic sites and therefore are a heterogeneous mixture of differentially processed proteins [44]. Moreover, due to denaturation, BMPs possess a shorter shelf-life relative to small-molecules which are considered to be more stable [45]. Added drawbacks to recombinant BMP therapy for renal disease are the limited routes of administration, which include intravenous infusion or subcutaneous injections. Intravenous infusion would necessitate inpatient care while self-administered subcutaneous injection may prove unappealing to patients. Both routes of administration have the potential to hinder patient adherence, especially for chronic illnesses such as kidney disease [45]. The option of oral administration of BMPs may be limited do to gastrointestinal tract degradation issues [46]. Moreover, intravenous infusion or subcutaneous injection would add to the already high manufacturing costs of recombinant BMP therapies.

Orally active small-molecules, in contrast, can be designed to stimulate BMP signaling at various levels of the pathway. In canonical BMP signaling, dimeric BMP ligands signal through a heterotetramer of two type I and type II BMP serine/threonine kinase receptors. BMP ligand binding triggers type II BMP receptors to phosphorylate the type I BMP receptors. Activated, the type I BMP receptor phosphorylates key intracellular transducers of canonical BMP signaling, SMADs-1/5/8/9. Extracellular enhancers and inhibitors regulate the bioavailability of BMP ligands in order to fine tune BMP signaling. While, intracellular factors such as inhibitory SMADs-6/7 fine tune intracellular levels of BMP signaling activation. Other molecules such as Smurfs target SMAD proteins for degradation by the proteasome. Furthermore, TGF- β signaling and its effectors SMADs-2/3 heavily oppose BMP signaling.

Using HTS methods, small-molecules have been identified that target various aspects of the BMP signaling pathway outlined in the previous section. These agents can be utilized for potential application toward a variety of BMP signaling related biological outputs. For example, BMPs are important regulators of stem/progenitor cell fate decisions. Additionally, BMPs are used for the maintenance and directed differentiation of embryonic stem cells toward different cell fates [47]. Therefore, cell-based HTS assays have been used to identify a BMP agonists/sensitizer for use in human embryonic stem cell differentiation. This particular cell-based HTS used a reporter construct containing the *Id2* (key BMP target gene) promoter transfected into C2C12 myoblasts to assay more than 4,000 small-molecules. The chemical library used contained kinase inhibitors, signaling pathway regulators, natural products, and United States Food and Drug Administration approved drugs [47].

The cell-based HTS assay yielded, PD407824, a checkpoint kinase inhibitor (CHK1), which was demonstrated to sensitize C2C12 myoblasts to sub-threshold levels of BMP4 treatment

and upregulated the expression of *Id1* and *Id2* [47]. Furthermore, PD407824, was found to synergize with BMP4 to reprogram C2C12 myoblasts cells to an osteoblasts fate [47]. As well as, quantitatively increased SMAD-1/5/9 levels in the presence of BMP4. Mechanistic experiments demonstrated that PD407824 inhibition by CHK1, downregulates P21 which leads to SMAD-2/3 degradation. This ultimately leads to increased association of SMAD-1/5/9 with co-SMAD-4, which leads to more effective activation of *Id1* and *Id2* [47].

Results

Validation of renal BRE-Luc cells for High-Throughput Screening (HTS)

A construct with a BMP responsive element (BRE) driving luciferase expression was stably integrated into the genome of human renal cells, which we termed BRE-Luc. Critically, the BRE-Luc construct contains distinct elements of the ID1 promoter that are necessary for p-SMAD-1/5/9 binding (**figure 2.1A**) [48]. Moreover, inverted repeats of the p-SMAD-1/5/9 binding elements confer high sensitivity to rh-BMP4 treatment and a wide dynamic range of detection of activated BMP signaling. Accordingly, in luciferase assays, we observed that rh-BMP4 treatment caused a dose-dependent increase in luciferase activity in BRE-Lucs ($EC_{50} = 2.405$ ng/ml); whereas, DMSO treatment did not (**figure 2.1B**).

Hence, our BRE-Luc cell line displayed a highly specific response to rh-BMP4 treatment. Additionally, 10 ng/ml of rh-BMP4 yielded a 10-fold increase in luciferase activity over DMSO (**figure 2.1B**). Furthermore, immunoblotting assays revealed that stimulation of BRE-Lucs with 0.4, 2, or 10 ng/ml of rh-BMP4, yielded a dose-dependent induction of p-SMAD-1/5/9 (**figure 2.1C**). With 2 ng/ml of rh-BMP4 yielding a 16-fold induction of p-SMAD-1/5/9 compared to untreated cells (**figure 2.1D**). Moreover, in the presence of increasing doses of rh-BMP4, basal levels of the TGF- β effectors, p-SMAD-2 and p-SMAD-3 remained virtually constant (**figure 2.2A**). Our BRE-Lucs, therefore, displayed the sensitivity and specificity needed to detect activated BMP signaling in a renal cell-based HTS assay for small-molecule agonists of BMP signaling.

Identification of BMP signaling agonists via a renal cell-based HTS

63,608 small-molecules from the Center for Chemical Genomics library were screened at a single concentration (10 μ M) in renal BRE-Lucs in our primary HTS (**figure 2.3A-B**). After applying the following MScreen [49] filters: activity of small-molecules \geq 18% activity of the positive control (25 ng/ml rh-BMP4) or \geq 3 standard deviations above the negative control (0.1% DMSO), 1,453 small-molecules from our primary screen were selected for confirmation retesting in triplicate. 1,218 small-molecules confirmed.

To select for compounds for our dose-response confirmation studies, we used the following criteria: activity of small-molecules \geq 10% of the positive control (25 ng/ml rh-BMP4) and active three out of the four times tested. 70 compounds met these criteria and passed an additional counter screen for non-specific activation of our BRE-Luc construct. Fresh powders of the top sixteen compounds were re-ordered for dose-response studies. Twelve of the sixteen small-molecules displayed dose-response activity with relatively potent EC_{50} 's (**figure 2.4A-B**). One compound, sb4, not only displayed a sigmoidal dose-response curve but also, the lowest EC_{50} (\sim 74nM) of the top twelve compounds (**figure 2.4A-B**). Luciferase activity after sb4 treatment was also increased 2.5-fold compared to DMSO at a top concentration of 1000 nM (**figure 2.4B**). The Hill Slope of sb4 was determined to be 1.24 (**figure 2.4B**). Of the twelve small-molecules some had similar structures (sb1 and sb2, sb3 and sb4, sb5 and sb6) while the remaining compounds were singletons with unique structures (sb-sb12) (**figure 2.4C**).

Discussion

This Chapter describes cell-based HTS methodologies that were carried out in order to identify small-molecules that activate the BMP signaling pathway for potential application toward treating Chronic Kidney Disease. Human renal cells (HEK-293s) expressing a genomically integrated BMP responsive element fused to firefly luciferase were employed to screen approximately 64,000 small-molecules in the Center for Chemical Genomics (CCG) library at the University of Michigan. The primary screening campaign and triage strategies identified twelve compounds that activated the BRE-Luc reporter construct in a dose-dependent manner. The half maximal effective concentration for these top twelve BMP signaling agonists were relatively low and ranged from approximately 74-1249 nM. However, it is important to bear in mind that the BRE-Luc reporter construct is an artificial tool that is highly responsive to BMPs because it contains inverted repeats of critical elements of the ID1 promoter that are necessary for p-SMAD-1/5/9 binding. Although a powerful tool for detecting subtle changes in BMP signaling, the results obtained from the artificial system may not translate directly when assessing endogenous levels of specific components of the BMP signaling pathway.

As explained in the introduction of this Chapter, cell-based HTS offers the advantage of testing small-molecules in an intact cellular environment. However, key mechanistic information about the direct binding target is unknown. Therefore, the top twelve BMP signaling agonists identified may act to enhance the BRE-Luc transcriptional response through an array of possible novel mechanisms. These top twelve compounds could also work to activate BRE-Luc through unwanted mechanisms. Therefore, after conducting the primary HTS screen described in this Chapter, secondary assays were used to characterize and gain mechanistic insights about the top twelve BMP signaling agonists. The results of these secondary assays are described in Chapter 3.

Figures

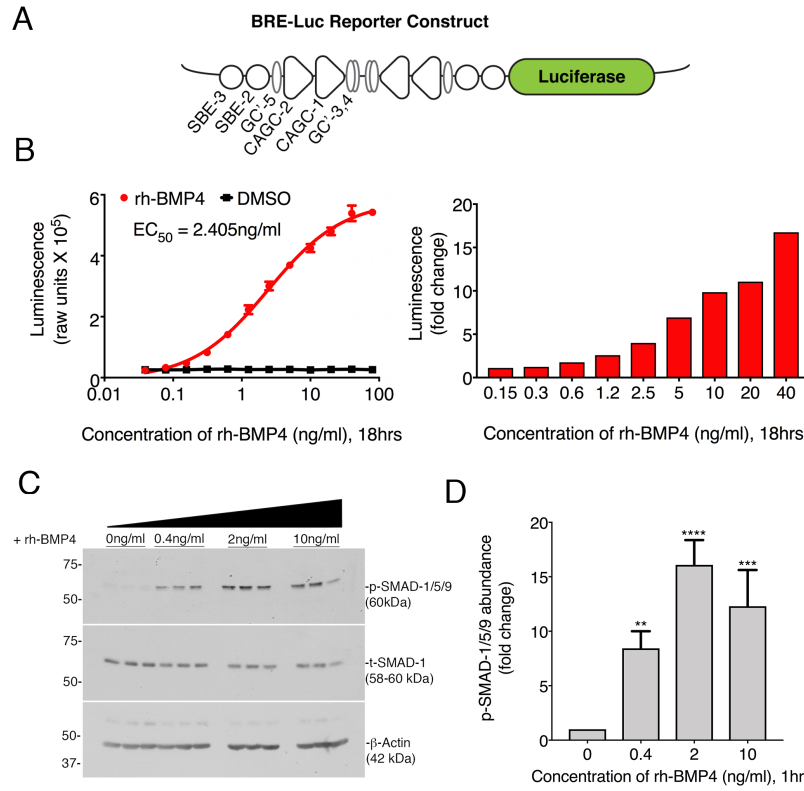


Figure 2.1 Characterization and validation of BRE-Luc cells for HTS.

(A) The BRE-Luc reporter construct contains an inverted repeat of BMP responsive elements driving luciferase. Elements of the ID1 promoter and SMAD binding sites are marked as originally identified by Korchynskiy *et al.* [48]. (B) A dose-response curve of BRE-Luc cells subjected to increasing concentrations of rh-BMP4 performed in triplicate. (C) Western blot of lysates from BRE-Luc cells treated with increasing concentrations of rh-BMP4. Membranes were probed with p-SMAD-1/5/9 and total-SMAD-1; β -Actin was used as an additional loading control. (D) p-SMAD-1/5/9 protein levels were quantified by densitometry. The signal of p-SMAD-1/5/9 was normalized to total-SMAD-1 to control for loading variability. Data are expressed as fold change relative to the media alone, which was set to 1. Error bars represent one standard deviation from the mean of 3 independent biological replicates. ANOVA, Dunnett's post-hoc multiple comparisons test generated P values of: ** $p < 0.01$ *** $p < 0.001$, **** $p < 0.0001$ relative to controls. This figure appears in—Bradford, S. T. J., E. J. Ranghini, E. Grimley, P. H. Lee and G. R. Dressler (2019). "High-throughput screens for agonists of bone morphogenetic protein (BMP) signaling identify potent benzoxazole compounds." *J Biol Chem.* PMID: 30602563 [50].

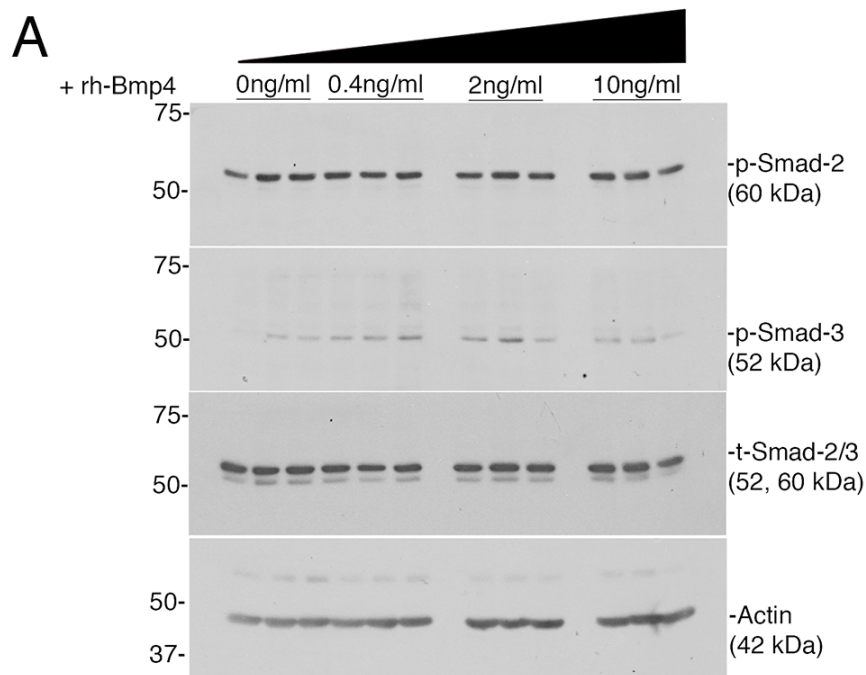


Figure 2.2 Assessment of TGF- β effectors p-SMAD-2 and p-SMAD-3 in BRE-Luc cells.

(A) Immunoblot of lysates from BRE-Luc cells treated with increasing concentrations of rh-BMP4 (0, 0.4, 2, and 10 ng/ml). Membranes were probed with p-SMAD-2, p-SMAD-3, and total-SMAD-2/3. β -Actin was used as an additional loading control. Blot shows 3 biological replicates of each dose. This figure appears in—**Bradford, S. T. J.**, E. J. Ranghini, E. Grimley, P. H. Lee and G. R. Dressler (2019). "High-throughput screens for agonists of bone morphogenetic protein (BMP) signaling identify potent benzoxazole compounds." *J Biol Chem.* PMID: 30602563 [50].

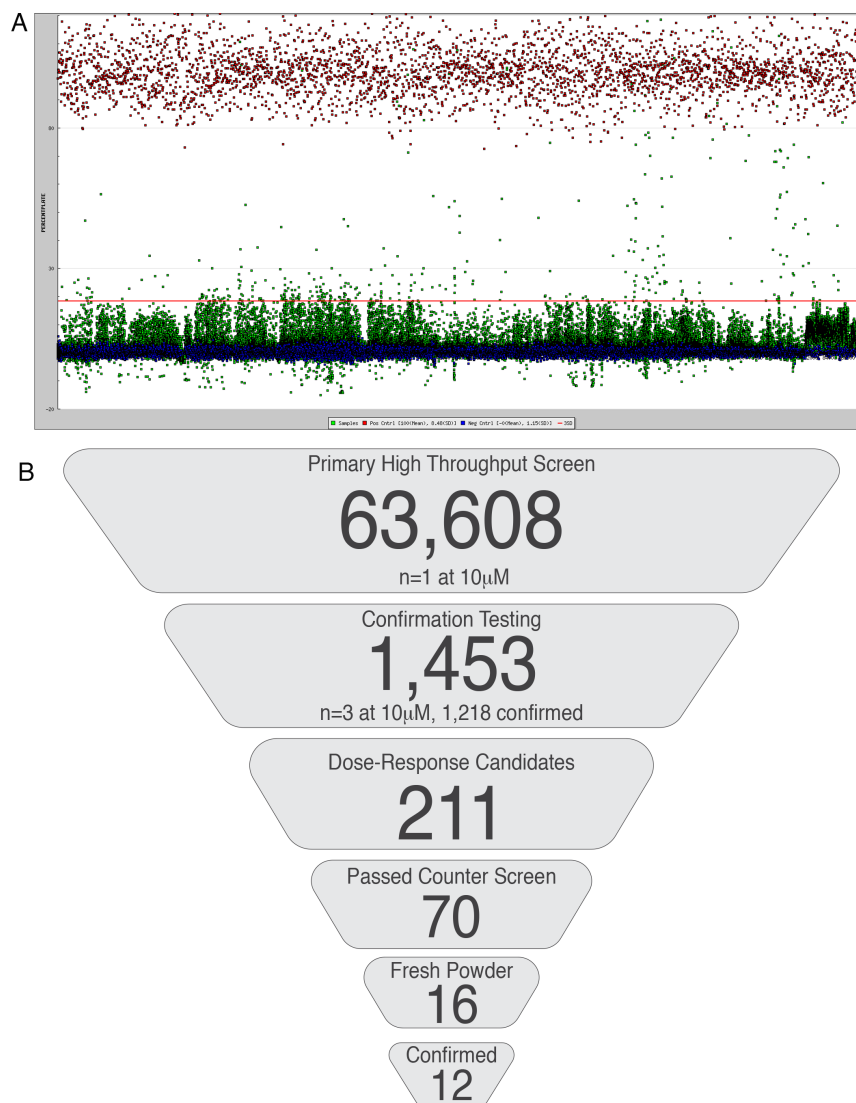


Figure 2.3 High-Throughput Screening strategy in BRE-Luc cells.

(A) A snapshot of the primary screen of 63,608 small-molecules (green dots) at a single concentration (10 μ M) in renal BRE-Luc cells. Positive controls were 25 ng/ml of rh-BMP4 (red dots) whereas negative controls were 0.1% DMSO (blue dots). The red line represents 3 standard deviations above the DMSO. The average luciferase induction for 25 ng/ml of rh-BMP4 was $355,000 \pm 34,000$, DMSO $44,000 \pm 4,300$, and for the small-molecules hits $127,000$. The average Z' score for all the plates screened was 0.71, indicating a high-quality screening assay. (B) Triage strategy used to winnow down the starting 63,608 small-molecules from the Primary HTS campaign which allowed identification of the top twelve BMP signaling agonists based on dose-response curves and structures. This figure appears in—Bradford, S. T. J., E. J. Ranghini, E. Grimley, P. H. Lee and G. R. Dressler (2019). "High-throughput screens for agonists of bone morphogenetic protein (BMP) signaling identify potent benzoxazole compounds." *J Biol Chem*. PMID: 30602563 [50].

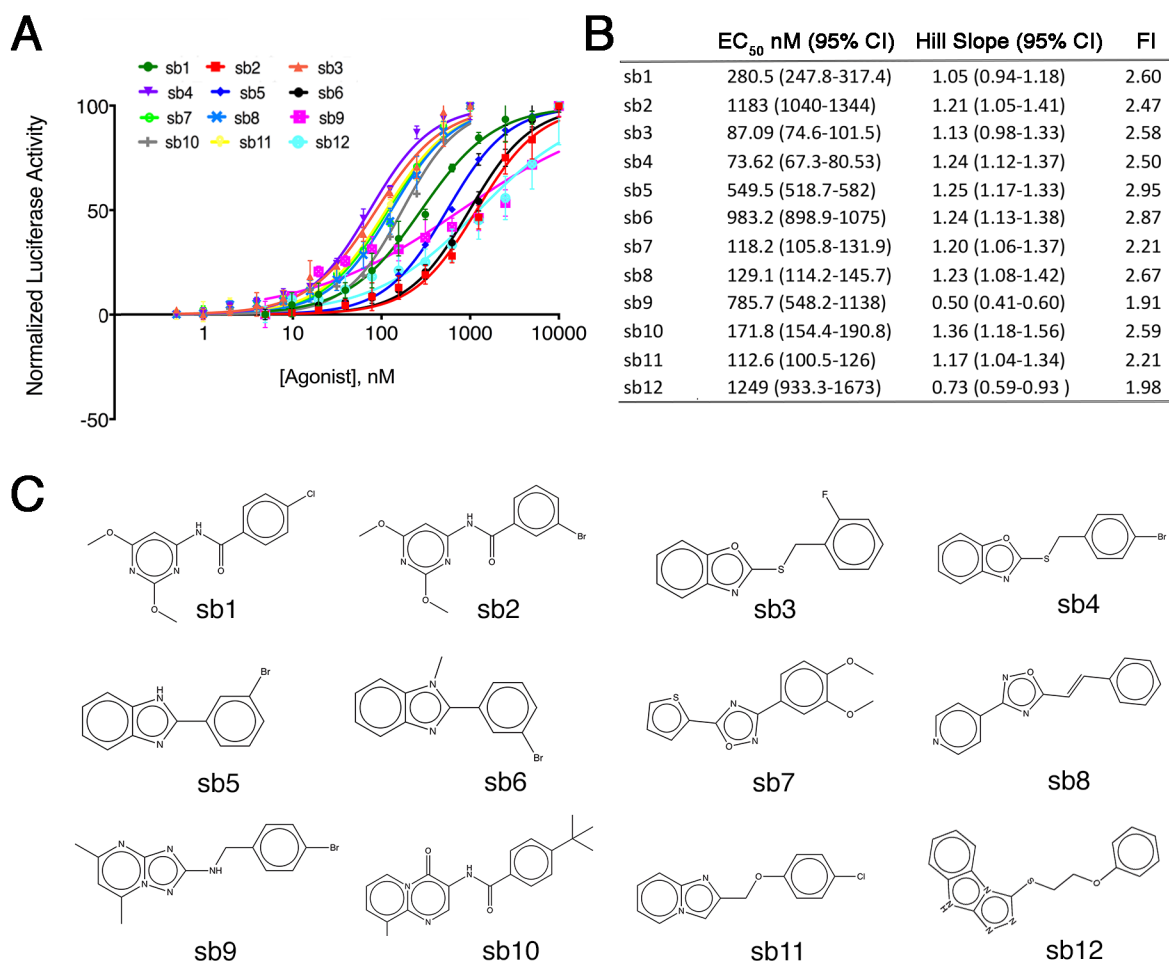


Figure 2.4 Dose-response curves of the top twelve potential BMP signaling agonists.

(A) Twelve compounds were tested for BRE-Luc dose-responses at two-fold increasing concentrations from 0.5 nM to 10 μ M in triplicate. (B) Effective concentrations at 50% maximum response (EC₅₀) and the Hill Slopes were calculated for each compound. Maximum fold induction (FI) above DMSO controls is reported. (C) Chemical structures of the 12 candidate BMP agonists are shown schematically. This figure appears in—**Bradford, S. T. J., E. J. Ranghini, E. Grimley, P. H. Lee and G. R. Dressler (2019). "High-throughput screens for agonists of bone morphogenetic protein (BMP) signaling identify potent benzoxazole compounds." J Biol Chem. PMID: 30602563 [50].**

Materials and Methods

Construction of BMP reporter cells (BRE-Luc cells)

Human embryonic kidney cells (HEK293) were transfected with a linearized plasmid containing two inverted repeats of a BMP responsive element containing SMAD binding sites and parts of the ID1 promoter as described [48]. Transformants were selected in 800 mg/ml of geneticin (G418) and clones were derived by single cell dilution. Individual BRE-Luc containing HEK-293 clones were tested for responsiveness to BMP4 and BMP7.

Cell culture

For testing of small-molecules, BRE-Lucs were maintained in complete medium (Dulbecco's modified Eagle's medium (DMEM) containing 4.5 g/L D-glucose and 584 mg/L L-glutamine supplemented with 10% fetal bovine serum and 1% Pen/Strep) and cultured to sub-confluency at 37°C and 5% CO₂.

Immunoblotting

BRE-Lucs were passaged in DMEM supplemented with 5% FBS (vol/vol) for both HTS and 6-well plate studies. Compounds were added in the presence of 5% FBS. PRECs were serum starved 1hr before addition of factors in Serum Free Medium (SFM). Sub-confluent BRE-Luc or PREC cultures were seeded into 6-well plates at 3.0×10^5 or 2.0×10^5 cells/well respectively, using an automated cell counter (Countess™ II). Cells were treated with rh-BMP4 (R & D Systems; 314-BP), vehicle (DMSO-D6), or compound (10 μ M) for 1hr or 24hrs. After the indicated time points, treatment medium was removed, adhered cells were washed once in 1X PBS and subsequently harvested in 1X PBS and pelleted by low centrifugation.

The cell pellet was then suspended in PK lysis buffer (50mM HEPES pH 7.5, 150mM NaCl, 1.5mM MgCl₂, 1mM EGTA, 10% Glycerol, 1% Triton X-100, 1mM Na₃VO₄ 50mM NaF) containing both phosphatase and protease inhibitors (PhosSTOP and cOmplete Mini; Roche) and allowed to lyse on ice for 30 minutes with intermittent vortexing. To pellet the insoluble fraction, the suspended pellet was centrifuged at 15,000 rpm for 15 minutes at 4°C. Supernatant was transferred to clean Eppendorf tubes and 6X sodium dodecyl sulfate was added 1:5 and heated for 5 minutes at 95°C. Equal amounts of total protein lysates were resolved on hand-casted 8% SDS-polyacrylamide gels.

Separated proteins were then electrophoretically transferred onto Immobilon®-FL polyvinylidene difluoride membranes. Membranes were dried and reactivated in methanol rinsed in 1X TBS and blocked for 1hr in 5% bovine serum albumin or 5% milk dissolved in 1X TBS-T (1X TBS + 0.1% Tween® 20) and then incubated overnight with primary antibodies consisting of one of the following: anti-Rb phospho-SMAD-1/5/9 1:1,000 (CST®; 13820), anti-Rb total-SMAD-1 1:2,000 (CST®; 9734), anti-Rb phospho-SMAD-2 1:1000 (CST®; 3104), anti-Rb phospho-

SMAD-3 1:1000 (CST®; 9520) anti-Rb total-SMAD-2/3 1:1000 (CST®; 3102), anti-β-Actin 1:10,000 (Proteintech®; 60008-1-Ig) The next day, membranes were washed in 1% non-fat dry milk prepared in 1X TBS-T and incubated for 1 hour at room temperature in anti-Rb HRP or anti-Ms-HRP diluted in 1% non-fat dry milk (1X TBS-T). Membranes were washed in TBS-T and rinsed twice with 1X TBS and incubated with ECL western blotting substrate (Pierce™; 32106). Finally, membranes were incubated with HyBlot ES™ autoradiography film (Denville Scientific) and developed on the Kodak X-OMAT 2000A processor and quantified using ImageJ (Version 2.0.0)

Small-molecule screening library

63,608 drug/lead-like structures were screened in the Center for Chemical Genomics (CCG) small-molecule library housed at the Life Science Institute at the University of Michigan. Small-molecules were selected for their drug/lead like physicochemical properties which fell within the Lipinski's space for bioavailable/orally active drugs having molecular weights < 500, hydrogen-bond donors < 5, hydrogen-acceptors < 10 and cLogP's < 5 [51]. The libraries utilized at the CCG consisted of compounds from the ChemDiv 100K diversity set in which 61,120 structures were screened returning a hit ratio 17.32%. 1,280 compounds from the Library of Pharmacologically Active Compounds (Sigma) returned a hit ratio of 9.06%. 1,280 compounds from the Prestwick library returned a hit ratio of 8.2% and screening 320 compounds from the NIH Clinical Compound library returned a 7.81% hit ratio.

Luciferase Assays

Compounds were dissolved in MagniSolv™ dimethyl sulfoxide-D6 (DMSO-D6, EMD Millipore; 2206-27-1) and then diluted in 5% FBS medium and added to 96-well plates. Recombinant proteins (rh-BMP4 or rh-Noggin, R&D Systems; 314-BP or 6057-NG) were reconstituted per manufactures' instructions and diluted in 5% FBS medium. BRE-Lucs were passaged in 5% FBS medium and seeded into factor containing 96-well plates at 3.0×10^3 cells/well using an automated cell counter (Countess™ II). BRE-Lucs were incubated overnight at 37°C and 5% CO₂. The next day, 85% of the culture medium was aspirated using a microplate washer (BioTek® ELx405™) and an equal volume of luciferase reagent (Steady-Glo® Promega) was added to the remaining culture medium in each well using a Multidrop™ dispenser. Following Steady-Glo® cell lysis, luminescence activity was measured on a luminometer (PHEARstar® BMG Labtech)

Bibliography

1. Parker, C.Z., J. H. , *High-Throughput Screening for small-molecule drug discovery*, in *Development of Therapeutic Agents Handbook*, S.C. Gad, Editor. 2012, John Wiley & Sons, Incorporated. p. 147-180.
2. Bleicher, K.H., et al., *Hit and lead generation: beyond high-throughput screening*. *Nat Rev Drug Discov*, 2003. **2**(5): p. 369-78.
3. Thorne, N., D.S. Auld, and J. Inglese, *Apparent activity in high-throughput screening: origins of compound-dependent assay interference*. *Curr Opin Chem Biol*, 2010. **14**(3): p. 315-24.
4. Auld, D.S. and J. Inglese, *Interferences with Luciferase Reporter Enzymes*, in *Assay Guidance Manual*, G.S. Sittampalam, et al., Editors. 2004: Bethesda (MD).
5. Thompson, J.F., L.S. Hayes, and D.B. Lloyd, *Modulation of firefly luciferase stability and impact on studies of gene regulation*. *Gene*, 1991. **103**(2): p. 171-7.
6. Bakhtiarova, A., et al., *Resveratrol inhibits firefly luciferase*. *Biochem Biophys Res Commun*, 2006. **351**(2): p. 481-4.
7. Kakkar, S., et al., *Benzoxazole derivatives: design, synthesis and biological evaluation*. *Chem Cent J*, 2018. **12**(1): p. 92.
8. Zhang, M., et al., *Chemical approaches to controlling cell fate*, in *Principles of developmental genetics* S.A. Moody, Editor. 2014: Amsterdam ; Boston : Elsevier/AP. p. 59-76.
9. Breyer, M.D. and K. Susztak, *The next generation of therapeutics for chronic kidney disease*. *Nat Rev Drug Discov*, 2016. **15**(8): p. 568-88.
10. Hewitson, T.D., *Fibrosis in the kidney: is a problem shared a problem halved?* *Fibrogenesis Tissue Repair*, 2012. **5**(Suppl 1): p. S14.
11. Leask, A. and D.J. Abraham, *TGF-beta signaling and the fibrotic response*. *FASEB J*, 2004. **18**(7): p. 816-27.

12. Zeisberg, M. and E.G. Neilson, *Mechanisms of tubulointerstitial fibrosis*. J Am Soc Nephrol, 2010. **21**(11): p. 1819-34.
13. Babickova, J., et al., *Regardless of etiology, progressive renal disease causes ultrastructural and functional alterations of peritubular capillaries*. Kidney Int, 2017. **91**(1): p. 70-85.
14. Hohenstein, B. and C. Hugo, *Peritubular capillaries: an important piece of the puzzle*. Kidney Int, 2017. **91**(1): p. 9-11.
15. Chevalier, R.L., M.S. Forbes, and B.A. Thornhill, *Ureteral obstruction as a model of renal interstitial fibrosis and obstructive nephropathy*. Kidney Int, 2009. **75**(11): p. 1145-1152.
16. Sharma, A.K., et al., *Interstitial fibrosis in obstructive nephropathy*. Kidney Int, 1993. **44**(4): p. 774-88.
17. Meng, X.M., D.J. Nikolic-Paterson, and H.Y. Lan, *Inflammatory processes in renal fibrosis*. Nat Rev Nephrol, 2014. **10**(9): p. 493-503.
18. Vukicevic, S., et al., *Osteogenic protein-1 (bone morphogenetic protein-7) reduces severity of injury after ischemic acute renal failure in rat*. J Clin Invest, 1998. **102**(1): p. 202-14.
19. Hruska, K.A., et al., *Osteogenic protein-1 prevents renal fibrogenesis associated with ureteral obstruction*. Am J Physiol Renal Physiol, 2000. **279**(1): p. F130-43.
20. Wang, S.N., J. Lapage, and R. Hirschberg, *Loss of tubular bone morphogenetic protein-7 in diabetic nephropathy*. J Am Soc Nephrol, 2001. **12**(11): p. 2392-9.
21. Wang, S., et al., *Bone morphogenic protein-7 (BMP-7), a novel therapy for diabetic nephropathy*. Kidney Int, 2003. **63**(6): p. 2037-49.
22. Zeisberg, M., et al., *Bone morphogenic protein-7 inhibits progression of chronic renal fibrosis associated with two genetic mouse models*. Am J Physiol Renal Physiol, 2003. **285**(6): p. F1060-7.
23. Rudnicki, M., et al., *Gene expression profiles of human proximal tubular epithelial cells in proteinuric nephropathies*. Kidney Int, 2007. **71**(4): p. 325-35.

24. Woroniecka, K.I., et al., *Transcriptome Analysis of Human Diabetic Kidney Disease*. *Diabetes*, 2011. **60**(9): p. 2354-2369.
25. Turk, T., et al., *BMP signaling and podocyte markers are decreased in human diabetic nephropathy in association with CTGF overexpression*. *J Histochem Cytochem*, 2009. **57**(7): p. 623-31.
26. Basile, D.P., M.D. Anderson, and T.A. Sutton, *Pathophysiology of acute kidney injury*. *Compr Physiol*, 2012. **2**(2): p. 1303-53.
27. Heung, M. and L.S. Chawla, *Predicting progression to chronic kidney disease after recovery from acute kidney injury*. *Curr Opin Nephrol Hypertens*, 2012. **21**(6): p. 628-34.
28. Basile, D.P., et al., *Progression after AKI: Understanding Maladaptive Repair Processes to Predict and Identify Therapeutic Treatments*. *J Am Soc Nephrol*, 2016. **27**(3): p. 687-97.
29. Manson, S.R., et al., *BMP-7 Signaling and its Critical Roles in Kidney Development, the Responses to Renal Injury, and Chronic Kidney Disease*. *Vitam Horm*, 2015. **99**: p. 91-144.
30. Hewitson, T.D., T. Ono, and G.J. Becker, *Small animal models of kidney disease: a review*. *Methods Mol Biol*, 2009. **466**: p. 41-57.
31. Walton, G., et al., *Renal growth factor expression during the early phase of experimental hydronephrosis*. *J Urol*, 1992. **148**(2 Pt 2): p. 510-4.
32. el-Dahr, S.S., et al., *Upregulation of renin-angiotensin system and downregulation of kallikrein in obstructive nephropathy*. *Am J Physiol*, 1993. **264**(5 Pt 2): p. F874-81.
33. Fern, R.J., et al., *Reduced angiotensinogen expression attenuates renal interstitial fibrosis in obstructive nephropathy in mice*. *J Clin Invest*, 1999. **103**(1): p. 39-46.
34. Vaughan, E.D., Jr., et al., *Pathophysiology of unilateral ureteral obstruction: studies from Charlottesville to New York*. *J Urol*, 2004. **172**(6 Pt 2): p. 2563-9.
35. *K/DOQI clinical practice guidelines on hypertension and antihypertensive agents in chronic kidney disease*. *Am J Kidney Dis*, 2004. **43**(5 Suppl 1): p. S65-73.

36. Kitada, M., Y. Ogura, and D. Koya, *Rodent models of diabetic nephropathy: their utility and limitations*. Int J Nephrol Renovasc Dis, 2016. **9**: p. 279-290.
37. Breyer, M.D., et al., *Mouse models of diabetic nephropathy*. J Am Soc Nephrol, 2005. **16**(1): p. 27-45.
38. Sugimoto, H., et al., *Renal fibrosis and glomerulosclerosis in a new mouse model of diabetic nephropathy and its regression by bone morphogenetic protein-7 and advanced glycation end product inhibitors*. Diabetes, 2007. **56**(7): p. 1825-33.
39. Li, J., X. Qu, and J.F. Bertram, *Endothelial-myofibroblast transition contributes to the early development of diabetic renal interstitial fibrosis in streptozotocin-induced diabetic mice*. Am J Pathol, 2009. **175**(4): p. 1380-8.
40. Boden, S.D., et al., *The use of rhBMP-2 in interbody fusion cages. Definitive evidence of osteoinduction in humans: a preliminary report*. Spine (Phila Pa 1976), 2000. **25**(3): p. 376-81.
41. Carragee, E.J., E.L. Hurwitz, and B.K. Weiner, *A critical review of recombinant human bone morphogenetic protein-2 trials in spinal surgery: emerging safety concerns and lessons learned*. Spine J, 2011. **11**(6): p. 471-91.
42. Chen, N.F., et al., *Symptomatic ectopic bone formation after off-label use of recombinant human bone morphogenetic protein-2 in transforaminal lumbar interbody fusion Report of 4 cases*. Journal of Neurosurgery-Spine, 2010. **12**(1): p. 40-46.
43. Muchow, R.D., W.K. Hsu, and P.A. Anderson, *Histopathologic inflammatory response induced by recombinant bone morphogenetic protein-2 causing radiculopathy after transforaminal lumbar interbody fusion*. Spine J, 2010. **10**(9): p. e1-6.
44. Swencki-Underwood, B., et al., *Expression and characterization of a human BMP-7 variant with improved biochemical properties*. Protein Expr Purif, 2008. **57**(2): p. 312-9.
45. Wen, N.X. and S. Venkatraman, *Protein delivery options: how well have we succeeded?* Ther Deliv, 2015. **6**(5): p. 537-9.
46. Bruno, B.J., G.D. Miller, and C.S. Lim, *Basics and recent advances in peptide and protein drug delivery*. Ther Deliv, 2013. **4**(11): p. 1443-67.

47. Feng, L., et al., *Discovery of a Small-Molecule BMP Sensitizer for Human Embryonic Stem Cell Differentiation*. Cell Rep, 2016. **15**(9): p. 2063-75.
48. Korchynskiy, O. and P. ten Dijke, *Identification and functional characterization of distinct critically important bone morphogenetic protein-specific response elements in the Id1 promoter*. J Biol Chem, 2002. **277**(7): p. 4883-91.
49. Jacob, R.T., et al., *MScreen: an integrated compound management and high-throughput screening data storage and analysis system*. J Biomol Screen, 2012. **17**(8): p. 1080-7.
50. Bradford, S.T.J., et al., *High-throughput screens for agonists of bone morphogenetic protein (BMP) signaling identify potent benzoxazole compounds*. J Biol Chem, 2019.
51. Lipinski, C.A., et al., *Experimental and computational approaches to estimate solubility and permeability in drug discovery and development settings*. Advanced Drug Delivery Reviews, 1997. **23**(1-3): p. 3-25.

Acknowledgements

We are grateful to the Center for Chemical Genomics at the University of Michigan Life Science Institute for providing their technical expertise and support. Specifically, M. Larsen for technical assistance with the High-Throughput Screening campaign and triage of active compounds. As well as, A. White, (Vahlteich Medicinal Chemistry Core) for also assisting with active compound triage and selection. This work was supported by the following United States National Institutes of Health grants: NIDDK 5R01DK054740-16 and NIDDK 3R01DK054740-16S1. Funding was also provided by the University of Michigan Center for the Discovery of New Medicines directed by V. Groppi.

Chapter 3 – Characterization of BMP signaling agonists identified using HTS

Abstract

After cell-based HTS assays are performed, multiple points along the molecular pathway under examination are usually interrogated as the direct molecular target is unknown. This can be accomplished by conducting secondary assays that measure activation of second messengers and/or activation of endogenous pathway genes. A plethora of other assays can also be utilized to help gain mechanistic insights about the “hits” identified in a cell-based HTS. Once a lead compound is established, structure-activity relationship (SAR) studies are also utilized to assess which features of the lead compound are critical to induce the observed effects of the compound. After screening nearly 64,000 small-molecules in a renal BRE-Luc reporter cell line we identified a lead compound termed sb4. We discovered that sb4 is a potent benzoxazole small-molecule that activates BRE-Luc in a dose-dependent manner. Furthermore, as assessed by western blotting, sb4 was found to activate the BRE-Luc reporter by stabilizing intracellular levels of p-SMAD-1/5/9. The increased levels of p-SMAD-1/5/9 observed with sb4 culminate in activation of endogenous BMP target genes such as ID1 and ID3. Significantly, sb4 mediated activation of the BMP signaling pathway is resistant to inhibition by Noggin and type I BMP receptor kinase inhibitors.

Introduction

As discussed in Chapter 2, cell-based HTS assays provide a more physiological approach for screening large libraries of small-molecules compared to biochemical HTS assays, which employ isolated purified proteins [1]. However, with cell-based HTS the direct molecular target and the chemotype class that will best modulate the molecular target are both unknown [1, 2]. Therefore, entire signaling pathways are usually the initial target of interrogation in primary cell-based HTS assays, which as detailed in chapter 2 employ artificial reporter gene systems [1]. Being able to interrogate along an entire signaling pathway in cell-based HTS assays provides two advantages: 1) expansion of the catalog of molecular targets that can be identified and 2) potentially produces more diverse chemotypes for drug/lead-like identification [1].

In secondary assays following a cell-based HTS and compound triage, endogenous components of the pathway can be interrogated after compound treatment to help gain mechanistic insights. Some secondary assays that can be used include immunoblotting for induction or activation of second messengers of the pathway. Or, assessing the influence of known chemical agents and endogenous factors of the interrogated pathway post compound treatment. Additionally, assessment of direct target genes in the pathway can also be evaluated after compound treatment. Furthermore, secondary assays also help reassure that compound treatment does not alter the artificial reporter gene system by unwanted mechanism [3-6].

Using various cell types, several laboratories have identified chemical entities that stimulate both canonical and non-canonical BMP signaling in luciferase-based HTS. The activity of these chemical entities was subsequently validated and characterized further by using a variety of secondary assays. For instance, in a primary HTS study using mouse myoblasts (C2C12 cells) stably expressing a BMP response element from the ID1 promoter linked to luciferase, FK506 was

found to activate BMP signaling [7, 8]. For secondary assays, FK506 was tested in human pulmonary arterial endothelial cells in order to investigate the mechanism of action of increased BMP signaling observed in the primary HTS [8]. By western blotting, levels of p-SMAD-1/5/8 were assessed after FK506 treatment for 15m, 1h, 6hrs, and 24hrs. BMP signaling as assessed by SMAD-1/5/8 phosphorylation, was the most robust after 15 minutes compared to the control after FK506 treatment. Additionally, ID1 (direct gene target of BMP signaling) levels were assessed by western blotting after FK506 treatment. ID1 levels after FK506 treatment were the most robust after 1hr of FK506 treatment.

Additionally, FK506 was tested in LDN-193189 (type I BMP receptor inhibitor) treated BRE-Luc C2C12 cells and failed to induce BMP signaling [8]. Knock-down of type I BMP receptors (Alk1/2/3) also compromised FK506 induced BMP signaling. Moreover, coimmunoprecipitation studies showed that FKBP12 binds to type I BMP receptors and that FK506 was able to release FKBP12 from Alk1, Alk2, and Alk3 [8]. Through the secondary assays conducted in this study, the investigators were able to conclude that FK506 activates BMP signaling via liberating the glycine/serine-rich domains of type I BMP receptors from FKBP12 inhibition which allows its interaction with constitutively active type II BMP receptors such as BMPRII [8].

Alongside secondary assays, structure-activity relationship (SAR) studies are also undertaken as another measure to further characterize as well as optimize the hits selected after cell-based HTS. The idea of SAR was initially postulated more than 150 years ago and describes the relationship between the chemical substituents of a compound and its observed biological effects. Gaining SAR knowledge allows a medicinal chemist to modify the chemical substituents of a drug/lead-like compound to potentially achieve higher potency and/or efficacy, as well as,

reduce toxicity and off-target activity. To initiate SAR studies after HTS, similar compounds are clustered into similar groups based on common chemical motifs and expanded if needed by various strategies (e.g. through the purchase of analogs or medicinal chemistry efforts). Generally, compounds with similar structures produce similar biological effects. However, changing a particular substituent could make the compound toxic or inactive, even though it may have a similar structure.

SAR studies have been utilized to identify potent inhibitors of the BMP signaling pathway. For example, using an *in vivo* zebrafish assay to screen over 7,500 compounds consisting of FDA approved and other commercially available diverse compounds, dorsomorphin (compound C) was identified. Dorsomorphin was found to produce substantial and reproducible dorsalization of zebrafish embryos [9]. Accordingly, was the first reported small-molecule inhibitor of the BMP signaling pathway [9]. However, dorsomorphin had been previously recognized as an inhibitor of AMP-activated protein kinase (AMPK) and labeled compound C. Moreover, within the characterization stages of dorsomorphin, significant off-target inhibitory effects were observed on vascular endothelial growth factor (VEGF) type 2 receptors [10]. Therefore, in an effort to find analogs of dorsomorphin that did not act on type 2 VEGF receptors or AMPK, SAR studies were performed. From these dorsomorphin SAR studies DMH1 (dorsomorphin homolog 1) was identified and found to have no activity against ALK5 (TGF β R-1), AMPK, or VEGFR2 [10]. Additional SAR studies have also identified LDN-193189 as potent type I BMP receptor inhibitor [11]. LDN-193189 is more selective than DMH1 but has activity at ALK5 and KDR [10]. Using SAR, LDN-212854 has also been identified as potent type I BMP receptor inhibitor [12].

Results:

p-SMAD-1/5/9 is induced after BMP signaling agonists treatment

Binding of BMP ligand causes heterotetramerization of type II and type I BMP receptors. After becoming phosphorylated by type II BMP receptors, the type I BMP receptor is activated and in turn rapidly phosphorylates SMADs-1/5/9—key intracellular transducers of canonical BMP signaling. To determine if phosphorylation of SMAD-1/5/9 was increased in the presence of our top twelve compounds, we treated renal BRE-Lucs for 1hr with 10 μ M of each compound and assayed for p-SMAD-1/5/9 induction by immunoblotting. 2 ng/ml of rh-BMP4 ligand + 0.04% DMSO (1hr) served as our positive control and induced p-SMAD-1/5/9 10.9-fold over 0.04% DMSO (negative control, vehicle) (**figures 3.1A-B**). Additionally, we found that 1hr of treatment with several of our top twelve BMP signaling agonists significantly increased the abundance of p-SMAD-1/5/9 at least 2-fold or more above the levels after 0.04% DMSO-D6 treatment (**figures 3.1A-B**). That several agonists increased levels of p-SMAD-1/5/9 within 1hr \geq 2-fold, suggests that our BMP signaling agonists may have the capacity to directly stimulate canonical BMP signaling. Similarly, Genthe and colleagues recently conducted a 643,432 compound HTS assay which identified three compounds that stimulate canonical BMP signaling within 1hr [13]. Collectively, this evidence supports the feasibility of identifying small-molecules using high-throughput screening that can mimic key downstream effects of endogenous BMP ligands.

Activation of non-canonical BMP signaling by our top twelve compounds was also assessed by immunoblotting for induction of mitogen-activated kinases p38, ERK1/2, and JNK. We found some of our BMP signaling agonists (sb7-sb11) decreased levels of p-ERK1/2 after 1hr of treatment but most all had little on p-p38 or p-JNK (**figure 3.2A and B-C**). In addition, BMPs stimulate the phosphorylation of transforming growth factor β -activated kinase 1 (p-TAK-1).

However, sb12 decreased levels of p-TAK-1, whereas there was no significant increase of p-TAK-1 by the other compounds (**figure 3.2D**). To ensure specificity, we also assessed levels of the TGF- β effectors, p-SMAD-2 and p-SMAD-3, after treatment with our top twelve BMP signaling agonists. Similar to rh-BMP4 dosing, the compounds had no significant effect on TGF- β signaling effectors. Specifically, BMP signaling agonists dosed at 10 μ M for 1hr did not change basal levels of p-SMAD-2/3 relative to levels of p-SMAD-2/3 after 0.04% DMSO treatment (**figure 3.3A**).

BMP signaling is stimulated in renal epithelial cells after sb4 treatment

To determine if SMAD-1/5/9 phosphorylation is induced in the presence of our top twelve compounds in other renal cell types, we employed serum-starved mouse primary renal epithelial cells (PRECs) for compound testing, which lack the BRE-Luc reporter construct. First, we assayed rh-BMP4 in dose-response in serum-starved PRECs. We observed that PRECs are highly sensitive to rh-BMP4 treatment by detection of robust and specific p-SMAD-1/5/9 induction (**figure 3.4A**). After 1hr, 2 ng/ml of rh-BMP4 resulted in a 35-fold induction of p-SMAD-1/5/9 over untreated PRECs (control) (**figure 3.4B**). PRECs were ~2-fold or greater more responsive to rh-BMP4 at each concentration tested (**figure 3.4A-B**) in comparison to BRE-Lucs (**figure 2.1C-D**). From the top twelve BMP signaling agonists, we assayed sb4 in serum-starved PRECs. We observed induction of phosphorylated SMAD-1/5/9 in a dose-dependent manner (**figure 3.4C-D**), with sb4 at 100 and 300 nM yielding a 2-fold induction over 0.004% DMSO after 24hrs of treatment. Although not as robust as rh-BMP4, our results suggest that sb4 can significantly increase p-SMAD-1/5/9 abundance in PRECs under serum-starved conditions.

Noggin and type I BMP receptor inhibition is bypassed by sb4

To gain insight about how our top twelve BMP signaling agonists act to induce p-SMAD-1/5/9 and luciferase gene induction, we conducted luciferase-based inhibitor studies with both endogenous and chemical inhibitors of the BMP signaling pathway. Noggin is an endogenous inhibitor of BMP signaling that acts by sequestering dimerized BMP ligands away from BMP receptors and thus suppressing BMP signaling [14]. We treated cells with one of our top twelve BMP signaling agonists, sb4, alone or with 250 ng/ml of rh-Noggin. Our results revealed that BMP signaling was not suppressed when sb4 was added in the presence of Noggin (**figure 3.5B**). This is in contrast to adding rh-BMP4 in the presence of Noggin where, BMP signaling is dramatically suppressed (**figure 3.5A**). This suggests that sb4 is able to bypass negative regulation by rh-Noggin and activate BMP signaling. Additionally, we tested the chemical inhibitor, LDN-193189, which selectively inactivates type I BMP receptors [11, 15]. Sb4 remained active in the presence of 1 μ M LDN-193189 (**figure 3.5D**), while rh-BMP4 activity was abolished (**figure 3.5C**). Taken together, our results indicate that sb4 works to activate BMP signaling downstream of Noggin and type I BMP receptors, which suggests that it works through an alternative mechanism.

BMP signaling efficacy is enhanced and maintained with sb4 treatment

To determine whether the efficacy of BMP signaling is enhanced in the presence of sb4 we assayed varying concentrations of rh-BMP4 in the presence of a constant concentration of sb4 (10 μ M). We found that sb4 enhanced the efficacy of BMP signaling at each concentration tested of rh-BMP4 (0.4, 1, 10, 40 ng). The enhancing effect of sb4 was best detected when low levels of rh-BMP4 ligand were present. As, sb4 increased BRE-Luc expression nearly 2-fold at 0.4 and 1 ng/ml of rh-BMP-4, the effect tapered off with higher concentrations of rh-BMP4 (**figure 3.6A**). These data show that sb4 not only activates BMP signaling independently of rh-BMP4 ligand (**figure 3.1A-B and figure 3.4C-D**) but, it also enhances BMP signaling activity. Furthermore, these data suggest that sb4 may act to stabilize p-SMAD-1/5/9 to enhance the transcriptional response. Feng and colleagues similarly discovered that compound, PD-407824, identified in a 4,000 compound HTS, functions as a BMP4 sensitizer in mouse C2C12 myoblasts [16].

To test more directly if sb4 stabilizes p-SMAD-1/5/9, we examined the decay of p-SMAD-1/5/9 after rh-BMP4 stimulation in the presence or absence of sb4. We stimulated BRE-Luc for 1hr with media containing 2 ng/ml rh-BMP4, removed the media, and immediately treated cells with either DMSO-D6 (0.004%) or 1 μ M sb4 and harvested cells at 0, 5, 15, 30, 45, and 60 minutes after treatments. Immunoblotted lysates of cells treated with 1 μ M sb4 at each timepoint had more levels of p-SMAD-1/5/9 than DMSO-D6 treated cells (**figure 3.6B-C**). In particular, cells treated with 1 μ M sb4 for 5 minutes had significantly more p-SMAD-1/5/9 than DMSO-D6 treated cells after 5 minutes. This suggests that sb4 may exert its effects by protecting p-SMAD-1/5/9 from decay and therefore preserves BMP signaling. Cao and colleagues identified two structurally distinct compounds (A01 and A17) that stabilized and prolonged total-Smad-1/5 levels in both dose and time dependent manners, respectively, by inhibiting the interaction between total-SMAD-

1/5 and Smurf (SMAD ubiquitination regulatory factors) which, promotes degradation of total-SMAD-1/5 [17].

Direct BMP4 gene targets are increased following sb4 treatment

Enhancement of BMP signaling efficacy in our luciferase and western blot studies prompted us to ask if endogenous direct BMP4 target genes are upregulated after sb4 dosing. Since our compounds mimic the activity of low-dose BMP4, we conducted a transcriptomic analysis in BRE-Lucs treated for 4hrs with 2ng/ml rh-BMP4. We identified thirty-one genes upregulated between 1.5-3.7-fold above medium only treated cells ($p < 0.05$) (**figure 3.7A-B**). We assayed two of the top thirty-one BMP4 target genes to determine if compound sb4 could modulate the expression of these genes. At 24 hrs, sb4 significantly increased the expression of ID1 and ID3 (**figure 3.7C-D**). We also assayed, COL2A1, a non-significant gene in our low-dose BMP4 transcriptomic analysis. Sb4, did not increase COL2A (**figure 3.7E**).

Analogs of sb4 increase BMP signaling in a dose-dependent manner

Testing of structural analogs of sb4 could identify compounds with increased efficacy and also reveal initial structure activity relationships (SARs). Thus, we compared 10 related compounds to sb4 and sb3 in our cell-based luciferase reporter assay and determined the EC₅₀'s (**figure 3.8**). Of these 10 compounds, 4 were inactive and 6 were active compounds with EC₅₀'s ranging from 16.2 nM to 274.4 nM. For these benzyl-thio-benzo-oxazole compounds, the substitution at the benzene ring of the benzyl group seems to be important. From the initial SAR analysis, the data shows a very tight structure-activity relationships. For example, benzyl or pyridyl for R₂ makes compounds inactive as in sb4.a1 and sb4.a4 but a methyl substituted benzyl at the *para* position makes the most active compound with EC₅₀ of 16.16 nM as in sb4.a2. Different substitutions of benzyl with fluorine, chlorine, and bromine at the *para* position as in sb4.a5, sb4.a3, and sb4, respectively also make compounds active but not as active as the methyl group. For *para* substitution, methyl is the best (sb4.a2: 16.16), followed by fluorine (sb4.a5: 60.14), bromine (sb4: 73.62), then by chlorine (sb4.a3: 77.05). Compared to substitution at the *para* position of the benzyl as in sb4.a5, substitution at the *ortho* position with F as in sb3 reduces activity. Compared to substitution at the *para* position of the benzyl as in sb4.a3, substitution at the *meta* position with Cl as in sb4.a6 makes compound 5 times less active. Substitution at the *ortho* position of the benzyl with methoxy is 2 times less active than fluorine. The fluorine-substituted compound at the *ortho* position is 10% more active when chlorine is substituted at the other *ortho* position at the same time as in sb4.a10. The inactivity of sb4.a7 could be either due to the steric effect of the substitution of methyl at the benzo-oxazole or due to the lack of aromatic ring at the right-hand side, or both. The oxazolo-pyridine in place of the benzo-oxazole as in sb4.a9 kills the activity. Overall, the substitutions at the *para* or *ortho* position of benzyl group is

preferred to at the *meta* position. These data suggest that modification of benzo-oxazole is not tolerated.

Discussion

In order to identify chemical compounds that could be the basis for developing therapeutic BMP signaling agonists, we designed a cell-based HTS and identified multiple specific small-molecules that enhance and/or stabilize p-SMAD-1/5/9, key second messengers in BMP signaling. Our unbiased cell-based HTS identified a novel compound, sb4, that rapidly activates BMP signaling in renal cell cultures. We found that sb4 increased levels of p-SMAD-1/5/9 within 1hr and increased the expression of direct key BMP4 target genes (ID1 and ID3). Additionally, our experiments revealed that sb4 acts downstream of type I BMP receptors and bypasses negative regulation by Noggin, an extracellular inhibitor of BMP signaling. Moreover, in the presence of rh-BMP4, sb4 enhances BMP signaling efficacy by slowing the turnover or decay of p-SMAD-1/5/9.

Several other laboratories have also reported the identification of activators/sensitizers of BMP signaling in other cell types. Of note, some of these previously published BMP activators such as Isoliquiritigenin [18], FK506 [8], PD-407824 [16], were tested in our primary HTS screen. However, they did not meet our cut off for further analysis due to either having low activity in our primary screen or not meeting the criteria to pass our counter screen. This may underscore the potential of diverse compound structures to induce cell type specific responses. In a broader sense, it stresses the importance of identifying direct targets and determining the mechanism of action of these diverse compounds. As, each molecule may target different levels/aspects of canonical or non-canonical BMP signaling. And therefore, induce varying intensities of activation of BMP signaling culminating in diverse biological effects.

Canonical receptor-SMAD-1/5/8/9 activation occurs via phosphorylation by type I BMP receptors. Phosphorylation at the c-terminal transcriptional domain of SMADs-1/5/8/9 facilitates

co-SMAD4 docking and heteromeric SMAD transcriptional complex formation. In addition, the linker interdomain of SMADs-1/5/8/9 undergo phosphorylation by cyclin dependent kinases (CDK8/9) and glycogen synthase 3 (GSK3), which renders R-SMADs fully functional [19]. To control activated BMP/SMAD-1/5/8/9 signaling duration and intensity, fundamental turnover mechanisms, such as dephosphorylation and ubiquitination, are necessary. In particular, small c-terminal domain ser/thr phosphatases (SCPs) have been identified that dephosphorylate the c-terminal transcriptional domain of SMAD-1 after type I BMP receptor phosphorylation [20, 21] and the linker interdomain after CDK8/9 phosphorylation [21]. Experimental siRNA mediated knockdown of SCPs-1/2 conferred increased BMP signaling and *Id1* expression in human keratinocytes and osteosarcoma cell lines [20]. Thus, small molecules such as sb4 could potentially inhibit such phosphatases and prove beneficial in disease states such as CKD.

The Smurf proteins (SMAD ubiquitination regulatory factors) also negatively regulate BMP/SMAD activity [22]. GSK3 phosphorylation recruits Smurfs to the BMP/SMAD linker interdomain to ubiquitinate activated BMP/SMADs for proteasomal degradation [23, 24]. Increased BMP signaling is also observed following siRNA mediated knockdown of Smurf [25]. Yes associated proteins (YAPs) are also recruited to the linker region of SMAD-1, but instead, function to enhance BMP/SMAD transcriptional activity and therefore signaling [25]. Because sb4 activates BMP signaling independent of Noggin or type I BMP receptor inhibition, it's plausible that increased levels of p-SMAD-1/5/9 observed in this study can be potentially attributed to inhibiting SCP or Smurf activity or promotion of YAP function. Further studies are needed to identify the direct targets of sb4 and its analogs to unravel the precise mechanism of action. Future studies in particular may include screens for molecules that dephosphorylate and

ubiquitinate SMADs-1/5/9 in BRE-Luc cells. Once identified, later assays to determine the effect of sb4 on these molecules will be pertinent.

Figures

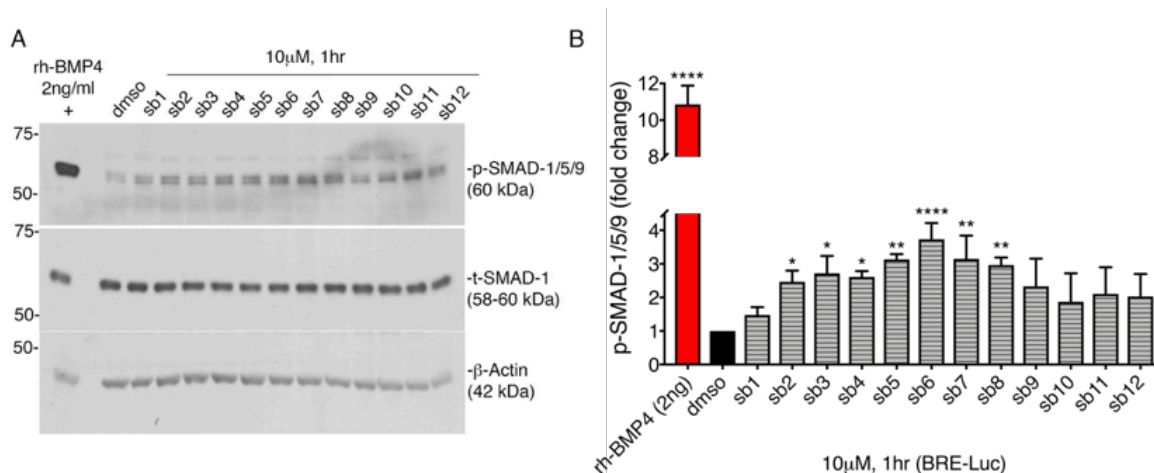


Figure 3.1 Activation of p-SMAD-1/5/9 by HTS small-molecules.

(A) Immunoblot of whole cell protein lysates from BRE-Luc cells treated with either 2 ng/ml rh-BMP4, 0.04% DMSO, or the top twelve BMP candidate agonists at 10 μM for 1 hour in BRE-Luc cells. Membranes were probed with anti-p-SMAD-1/5/9 and anti-total-SMAD-1. β-Actin served as an additional loading control. (B) Quantitation of p-SMAD-1/5/9 protein levels as determined by densitometry of three independently derived western blots. The p-SMAD-1/5/9 levels were normalized to total-SMAD-1. Final data are expressed as fold change relative to the mean negative control signal, with error bars representing one standard deviation (*p < 0.05, **p < 0.01, ****p < 0.0001 relative to control). ANOVA, Dunnett's post-hoc multiple comparisons test was used to determine significance. This figure appears in—**Bradford, S. T. J., E. J. Ranghini, E. Grimley, P. H. Lee and G. R. Dressler (2019). "High-throughput screens for agonists of bone morphogenetic protein (BMP) signaling identify potent benzoxazole compounds." J Biol Chem. PMID: 30602563 [26].**

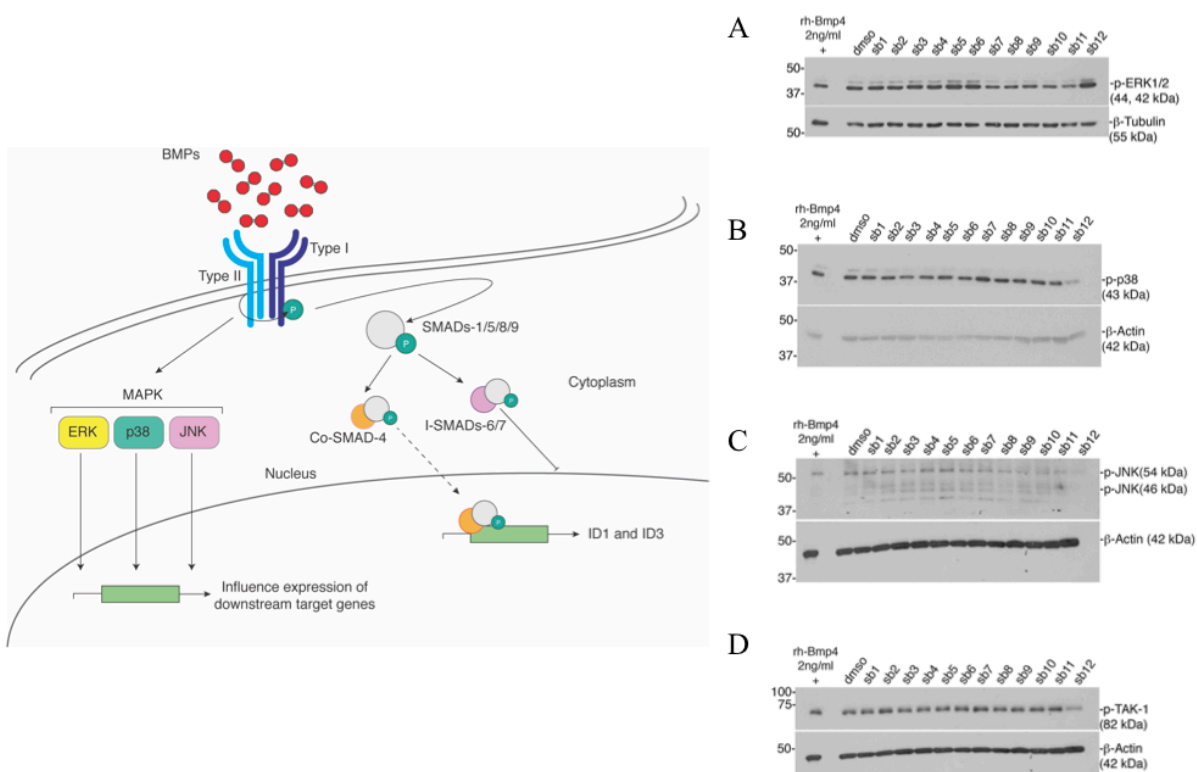


Figure 3.2 Evaluation of the top twelve agonists in non-canonical BMP signaling activation.

In non-canonical BMP signaling, dimerized BMP ligands binding to their receptors can activate mitogen-activated kinases p38, ERK1/2, and JNK. Non-canonical BMP signaling can also activate p-TAK-1. Above, immunoblots of lysates from BRE-Luc cells treated with either 2 ng/ml rh-BMP4 (positive control), 0.04% DMSO-D6 (negative control), or top twelve BMP signaling agonists at 10 μ M for 1 hour in BRE-Luc cells. Membranes were probed with either (A) p-ERK-1/2, β -Tubulin was used as a loading control or (B) p-p38 (C) p-JNK (D) p-TAK-1, β -Actin was used as at loading control. This figure appears in—Bradford, S. T. J., E. J. Ranghini, E. Grimley, P. H. Lee and G. R. Dressler (2019). "High-throughput screens for agonists of bone morphogenetic protein (BMP) signaling identify potent benzoxazole compounds." *J Biol Chem*. PMID: 30602563 [26].

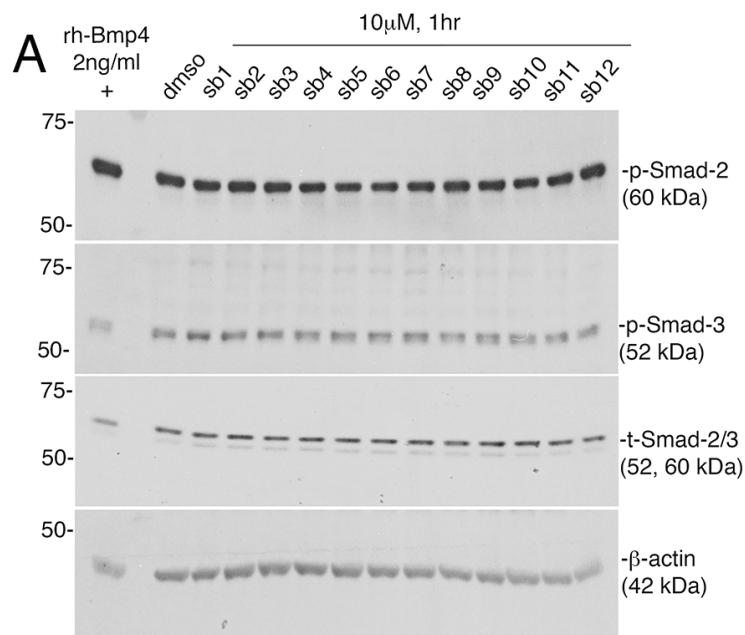


Figure 3.3 Assessment of the top twelve agonists in TGF-β signaling effector induction.

(A) Immunoblot of lysates from BRE-Luc cells treated with either 2 ng/ml rh-BMP4 (positive control), 0.04% DMSO-D6 (negative control), or top twelve BMP signaling agonists at 10 μM for 1 hour in BRE-Luc cells. Membranes were probed with p-SMAD-2, p-SMAD-3, and total-SMAD-2/3. β-Actin was used as an additional loading control. This figure appears in—**Bradford, S. T. J.**, E. J. Ranghini, E. Grimley, P. H. Lee and G. R. Dressler (2019). "High-throughput screens for agonists of bone morphogenetic protein (BMP) signaling identify potent benzoxazole compounds." *J Biol Chem*. PMID: 30602563 [26].

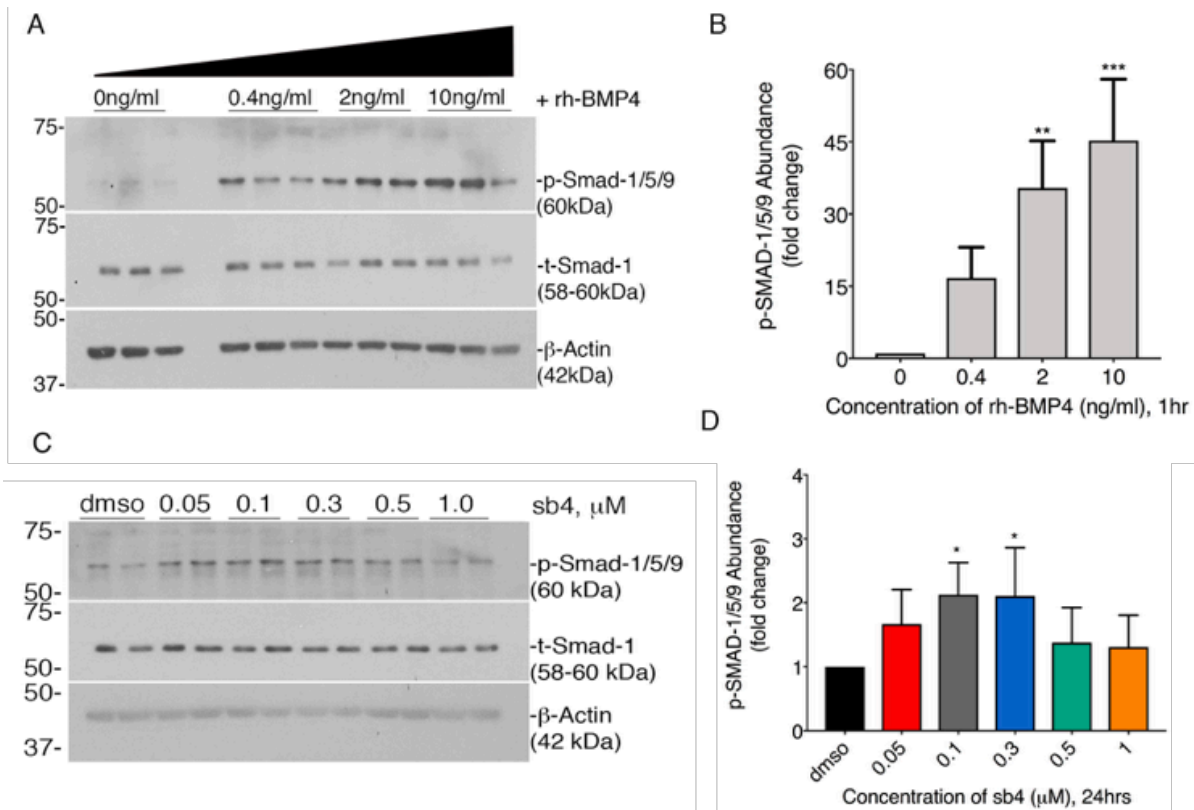


Figure 3.4 Activation of p-SMAD-1/5/9 by sb4 in PRECs.

(A) Immunoblot of lysates from 1hr serum-starved PRECs subsequently treated for 1hr with increasing concentrations of rh-BMP4 prepared in serum free medium. (B) p-SMAD-1/5/9 abundance, semi-quantified by densitometry. (C) Immunoblot of lysates from 1hr serum-starved PRECs subsequently treated for 24hrs with increasing concentrations of sb4 prepared in serum free medium. (D) p-SMAD-1/5/9 abundance, semi-quantified by densitometry. Membranes were probed with p-SMAD-1/5/9 and total-SMAD-1, β -Actin was used as an additional loading control. The signal of p-SMAD-1/5/9 was normalized to total-SMAD-1 to control for loading variability. Final data are expressed as fold change relative to the mean negative control signal (0ng/ml rh-BMP4 or 0.004% DMSO-D6 which, were set to 1). Means \pm SD (error bars) are reported. * $p < 0.05$, ** $p < 0.01$ *** $p < 0.001$, for rh-BMP4 at 0.4ng/ml and sb4 at 0.05, 0.5, and 1 μ M $p > 0.05$ relative to control, 0ng/ml rh-BMP4 or 0.004% DMSO-D6 (ANOVA; Dunnett's post-hoc multiple comparisons test). $n = 3-4$ independent biological replicates. Panels C and D appear in—**Bradford, S. T. J., E. J. Ranghini, E. Grimley, P. H. Lee and G. R. Dressler (2019). "High-throughput screens for agonists of bone morphogenetic protein (BMP) signaling identify potent benzoxazole compounds." J Biol Chem. PMID: 30602563 [26].**

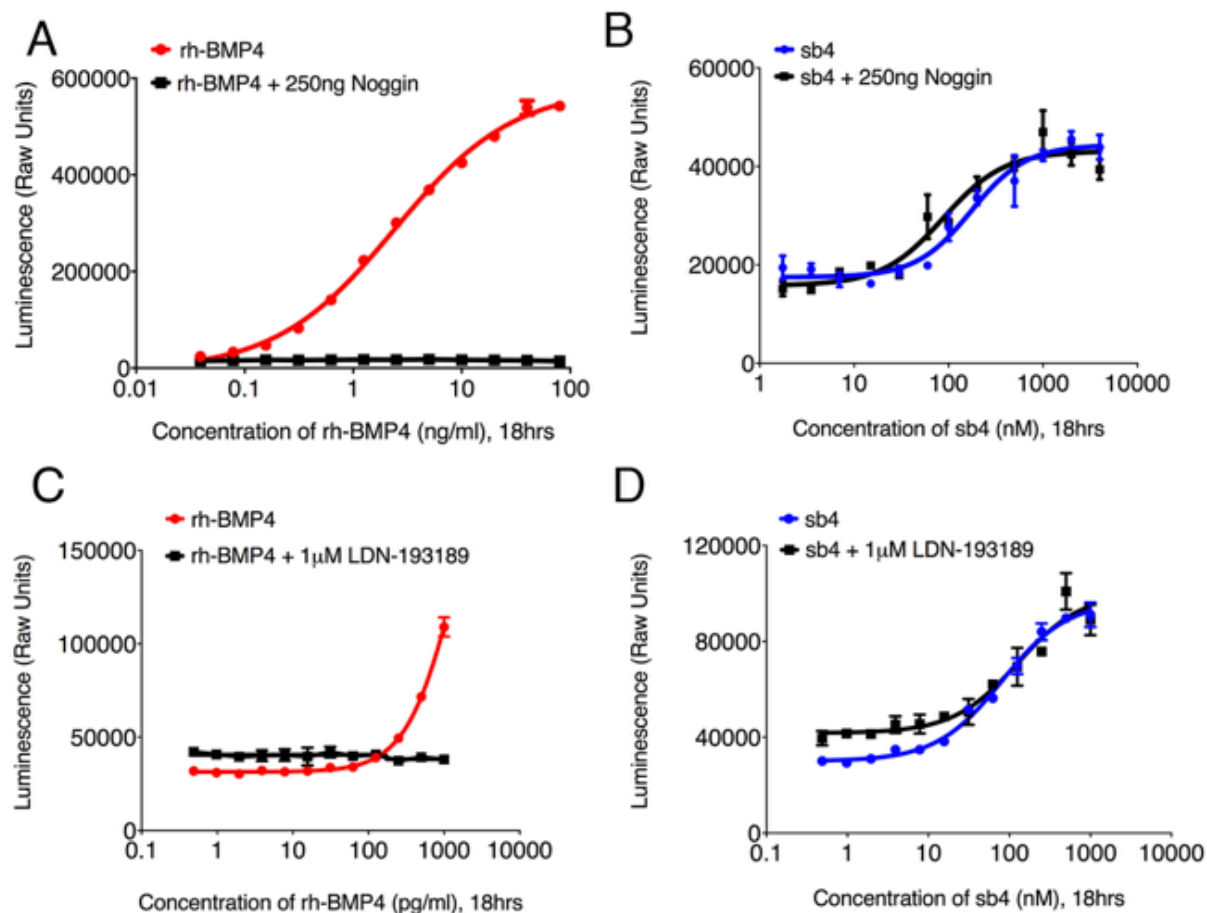


Figure 3.5 Effects of endogenous and chemical BMP inhibitors on sb4 activity.

(A) BRE-Luc cells were subjected to increasing concentrations of rh-BMP4 with (black) or without (red) 250 ng/ml of rh-Noggin. Maximum concentrations of 80 ng/ml for rh-BMP4 were used and cells were incubated for 18hrs before measuring luminescence. (B) A dose-response for sb4 was measured in BRE-Luc cells alone (blue) or in the presence of 250 ng/ml rh-Noggin (black). A maximum concentration of 4 µM of sb4 was used. (C) Activity of increasing concentrations of rh-BMP4 in BRE-Luc cells alone (red) or with a constant dose of 1 µM type I BMP receptor inhibitor (LDN-193189, black). For both curves a maximum concentration of 1000 pg/ml rh-BMP4 was used and cells were incubated for 18hrs before measuring luminescence. (D) Increasing concentrations of sb4 were added to BRE-Luc cells alone (blue) or in the presence of 1 µM LDN-193189 (black). A maximum of 1000 nM of sb4 was used. Experiments were conducted in triplicate. This figure appears in—**Bradford, S. T. J.**, E. J. Ranghini, E. Grimley, P. H. Lee and G. R. Dressler (2019). "High-throughput screens for agonists of bone morphogenetic protein (BMP) signaling identify potent benzoxazole compounds." *J Biol Chem*. PMID: 30602563 [26].

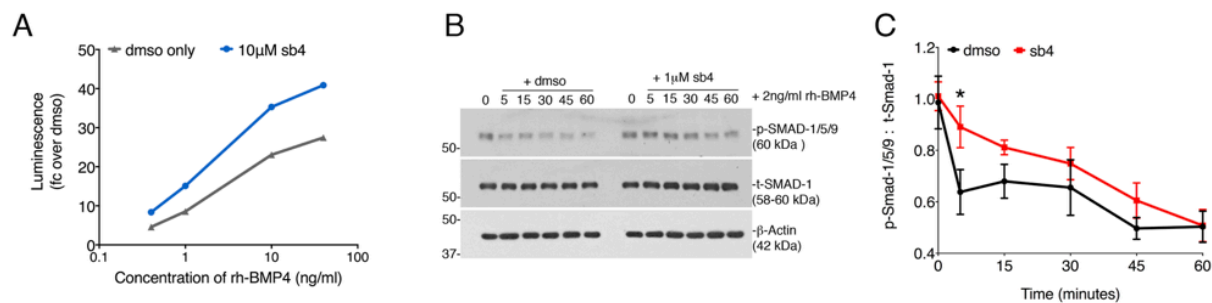


Figure 3.6 BMP signaling agonists enhance the efficacy of BMPs.

(A) BRE-Luc cells were treated with DMSO (grey) or sb4 (blue) at a constant concentration of 10 μ M in the presence of increasing concentrations of rh-BMP4 (0.4, 1, 10 and 40 ng/ml) for 18 hours. Representative experiment conducted in triplicate, reported as fold change over DMSO. (B) Western blot of protein lysates from BRE-Luc cells treated for 1 hour with rh-BMP4 (2 ng/ml) followed by fresh media containing either vehicle (DMSO) or 1 μ M sb4. Samples were harvested at 0, 5, 15, 30, 45, and 60 minutes after sb4 addition. A representative western blot for p-SMAD-1/5/9 from three independent biological experiments is shown. (C) Ratio of p-SMAD-1/5/9 to total-SMAD-1 as quantified by densitometry is shown for experiments outlined in C. Ratio of p-SMAD-1/5/9 to total-SMAD-1 over time was compared by unpaired multiple t-tests. *p-value = 0.02. Note the increased stability of p-SMAD-1/5/9 in sb4 treated cells. This figure appears in—**Bradford, S. T. J., E. J. Ranghini, E. Grimley, P. H. Lee and G. R. Dressler (2019). "High-throughput screens for agonists of bone morphogenetic protein (BMP) signaling identify potent benzoxazole compounds." J Biol Chem. PMID: 30602563 [26].**

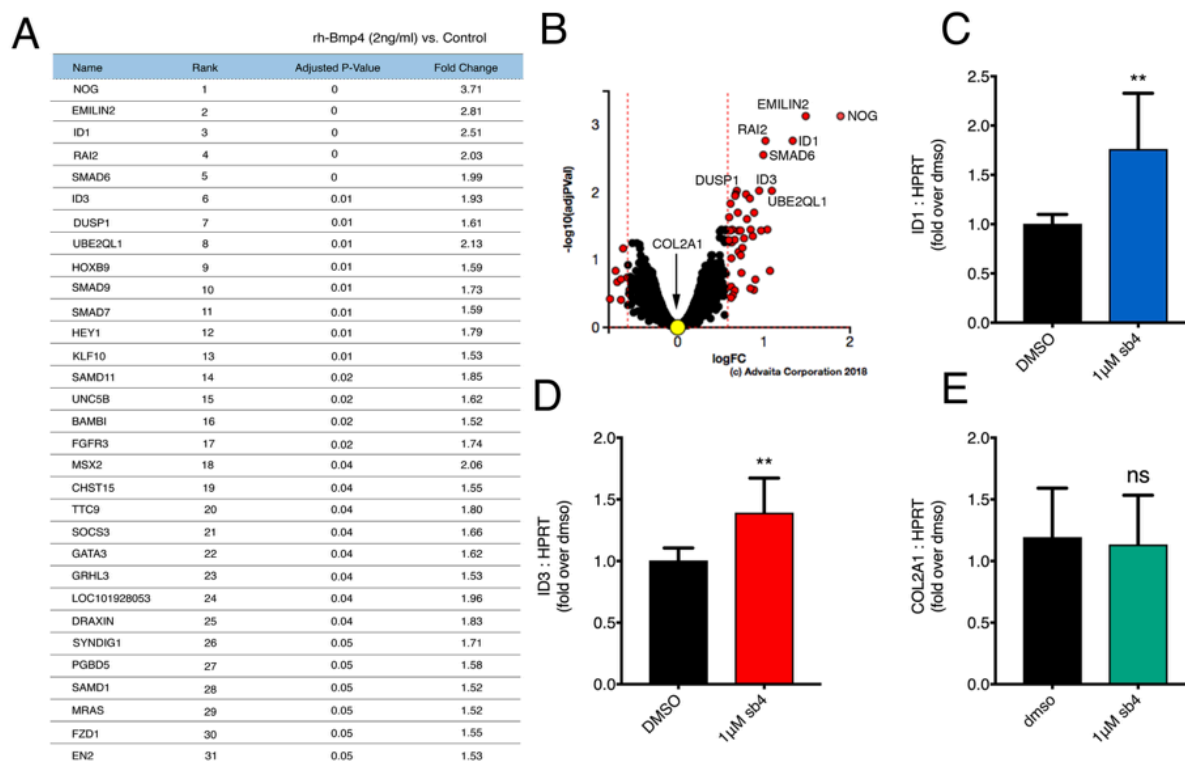


Figure 3.7 Sb4 activates endogenous BMP4 target genes.

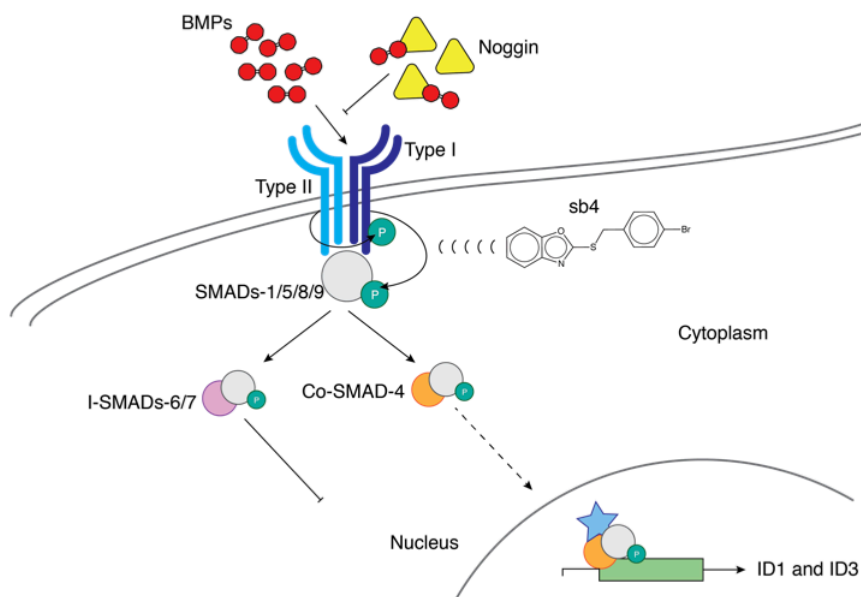
(A) The top 31 genes with increased transcriptional activation after 4 hours of rh-BMP4 (2 ng/ml) as determined by Affymetrix microarrays. Triplicate biological replicates were performed for treated and untreated groups. The p-values ≤ 0.05 and fold changes ≥ 1.5 are reported for treated vs. untreated groups. (B) Volcano plot of 6,643 genes that were measured for expression. 51 genes were differentially expressed between treated and untreated groups. Significant differentially expressed genes are shown in red dots, black and selected yellow dots represent non-significant genes. The volcano plot was generated by uploading transcriptomic data into iPathwayGuide, with cut off fold change and p-values set to 0.58 and 1 respectively. (C-E) Quantitative RT-PCR analysis was used to determine the relative mRNA levels of endogenous rh-BMP4 target genes after 1 μ M sb4 treatment. The *ID1* (C) and *ID3* (D) genes show significant upregulation, whereas *COL2A1* (E) remains unchanged. Data represent the mean and one standard deviation from three independent biological experiments performed in triplicate (**p-value < 0.01, ns = not significant: unpaired t-test). This figure appears in—Bradford, S. T. J., E. J. Ranghini, E. Grimley, P. H. Lee and G. R. Dressler (2019). "High-throughput screens for agonists of bone morphogenetic protein (BMP) signaling identify potent benzoxazole compounds." *J Biol Chem.* PMID: 30602563 [26].

Compound	R ₁	R ₂	EC ₅₀ (nM)	Max Response at 500 nM (Fold Induction)	Max Response at 1000 nM (Fold Induction)
SB3			87.09	2.89	2.89
SB4			73.62	2.97	3.10
SB4.a1			NA	NA	NA
SB4.a2			16.16	3.36	3.02
SB4.a3			77.05	2.85	3.79
SB4.a4			NA	NA	NA
SB4.a5			60.14	3.07	2.83
SB4.a6			274.4	1.57	2.03
SB4.a7			NA	NA	NA
SB4.a8			184	1.79	2.31
SB4.a9			NA	NA	NA
SB4.a10			78.91	2.64	2.67

Figure 3.8 Initial Structure Activity Relationships (SAR) among 11 sb4-like compounds.

Dose-response curves for analog structures of sb4 were tested in BRE-Luc cells. The effective concentration at 50% maximum activity (EC₅₀) was calculated and units are reported in nM for each structure as shown. Compounds that were not active at the concentrations tested are labeled NA. The PubChem ID numbers are listed below the designated name. A portion of this figure this figure appears in—**Bradford, S. T. J.**, E. J. Ranghini, E. Grimley, P. H. Lee and G. R. Dressler (2019). "High-throughput screens for agonists of bone morphogenetic protein (BMP) signaling identify potent benzoxazole compounds." *J Biol Chem*. PMID: 30602563 [26].

sb4



- Low $EC_{50} = 74$ nM
Hill Slope = 1.24,
Acts rapidly
- Resistant to endogenous BMP and chemical inhibition
- Stabilizes p-SMAD-1/5/9
- Activates direct targets of BMP signaling: ID1, ID3
- Sb4 analogs: dose-dependent BRE-Luc activation
- SAR: substitution at the benzene ring for R_2 seems to be important

Figure 3.9 Profile of sb4 and key mechanistic insights gained.

Materials and Methods

Immunoblotting

BRE-Lucs were passaged in DMEM supplemented with 5% FBS (vol/vol) for both HTS and 6-well plate studies. Compounds were added in the presence of 5% FBS. PRECs were serum starved 1hr before addition of factors in Serum Free Medium (SFM). Sub-confluent BRE-Luc or PREC cultures were seeded into 6-well plates at 3.0×10^5 or 2.0×10^5 cells/well respectively, using an automated cell counter (Countess™ II). Cells were treated with rh-BMP4 (R & D Systems; 314-BP), vehicle (DMSO-D6), or compound (10 μ M) for 1hr or 24hrs. After the indicated time points, treatment medium was removed, adhered cells were washed once in 1X PBS and subsequently harvested in 1X PBS and pelleted by low centrifugation.

The cell pellet was then suspended in PK lysis buffer (50mM HEPES pH 7.5, 150mM NaCl, 1.5mM MgCl₂, 1mM EGTA, 10% Glycerol, 1% Triton X-100, 1mM Na₃VO₄ 50mM NaF) containing both phosphatase and protease inhibitors (PhosSTOP and cOmplete Mini; Roche) and allowed to lyse on ice for 30 minutes with intermittent vortexing. To pellet the insoluble fraction, the suspended pellet was centrifuged at 15,000 rpm for 15 minutes at 4°C. Supernatant was transferred to clean Eppendorf tubes and 6X sodium dodecyl sulfate was added 1:5 and heated for 5 minutes at 95°C. Equal amounts of total protein lysates were resolved on hand-casted 8% SDS-polyacrylamide gels.

Separated proteins were then electrophoretically transferred onto Immobilon®-FL polyvinylidene difluoride membranes. Membranes were dried and reactivated in methanol rinsed in 1X TBS and blocked for 1hr in 5% bovine serum albumin or 5% milk dissolved in 1X TBS-T (1X TBS + 0.1% Tween® 20) and then incubated overnight with primary antibodies consisting of one of the following: anti-Rb phospho-SMAD-1/5/9 1:1,000 (CST®; 13820), anti-Rb total-SMAD-

1 1:2,000 (CST®; 9734), anti-Rb phospho-SMAD-2 1:1000 (CST®; 3104), anti-Rb phospho-SMAD-3 1:1000 (CST®; 9520) anti-Rb total-SMAD-2/3 1:1000 (CST®; 3102) anti-Rb-phospho-TAK1 (CST®; 9339), anti-Rb-phospho-MAPK Family Sampler kit (CST®; 9910T), anti-β-Actin 1:10,000 (Proteintech®; 60008-1-Ig) The next day, membranes were washed in 1% non-fat dry milk prepared in 1X TBS-T and incubated for 1 hour at room temperature in anti-Rb HRP or anti-Ms-HRP diluted in 1% non-fat dry milk (1X TBS-T). Membranes were washed in TBS-T and rinsed twice with 1X TBS and incubated with ECL western blotting substrate (Pierce™; 32106). Finally, membranes were incubated with HyBlot ES™ autoradiography film (Denville Scientific) and developed on the Kodak X-OMAT 2000A processor and quantified using ImageJ (Version 2.0.0)

Statistical Analysis

The following statistical test were used to assess significance and derive p-values, for each test, alpha = 0.05%: one-way ANOVA with post-hoc Dunnett's multiple comparison test, unpaired two-tailed t-test, and multiple t-test's (one unpaired t-test per row) by using GraphPad Prism7 version 7.0d

BRE-Luc cell Transcriptome profiling

To identify direct gene targets of low dose rh-BMP4 (2ng/ml) specifically in BRE-Lucs, cells were seeded at 3.0×10^5 cells in 6-well plates in triplicate for each sample. Cells were cultured in 5% FBS medium overnight and treated the next day with or without 2ng/ml rh-BMP4 for 4 hours. After treatment, BRE-Lucs were harvested to isolate total RNA using the RNeasy[®] Mini Kit (Qiagen) by following the manufactures' protocol. Transcriptome profiles of low-dose rh-BMP4 (2ng/ml) (treated) and 5% FBS medium only (untreated) cells were assessed via Affymetrix[™] microarray analysis performed by the Microarray Core housed within University of Michigan DNA Sequencing core. Concisely, the integrity and yield of total RNA was assessed by using the RNA 6000 Nano kit on the 2100 Bioanalyzer (Agilent Technologies). Reported RNA integrity numbers were above 9 for the two samples submitted in triplicate. 400ng of total RNA was used to generate fragmented and biotin conjugated single-stranded cDNA (ss-cDNA) using the GeneChip[™] Whole Transcript PLUS reagent kit (Applied Biosystems). ss-cDNA was then hybridized to the Affymetrix[®] GeneAtlas Human Gene 2.1 Sense Target microarray. Following hybridization—wash, stain, and imaging procedures were carried out according to the manufactures protocol. The robust multi-array average method [27] was used to correct for variations between microarrays. Oligo and Limma packages of Bioconductor/R were used to identify differentially expressed genes by fitting normalized gene expression data to weighted linear models [28]. Probe sets with a variance above 0.025 and fold changes greater than 1.5 were selected. Multiplicity assessment was carried out by using the false discovery rate method to adjust p-values [29]. Final data was loaded into iPathwayGuide to generate volcano plot (Advaita Bioinformatics).

qRT-PCR

To assess the capacity of HTS compounds to induce the expression of endogenous direct gene targets of BMP signaling, BRE-Lucs were seeded in 6-well plates at 3.0×10^5 cells/well and cultured in 5% FBS medium overnight. The following day, BRE-Lucs were treated with low dose rh-BMP4 (2ng/ml), 0.04% DMSO-D6, or increasing concentrations of compounds (all with 0.04% DMSO-D6). After 24hrs of treatment, BRE-Lucs were harvested for total RNA isolation using the RNeasy[®] Mini Kit (Qiagen) by following the manufactures protocol. Synthesis of first-strand cDNA was prepared by using 1 µg of total RNA, Superscript[™] III (Invitrogen) reverse transcriptase, and 100ng of random primers.

Amplified cDNA templates were diluted 1:50 and SYBR[®] green Master Mix was used to monitor cDNA template amplification on the Applied Biosystems[®] 7500 real-time PCR system. HPRT was used to normalize gene expression. For each sample, fold change of gene expression over 0.04% DMSO-D6 was calculated. Human primer pair sequences used were obtained from PrimerBank [30] (except for HPRT) and include the following:

ID1-(f)-CTGCTCTACGACATGAACGG, (r)-GAAGGTCCCTGATGTAGTCGAT

ID3-(f)-GAGAGGCACTCAGCTTAGCC, (r)-TCCTTTTGTCGTTGGAGATGAC

COL2A1-(f)-CCAGATGACCTTCCTACGCC, (r)-TTCAGGGCAGTGTACGTGAAC

HPRT-(f)-ATGGACAGGACTGAACGTCTT, (r)-TCCAGCAGGTCAGCAAAGAA

Bibliography

1. An, W.F. and N. Tolliday, *Cell-based assays for high-throughput screening*. Mol Biotechnol, 2010. **45**(2): p. 180-6.
2. Hughes, J.P., et al., *Principles of early drug discovery*. Br J Pharmacol, 2011. **162**(6): p. 1239-49.
3. Auld, D.S. and J. Inglese, *Interferences with Luciferase Reporter Enzymes*, in *Assay Guidance Manual*, G.S. Sittampalam, et al., Editors. 2004: Bethesda (MD).
4. Auld, D.S., et al., *A specific mechanism for nonspecific activation in reporter-gene assays*. ACS Chem Biol, 2008. **3**(8): p. 463-70.
5. Thorne, N., D.S. Auld, and J. Inglese, *Apparent activity in high-throughput screening: origins of compound-dependent assay interference*. Curr Opin Chem Biol, 2010. **14**(3): p. 315-24.
6. Thorne, N., J. Inglese, and D.S. Auld, *Illuminating insights into firefly luciferase and other bioluminescent reporters used in chemical biology*. Chem Biol, 2010. **17**(6): p. 646-57.
7. Zilberberg, L., et al., *A rapid and sensitive bioassay to measure bone morphogenetic protein activity*. BMC Cell Biol, 2007. **8**: p. 41.
8. Spiekerkoetter, E., et al., *FK506 activates BMPR2, rescues endothelial dysfunction, and reverses pulmonary hypertension*. J Clin Invest, 2013. **123**(8): p. 3600-13.
9. Yu, P.B., et al., *Dorsomorphin inhibits BMP signals required for embryogenesis and iron metabolism*. Nat Chem Biol, 2008. **4**(1): p. 33-41.
10. Hao, J., et al., *In vivo structure-activity relationship study of dorsomorphin analogues identifies selective VEGF and BMP inhibitors*. ACS Chem Biol, 2010. **5**(2): p. 245-53.
11. Cuny, G.D., et al., *Structure-activity relationship study of bone morphogenetic protein (BMP) signaling inhibitors*. Bioorg Med Chem Lett, 2008. **18**(15): p. 4388-92.
12. Williams, E. and A.N. Bullock, *Structural basis for the potent and selective binding of LDN-212854 to the BMP receptor kinase ALK2*. Bone, 2018. **109**: p. 251-258.

13. Genthe, J.R., et al., *Ventromorphins: A New Class of Small Molecule Activators of the Canonical BMP Signaling Pathway*. ACS Chem Biol, 2017. **12**(9): p. 2436-2447.
14. Zimmerman, L.B., J.M. DeJesusEscobar, and R.M. Harland, *The Spemann organizer signal noggin binds and inactivates bone morphogenetic protein 4*. Cell, 1996. **86**(4): p. 599-606.
15. Yu, P.B., et al., *BMP type I receptor inhibition reduces heterotopic [corrected] ossification*. Nat Med, 2008. **14**(12): p. 1363-9.
16. Feng, L., et al., *Discovery of a Small-Molecule BMP Sensitizer for Human Embryonic Stem Cell Differentiation*. Cell Rep, 2016. **15**(9): p. 2063-75.
17. Cao, Y., et al., *Selective small molecule compounds increase BMP-2 responsiveness by inhibiting Smurf1-mediated Smad1/5 degradation*. Sci Rep, 2014. **4**: p. 4965.
18. Vrijens, K., et al., *Identification of small molecule activators of BMP signaling*. PLoS One, 2013. **8**(3): p. e59045.
19. Aragon, E., et al., *A Smad action turnover switch operated by WW domain readers of a phosphoserine code*. Genes Dev, 2011. **25**(12): p. 1275-88.
20. Knockaert, M., et al., *Unique players in the BMP pathway: small C-terminal domain phosphatases dephosphorylate Smad1 to attenuate BMP signaling*. Proc Natl Acad Sci U S A, 2006. **103**(32): p. 11940-5.
21. Sapkota, G., et al., *Dephosphorylation of the linker regions of Smad1 and Smad2/3 by small C-terminal domain phosphatases has distinct outcomes for bone morphogenetic protein and transforming growth factor-beta pathways*. J Biol Chem, 2006. **281**(52): p. 40412-9.
22. Zhu, H., et al., *A SMAD ubiquitin ligase targets the BMP pathway and affects embryonic pattern formation*. Nature, 1999. **400**(6745): p. 687-93.
23. Bruce, D.L. and G.P. Sapkota, *Phosphatases in SMAD regulation*. FEBS Lett, 2012. **586**(14): p. 1897-905.
24. Sapkota, G., et al., *Balancing BMP signaling through integrated inputs into the Smad1 linker*. Mol Cell, 2007. **25**(3): p. 441-54.

25. Alarcon, C., et al., *Nuclear CDKs drive Smad transcriptional activation and turnover in BMP and TGF-beta pathways*. Cell, 2009. **139**(4): p. 757-69.
26. Bradford, S.T.J., et al., *High-throughput screens for agonists of bone morphogenetic protein (BMP) signaling identify potent benzoxazole compounds*. J Biol Chem, 2019.
27. Irizarry, R.A., et al., *Exploration, normalization, and summaries of high density oligonucleotide array probe level data*. Biostatistics, 2003. **4**(2): p. 249-64.
28. Smyth, G.K., *Linear models and empirical bayes methods for assessing differential expression in microarray experiments*. Stat Appl Genet Mol Biol, 2004. **3**: p. Article3.
29. Benjamini, Y. and Y. Hochberg, *Controlling the False Discovery Rate: A Practical and Powerful Approach to Multiple Testing*. Journal of the Royal Statistical Society. Series B (Methodological), 1995. **57**(1): p. 289-300.
30. Wang, X., et al., *PrimerBank: a PCR primer database for quantitative gene expression analysis, 2012 update*. Nucleic Acids Res, 2012. **40**(Database issue): p. D1144-9.

Acknowledgements

We are grateful to the Center for Chemical Genomics at the University of Michigan Life Science Institute for providing their technical expertise and support. Specifically, M. Larsen for technical assistance with the High-Throughput Screening campaign and triage of active compounds. As well as, A. White, (Vahlteich Medicinal Chemistry Core) for also assisting with active compound triage and selection. This work was supported by the following United States National Institutes of Health grants: NIDDK 5R01DK054740-16 and NIDDK 3R01DK054740-16S1. Funding was also provided by the University of Michigan Center for the Discovery of New Medicines directed by V. Groppi.

Chapter 4 – Proliferative renal diseases: Re-mining screens for Pax2 inhibitors

Abstract

Proliferative diseases of the kidney include polycystic kidney disease (PKD) and clear cell renal cell carcinoma (ccRCC). The DNA binding protein, Pax2, is implicated in the progression of both diseases. In the developing kidney, upregulation of Pax2 is required for the conversion of mesenchymal cells into epithelial cells, which upon maturation form nephrons. Once epithelial cells are terminally differentiated, Pax2 expression is downregulated in mature epithelial compartments of the nephron. In PKD, Pax2 is re-expressed and detected in the nucleus of cystic epithelial cells. Additionally, in the majority of ccRCCs, Pax2 is re-activated and detected in the diseased renal tissues. Reducing the activity of Pax2 arrests cystogenesis, as well as, decelerates the growth and proliferation of renal tumor cells.

Recently, a small-molecule inhibitor of Pax2 activity, EG1, was discovered with the capacity to limit Pax2 mediated ureteric branching morphogenesis and aggregation of Pax2⁺ cells at ureter tip buds [1]. Additionally, EG1 limited the expression of Cited1, a Pax2 target gene [1]. Following the discovery of EG1, a high-throughput screening campaign was carried out to discover more small-molecule inhibitors of Pax2 with different mechanisms of action [2]. The HTS campaign yielded 48 Pax2 inhibitors and 2 activators [2]. Most were unique structures precluding cluster formation needed for SAR analysis. This chapter, therefore, describes re-mining screens for small-molecule inhibitors of Pax2 activity, which were employed to identify a lead series for SAR analysis. An emerging lead series has been identified and an initial SAR analysis

is reported in this Chapter. These agents will require follow up studies in chromatin immunoprecipitation assays, kidney organoid cultures, and other assays to confirm the compounds in the lead series exert their effects through desirable mechanisms.

Introduction

As discussed in Chapters 2 and 3, theoretically, cell-based HTS methods can be implemented to discover disease specific drugs with innovative mechanisms of action. Specifically, agents identified using HTS may harbor the capacity to modulate various signaling pathways and molecular factors implicated in a variety of diseases. As indicated in Chapter 1, several unmet clinical needs exist for treating proliferative diseases of the kidney such as Polycystic Kidney Disease (PKD) and clear cell Renal Cell Carcinoma (ccRCC). Therefore, applying cell-based HTS methodologies to discover novel drug entities that can directly modulate molecular targets implicated in proliferative kidney diseases is warranted.

Many of the therapeutics currently under evaluation and in use for PKD management were not originally characterized for PKD treatment [3]. For instance, Tolvaptan is a highly selective vasopressin V_2 -receptor antagonist with actions in the distal portions of the nephron and it is used clinically for diseases associated with fluid overload [4, 5]. Under normal physiological conditions, arginine vasopressin, an anti-diuretic hormone, acts at vasopressin V_2 -receptors located in the distal nephrons and collecting ducts. This causes increased reabsorption of free water in the kidneys and stimulates increased levels of cyclic AMP [4]. Therefore, Tolvaptan under the trade name Samsca[®] (Japan), was originally indicated for use in hospitalized patients with dilutional hyponatremia (low sodium serum levels) for short-term/30-day use [6].

Although Tolvaptan was not initially approved for cystic kidney disease, it was speculated early on that it might have clinical use for the treatment of diseases associated with fluid retention such as PKD [4]. And recently, Tolvaptan under the trade name Jynarque[®] (USA), was approved by the FDA for management of the autosomal dominant form of PKD. By competing for access to

arginine vasopressin V₂-receptors, Tolvaptan, blocks binding of circulating endogenous levels of arginine vasopressin which results in inhibited cAMP activity.

The vasopressin/cAMP signaling pathway is disrupted in PKD. Specifically, high levels of intracellular cAMP promote cystogenesis in PKD [7-9]. In both the *pcy* mouse model of nephronophthisis and the *PCK* rat model of the autosomal recessive form of PKD, intracellular levels of cAMP are significantly higher than in wild type animals [10]. Furthermore, these cystic animals are unable to concentrate urine and ultimately progress to renal failure [10]. Treatment of both *pcy* mice and *PCK* rats with the vasopressin inhibitor OPC31260 (Tolvaptan) significantly improved several measures of renal function and disease development including: increased kidney weight, plasma creatinine levels, blood urea nitrogen, renal cyst volumes, and mitotic and apoptotic indices [10]. Of note, *pcy* animals treated with OPC31260 experienced not only arrested disease progression but also induced disease regression [10]. Induced disease regression in *pcy* animals was indicated by the observation that the kidney weights of *pcy* animals undergoing OPC31260 therapy for 15 weeks (initiated at 15 weeks old and sacrificed at week 30) weighed significantly less than kidneys of untreated mice at 15 weeks of age [10].

Even more, cystic animals with genetically ablated circulating levels of arginine vasopressin are protected from cyst formation and have reduced levels of cAMP. *PCK* animals with deleted *Pkhd1* crossed with animals with deleted arginine vasopressin (*PCK AVP^{-/-}* animals) have significantly less levels of cAMP, as well as, protection against cystogenesis compared to *PCK AVP^{+/+}* and *PCK AVP^{+/-}* animals [11]. However, when treated with the AVP V₂-receptor agonists, 1-deamino-8-d-arginine vasopressin (dDVAP), elevated cAMP levels return and the complete cystogenic phenotype is reinstated [11]. Furthermore, compared to *PCK AVP^{+/+}* and *PCK AVP^{+/-}* animals *PCK AVP^{-/-}* animals possessed strikingly improved cysts volumes,

significantly lower kidney weights and volumes of fibrosis [11]. Additionally, and of note, *PCK AVP^{-/-}* animals had enormous volumes of urine output compared to *PCK AVP^{+/+}* and *PCK AVP^{-/+}* animals [11].

Although Jynarque[®] (Tolvaptan, USA) was recently FDA approved for the autosomal dominant form of PKD, it is only available to a subset of patients with the disease. Only patients with rapidly progressing autosomal dominant PKD or patients with a high risk of rapid progression are suitable candidates for Jynarque[®] treatment. Many factors are taken into consideration to determine if a patient has a rapidly progressing form of PKD. For example, young PKD patients with high total kidney volume and rapid PKD progression are predicted to benefit most from Jynarque[®] treatment [12]. Patients with a truncating PKD1 mutation are also expected to benefit from Jynarque[®] treatment due to its association with rapid disease progression [12].

While rare, a serious adverse side effect of Jynarque[®] treatment is hepatotoxicity which may necessitate liver transplantation if left unchecked. Accordingly, frequent tests to monitor liver function are required for all patients on Jynarque[®] in order to continue therapy. Jynarque[®] treatment must be discontinued if elevated liver enzymes fail to return to acceptable levels. More common side effects of Jynarque[®] treatment include frequent urination and intense thirst. Jynarque[®] treatment induces high sodium serum levels; therefore, patients must drink several liters of water per day in order to prevent severe dehydration. To reach more patients and reduce the chance of severe side effects, alternative therapeutic strategies are needed for safe and effective long-term treatment of both the autosomal recessive and dominant forms of PKD.

The transcription factor, Pax2, has been implicated in the progression of proliferative kidney diseases and is an emerging target for small-molecule inhibition. In renal epithelial cells (MDCKs) Pax2 has been shown to be repressed by the commonly mutated PKD gene *Pkd1* which

encodes Polycystin-1 [13]. Specifically, in overexpressing *Pkd1* renal epithelial cells, Pax2 protein levels and promoter activity are significantly repressed relative to control cells lacking the *Pkd1* transgene [13]. In normal developing kidneys, Pax2 is required for mesenchymal-to-epithelial cell conversion and Pax2 expression is classically detected in emerging nephrons [14, 15]. Mature nephrons, however, terminate Pax2 expression prior to completing the epithelial differentiation program [13, 15, 16]. In mice mimicking the recessive form of PKD, *cpk* and the autosomal dominant form of PKD, *Pkd1^{del34/del34}*, Pax2 is re-expressed and detected in the nucleus of cystic epithelial cells [13, 17]. Importantly, transgenic overexpressing Pax2 animals develop microcysts in the glomerulus and proximal tubules [16]. Similar to the vasopressin deficient cystic animals (*PCK AVP^{-/-}*) described above, *cpk* and *Pkd1^{del34/del34}* cystic animals with reduced Pax2 dosage have arrested cystogenesis [13, 17]. Moreover, there is a marked reduction in the weight of kidneys from *cpk* and *Pkd1^{del34/del34}* animals heterozygous for Pax2 relative to the weight of kidneys from cystic animals homozygous for Pax2 [13, 17]. Inhibiting Pax2 activity arrests cystogenesis in these animals and decreases total kidney weight. Therefore, inhibiting Pax2 activity with small-molecule inhibitors may also slow the growth of cysts in both autosomal recessive and dominant PKD.

Clear cell renal cell carcinoma (ccRCC) like polycystic kidney disease is another proliferative kidney disease that ultimately progresses toward end-stage renal failure. Unlike polycystic kidney disease which has only one FDA approved therapy, several targeted FDA therapies with different mechanisms of action exist for managing ccRCC. The development of resistance to these therapies, however, hinders effective long-term treatment of ccRCC. Lesions in the VHL gene are suggested to occur in 90% of ccRCC cases through genetic or epigenetic mechanisms [18]. Under normal physiological conditions, VHL regulates HIF-1 α activity. Consequently, in ccRCC, VHL lesions lead to constitutively active HIF-1 α and the pathological

activation of HIF-1 α target genes. HIF-1 α target genes such as vascular endothelial growth factor (VEGF) and mechanistic target of rapamycin (mTOR) are important mediators that drive malignant tumor behavior.

With early detection, partial or total nephrectomy can be implemented to treat ccRCC. Commonly, however, ccRCC progresses without noticeable symptoms which can result in metastasis and 30% of nephrectomy patients will develop metastatic spread of ccRCC [19, 20]. First- and second-line targeted treatments, therefore, are employed for the treatment of metastatic ccRCC. First-line targeted therapies for metastatic ccRCC include small-molecules Sorafenib and Sunitinib which inhibit VEGF receptor tyrosine kinases. Sorafenib and Sunitinib have activity on other tyrosine kinases such as PDGFRB (platelet-derived growth factor receptor β), Flt-3 (FMS-like tyrosine kinase), c-Kit (receptor of stem cell factor), and RET receptor tyrosine kinases [21]. Sorafenib and Sunitinib primarily exert their effects through inhibition of tumor angiogenesis and proliferation [21, 22]. The average duration of clinical control of ccRCC under first-line therapeutics is 8-9 months [19]. Side effects of both Sorafenib and Sunitinib include: hypertension, diarrhea, hand-foot syndrome, rash, and mucositis [19].

In patients with metastatic ccRCC that have experienced disease progression on first-line VEGF receptor inhibitors, second-line targeted therapies for metastatic ccRCC are implemented. Second-line targeted therapies for metastatic ccRCC include Everolimus and Temsirolimus which inhibit the serine-threonine kinase mTOR, a central regulator of cell growth [23]. Everolimus and Temsirolimus bind to FKBP-12 and form an inhibitory complex that inactivates mTOR signaling [24, 25]. Everolimus and Temsirolimus inhibitory actions on mTOR result in a decrease in proteins that regulate cell cycle progression and angiogenesis [24]. The average duration of controlling ccRCC under second-line therapeutics is 5-6 months [19]. Side effects of both Everolimus and

Temsirolimus include: stomatitis, hypercholesterolemia, hyperglycemia, pneumonitis, and edema [19].

In developing renal tissues, Pax2, is essential for specifying and restricting the fates of renal stem cells [15]. Pax2, therefore, is activated in the renal mesenchyme and proliferating renal epithelial cells [15]. Once terminally differentiated, however, mature renal epithelial cells silence Pax2 activity. Conversely, in the majority of ccRCC, Pax2 is re-activated and detected in the malignant renal epithelium [26]. As detailed above, mutated VHL is unable to negatively regulate HIF-1 α , causing pathogenic activation of a number of HIF-1 α target genes. And, along with the negative regulation of HIF-1 α , VHL also suppresses Pax2; as, loss of VHL induces Pax2 up-regulation in ccRCC [27]. In addition, a correlation between HIF-1 α and Pax2 in ccRCC has been identified in patient tumors [27]. Furthermore, it has been suggested that prolonged activation of Pax2 may restrict the differentiation potential of renal epithelial cells [16]. Downregulation of Pax2 activity, however, by antisense oligonucleotides decelerates the growth and proliferation of renal tumor cells [28]. Moreover, downregulated Pax2 enhances cisplatin-induced apoptosis in renal carcinoma cells and RCC derived xenographs with ablated Pax2 (shPax2) [29, 30]. Therefore, inhibiting Pax2 activity with small-molecule inhibitors may also slow the growth and proliferation of renal carcinoma cells alone or in combination with other currently approved targeted therapeutics.

Results

To identify small-molecule inhibitors of Pax2 that could potentially be developed to slow the progression of polycystic kidney disease (PKD) and clear-cell renal cell carcinoma (ccRCC) we designed a cell-based HTS assay that allowed initial screening of 69,125 chemical compounds, which was carried out by Grimley [2]. After applying triage criteria, Grimley tested 233 inhibitors and 110 activators of Pax2 in dose-response [2]. This was followed by fresh powder stock retesting of 146 confirmed inhibitors and 8 confirmed activators in dose-response [2]. After running counterscreening assays, Grimley found a total of 50 “hits” that remained promising candidates for modulating Pax2 activity [2]. 48 were inhibitors and 2 were activators of Pax2 activity [2].

Many of the top 50 “hits” displayed favorable dose-response activity with some having single digit micromolar IC_{50} 's, selection of a lead series for SAR analysis, however, was stalled. This was because most of the compounds were singletons/unique structures (at least 37 structures were unique) [2]. Grimley, however, did report one cluster with 7 members and 2 clusters with 2 members [2]. To expand the on the 50 “hits” found by Grimley, we initiated re-mining screens in order to identify molecules with similar structures to the 50 “hits” identify by Grimley that had not been tested in the initial small-molecule screening assays. Overall, we wanted to improve our prospects of identifying the best chemical series with satisfactory SAR for Pax2 inhibition.

We performed a similarity search of the entire Center for Chemical Genomics (CCG) screenable library using the 50 “hits” as queries with structure similarity set to 75%. From this search criteria, we identified over 300 compounds that had not been previously screened in our initial assays. We performed dose-response assays using 8-point titration curves generated with a 1.67 dilution factor in renal cells containing an integrated Pax Response Sequence (PRS4-Luc cells). The titration curves had a top concentration of 50 μ M and a final concentration of 1.38 μ M.

PRS4-Luc reporter cells were transiently transfected with a Pax2 expression construct and treated with either DMSO or compounds using the titration curve described above. 122 compounds out of 373 compounds in our re-mining screen were active in the concentration response curve (CRC) assays (hit rate of 33%).

Cluster analysis was performed on 122 active compounds using DataWarrior software [31]. 47 clusters were identified with 80% similarity and 34 clusters were identified with 70% similarity. 17 clusters were eliminated based on reactive filters flags, range of activities within the cluster, chemical structures, etc. The most active compound was selected from each of the 17 remaining clusters to purchase fresh powder. 15 compounds were available for purchase through our selected vendor. The activities in CRC for compounds from the fresh powder confirmed the original CRC activities even though activities were slightly higher from fresh powder than the original for most of the compounds (**table 4.1**).

Since the original CRC activities were confirmed by the fresh powder, we went back to perform an initial SAR for the original 122 CRC active compounds. From the 34 clusters, one series of compounds are beginning to clearly emerge in terms of the number of compounds in the cluster, the range of activities, and compounds with related structures to the other clusters (**figure 4.2**). There are 23 compounds in this particular cluster, and they were combined with 12 compounds from other clusters since they had related structures. A set of 35 compounds in total was tabulated for an initial SAR analysis. The activities (pAC_{50}) range from 3.8 – 5.48. The IC_{50} values are also reported in Table 4.2. The CRC activities of the original CCG powder and the fresh powder for 6 compounds in this set were compared in Table 4.1.

The initial SAR analysis and the R group analysis are in Table 4.2. In this set of 35 compounds, there are five compounds with quinazoline cores. The open chain as R_2 is more active

than the cyclized group. The methyl substitution of the benzene ring of R₁ decreases the activity. There are 21 compounds with a piperazine core showing an excellent initial SAR. In this series, [1,2,4]triazolo[1,5-a]pyrimidine group is prevalent as either R₁ or R₂, 5 compounds have it as R₁ and 6 compounds have it as R₂. Also, the structurally related group, 5,6,7,8-tetrahydro-[1,2,4]triazolo[5,1-b]quinazoline is in 4 compounds as R₁ and in 6 compounds as R₂. The most active compound has [1,2,4]triazolo[1,5-a]pyrimidine group as R₁ and a di-methyl substituted benzene at the ortho and meta positions. For the same R₂, having [1,2,4]triazolo[1,5-a]pyrimidine as R₁ makes the compound more active than 5,6,7,8-tetrahydro-[1,2,4]triazolo[5,1-b]quinazoline.

Discussion

Although Pax2 is an established target in proliferative disease of the kidney, currently, there is a dearth of chemical agents/tools available to modulate this molecule proved to be critical in both kidney development and disease. *In silico*/virtual screening methodologies combined with the use of a homology model of the Pax2 paired domain, led to the discovery of the first ever reported small-molecule inhibitor of Pax2, EG1, by Grimley and colleagues [1]. In the study by Grimley and colleagues, renal carcinoma cell lines harboring re-activated Pax2 expression exhibited decreased viability and proliferation following EG1 treatment. Moreover, cultured embryonic kidney rudiments treated with EG1 displayed defects in Pax2 mediated ureteric branching morphogenesis and incomplete aggregation of Pax2⁺ cells at ureter tip buds [1].

As discussed in Chapters 2 and 3, cell-based high-throughput screening methodologies provides investigators with an unbiased means to discover drug entities that can potentially modulate disease targets. As well as, a method to discover drugs with novel mechanisms of action. Therefore, using high-throughput screening methodologies, Grimley was able to identify at least 50 more small-molecules with the capacity to modulate Pax2 transcription activation [2]. This Chapter discusses re-mining efforts to find compounds with similar structures to the 50 small-molecules identified by Grimley.

Collectively, the aim of these studies is to discover molecules that have the capacity to not only inhibit Pax2-DNA-binding interactions but that also have the capacity to inhibit the formation of complexes between Pax2 and its binding partners, i.e., protein-protein interactions (PPIs). For example, the Pax transactivation domain interacting protein (PTIP) interacts with the carboxy-terminal transactivation domain of Pax2 [32]. The Pax2 and PTIP complex co-localize to sites of actively expressed chromatin in the cell nucleus [32]. PTIP then recruits and links the MLL3/4

histone H3K4 methyltransferase complex to Pax2 [33]. Whereby, the Pax2-PTIP-MLL complex is able to imprint and maintain active epigenetic marks on chromatin [15]. Some Pax2 binding partners act in a repressive manner to inhibit Pax2 transactivation activity and thus silence the genome. For instance, the groucho-related gene 4 (Grg4) is a binding partner of Pax proteins [34, 35]. Grg4 inhibits Pax protein transcriptional activity in an octapeptide dependent manner to permit silencing of specific genes [34, 35]. Hence, inhibiting the ability of Pax2 to interact with proteins such as PTIP or enhancing interactions between Pax2 and Grg4 may provide additional therapeutic strategies to arrest cystogenesis in PKD and decelerate ccRCC. Furthermore, agents that work by modulating Pax2 protein-protein interactions could potentially improve the ability to potentially control tissue specific protein-protein interactions with precision and efficacy. By comparing such compounds to the activity of EG1 we can assess the extent of Pax2 inhibition.

Ectopic expression or re-activation of Pax2 is implicated in the progression of both PKD and ccRCC. Therefore, efforts to identify agents that have the capacity to modulate Pax2 activity by novel mechanisms is warranted. Currently, Jynarque[®] (Tolvaptan, USA) is only FDA approved treatment for the autosomal dominant form of PKD and is only accessible to a sub-group of PKD patients. On the other hand, several approved FDA therapies exist for ccRCC management (e.g. Sorafenib, Sunitinib, Everolimus, and Temsirolimus). However, the development of resistance to inhibitor drug therapy is a huge barrier which prevents effective long-term treatment. Available *in vitro* systems and *in vivo* models of both PDK and ccRCC will aid the process of validating the efficacy of potential novel small-molecule modulators of Pax2 transactivation activity.

Figures

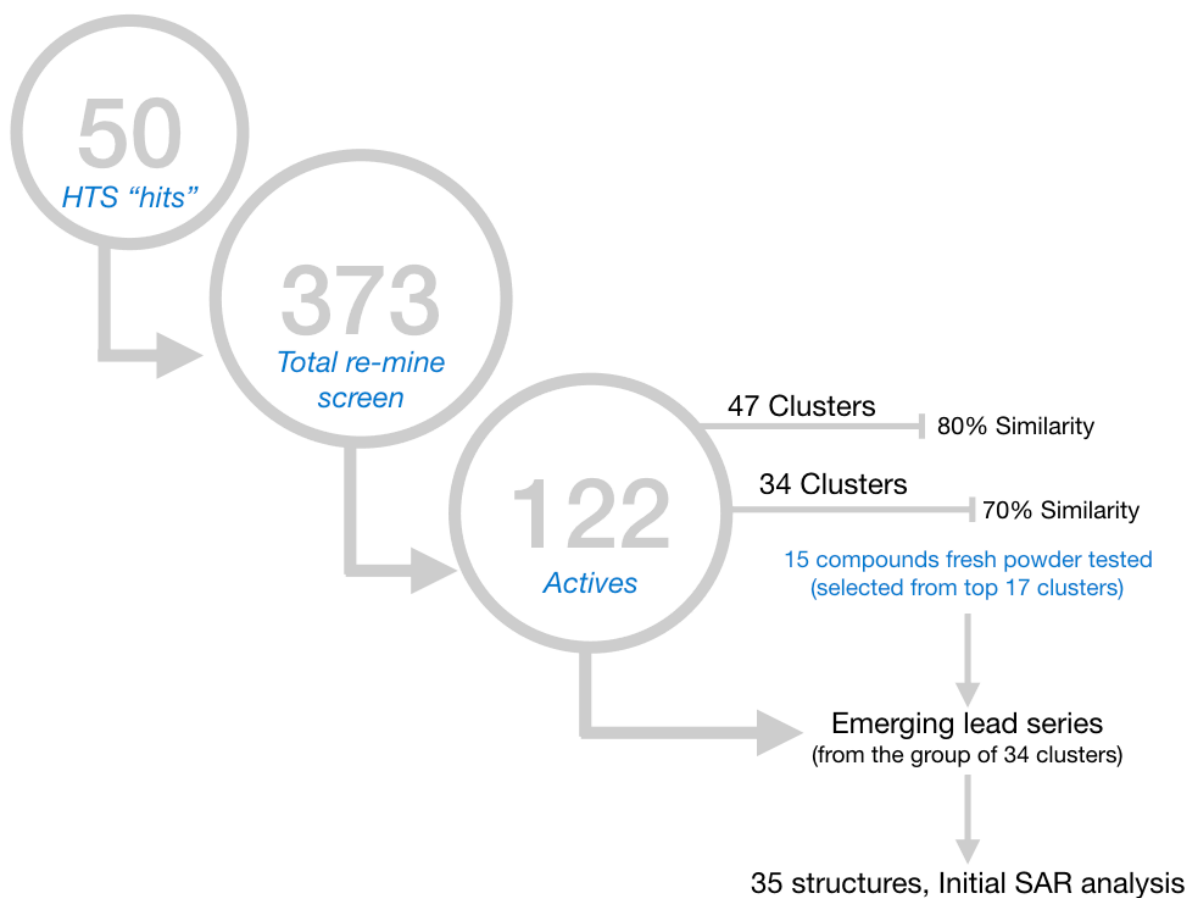
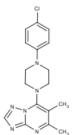
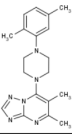
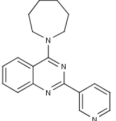
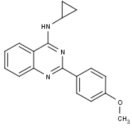
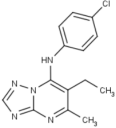
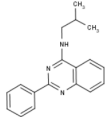


Figure 4.1 Re-mining strategy to test additional small-molecules in PRS4-Luc cells.

Table 4.1 Comparison of CRC activities between original and fresh powder compounds

Compound ID	Structure	PUBCHEM_SID	pAC ₅₀ , original	pAC ₅₀ , fresh powder	IC ₅₀ (M)	IC ₅₀ (μM)
eg-h26/ 130202		124682279	5.18	5.48	6.60693E-06	6.61
sbeg-1/ 191845		124738812	5.48	5.96	3.31131E-06	3.31
sbeg-2/ 17812		124615728	4.83	5.42	1.47911E-05	14.79
sbeg-3/ 188489		124735674	4.55	5.42	2.81838E-05	28.18
sbeg-4/ 191087		124738112	5.38	5.41	4.16869E-06	4.17
sbeg-5/ 16542		124614458	5.12	5.06	7.58578E-06	7.59

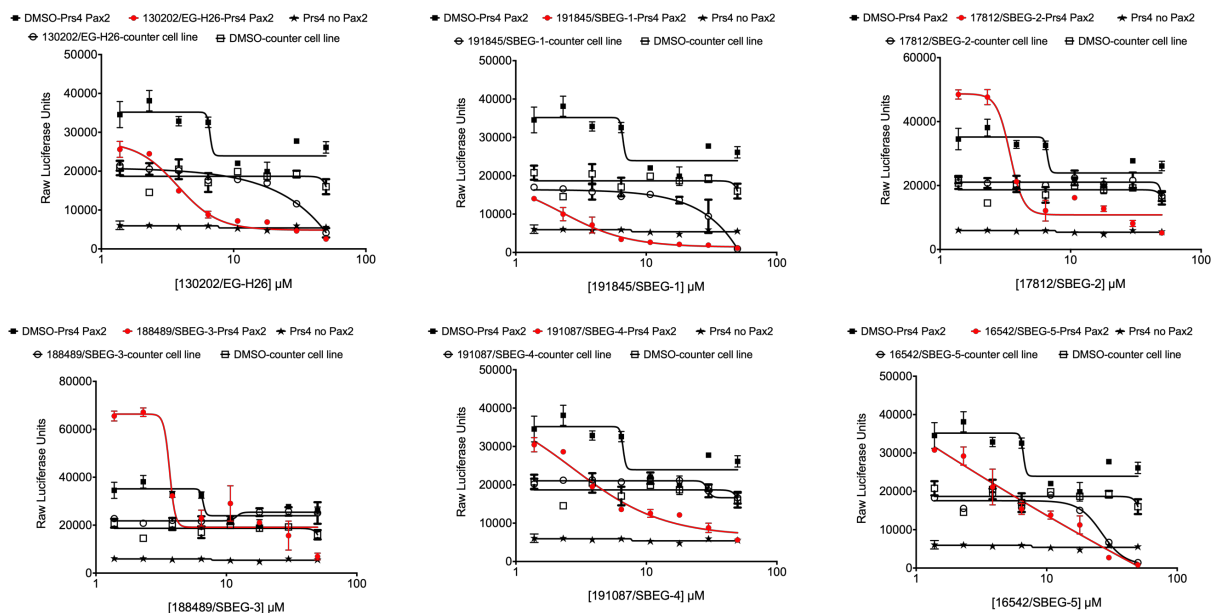
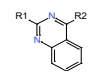
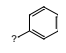
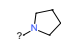
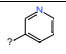
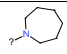
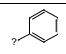
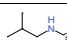
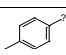
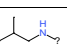
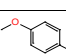
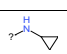
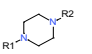
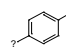
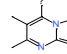
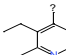
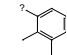
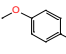
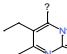
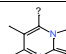
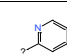
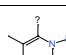
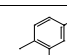
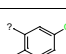
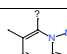
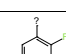
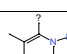
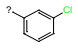
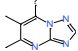
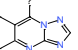
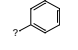
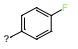
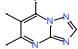
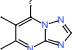
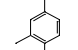
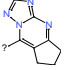
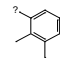
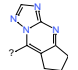
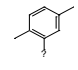
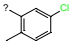
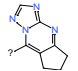
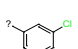
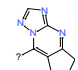
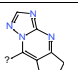
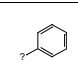
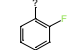
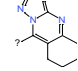
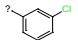
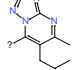
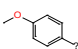
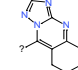


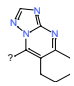
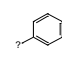
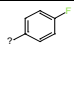
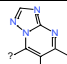
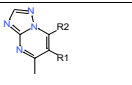
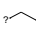
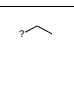
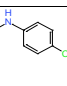
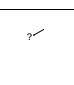
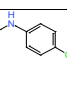
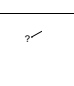
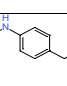
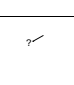
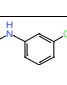
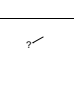
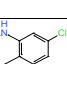
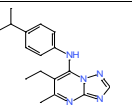
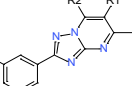
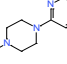
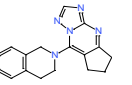
Figure 4.2 Fresh powder dose-response curves of emerging lead series of Pax2 inhibitors.

Using fresh powder isolates, we performed dose-response assays using 8-point titration curves generated with a 1.67 dilution factor in renal cells containing an integrated Pax Response Sequence (PRS4-Luc cells). The titration curves had a top concentration of 50 μM and a final concentration of 1.38 μM . (**open squares**): DMSO/D6 was tested in a counter-cell line which lacks PRS4-Luc. The hypothesis was that DMSO would have no effect in the counter cell line and accordingly, these experimental conditions were used as a control. (**filled squares**): DMSO/D6 was tested in PRS4-Luc cells transiently transfected with a Pax2 expression construct. The hypothesis was that DMSO/D6 would have no effect on Pax2 transactivation activity. (**open circle**): Assessment of compound activity in the counter-cell line which lacks PRS4-Luc. The hypothesis was that Pax2 inhibitors would have no activity in the counter cell line. Suitably, these conditions were used to screen for non-specific activity of Pax2 inhibitors. (**filled circle/red curve**): Pax2 actives tested in PRS4-Luc cells transiently transfected with Pax2. The hypothesis is that Pax2 actives would have an inhibitory effect on Pax2 transactivation activity. (**filled star**): Baseline activity of PRS4-Luc cells without transfected Pax2. The hypothesis was that identified Pax2 inhibitors would produce a curve similar to cells lacking transfected Pax2. Thus, these conditions were used as a positive control. Note the range of inhibitory activities in the compounds within the emerging lead series of Pax2 inhibitors (**red curves**).

Table 4.2 Initial SAR analysis of a set of 35 CRC active compounds

Core Structure	R1	R2	Compound #	PUBCHEM_SID	pAC ₅₀	IC ₅₀ (M)	IC ₅₀ (μM)
			sbeg-6/ 16541	124614457	4.58	2.63E-05	26.30
			sbeg-2/ 17812	124615728	4.83	1.48E-05	14.79
			sbeg-5/ 16542	124614458	5.12	7.59E-06	7.59
			sbeg-7/ 24110	124622026	4.75	1.78E-05	17.78
			sbeg-3/ 188489	124735674	4.55	2.82E-05	28.18
			eg-h26/ 130202	124682279	5.18	6.61E-06	6.61
			sbeg-8/ 191082	124738107	4.16	6.92E-05	69.18
			sbeg-9/ 191088	124738113	4.97	1.07E-05	10.72
			sbeg-10/ 191843	124738810	4.48	3.31E-05	33.11
			sbeg-1/ 191845	124738812	5.48	3.31E-06	3.31
			sbeg-11/ 191847	124738814	5.04	9.12E-06	9.12
			sbeg-12/ 191861	124738828	4.26	5.5E-05	54.95

		sbeg-13/ 191865	124738832	4.58	2.63E-05	26.30
		sbeg-14/ 191876	124738843	4.45	3.55E-05	35.48
		sbeg-15/ 191879	124738846	4.68	2.09E-05	20.89
		sbeg-16/ 191880	124738847	3.94	0.000115	114.82
		sbeg-17/ 191895	124738862	4.38	4.17E-05	41.69
		sbeg-18/ 191896	124738863	4.75	1.78E-05	17.78
		sbeg-19/ 191897	124738864	4.25	5.62E-05	56.23
		sbeg-20/ 191916	124738883	4.64	2.29E-05	22.91
		sbeg-21/ 191920	124738887	4.05	8.91E-05	89.13
		sbeg-22/ 191941	124738908	4.24	5.75E-05	57.54
		sbeg-23/ 191944	124738911	4.34	4.57E-05	45.71
		sbeg-24/ 191949	124738916	4.34	4.57E-05	45.71

		sbeg-25/ 191952	124738919	4.55	2.82E-05	28.18
		sbeg-26/ 191955	124738922	4.46	3.47E-05	34.67
		sbeg-27/ 191086	124738111	3.8	0.000158	158.49
		sbeg-4/ 191087	124738112	5.38	4.17E-06	4.17
		sbeg-28/ 191866	124738833	4.26	5.5E-05	54.95
		sbeg-29/ 191872	124738839	4.19	6.46E-05	64.57
		sbeg-30/ 191874	124738841	4.24	5.75E-05	57.54
		sbeg-31/ 191884	124738851	4.08	8.32E-05	83.18
		sbeg-32/ 191091	124738116	4.34	4.57E-05	45.71
		sbeg-33/ 190303	124737434	4.46	3.47E-05	34.67
		sbeg-34/ 191912	124738879	4.47	3.39E-05	33.88

Materials and Methods

Cell-Culture

For testing of small-molecules, HEK293 cells carrying an integrated Pax Response Sequence driving luciferase (PRS4-Luc) were maintained in complete medium (Dulbecco's modified Eagle's medium (DMEM) containing 4.5 g/L D-glucose and 584 mg/L L-glutamine supplemented with 10% fetal bovine serum and 1% Pen/Strep) and cultured to sub-confluency at 37°C and 5% CO₂.

Transfection Procedure

As described previously [1], PRS4-Luc cells were seeded into Corning® 100 mm tissue culture-treated culture dishes at 3.0×10^6 and grown overnight. The following morning, PRS4-Luc cells were approximately 50% confluent and media exchange was performed with 5 mls of fresh complete media lacking 1% Pen/Strep. PRS4-Luc cells were then transiently transfected with or without CMV-Pax2b. The transfection plasmid DNA-lipid complex consisted of: 4 µg of CMV-Pax2b plasmid DNA (4 µL obtained from 1 µg/µl plasmid DNA stock) combined with 910 µL of Opti-MEM™ I (Gibco™) for a total of 914 µL, as well as, 14 µL of Lipofectamine 2000® reagent (Life Technologies™) and 900 µL of Opti-MEM™ I (Gibco™) for a total of 914 µL. The transfection plasmid DNA-lipid complex reagent was mixed and allowed to incubate for 20 minutes at room temperature. The plasmid DNA-lipid complex consisting of 1828 µL was then added dropwise to the overnight cultured PRS4-Luc cells described above. The PRS4-Luc cells containing the transfection reaction was then allowed to incubate for 6 hours at 37°C and 5% CO₂. Transfection reaction plates were gently shaken at 30 mins and 60 mins post-transfection.

Luciferase Assays

PRS4-Luc cells transfected with CMV-Pax2b were trypsinized and counted using an automated cell counter (Countess™ II). 6×10^3 cells/well were then seeded into 384-well plates containing small-molecules using complete medium. Under 37°C and 5% CO₂ conditions, PRS4-Lucs were incubated overnight with the small-molecules for the re-mine screen. The next day, culture medium was aspirated using a microplate washer (BioTek® ELx405™) so that 10 µL remained and an equal volume of luciferase reagent (Steady-Glo® Promega) was added to the remaining culture medium in each well using a Multidrop™ dispenser. Following Steady-Glo® cell lysis, luminescence activity was measured on a luminometer (PHEARstar® BMG Labtech).

Small-molecule screening library utilized for re-mining efforts

Over 300 drug/lead-like structures were screened from the Center for Chemical Genomics (CCG) small-molecule library housed at the Life Science Institute at the University of Michigan. Small-molecules were selected for their drug/lead like physicochemical properties which fell within the Lipinski's space for bioavailable/orally active drugs having molecular weights < 500, hydrogen-bond donors < 5, hydrogen-acceptors < 10 and cLogP's < 5 [36]. Compounds utilized for re-mining efforts were sourced from the ChemDiv 20K collection (65 active compounds), ChemDiv 100K collection (53 active compounds), NCI collection (1 active compound), MB_24K collection (2 active compounds) and the CMLD collection (1 active compound) which are all housed in the CCG library.

Fresh-powder sources for confirmation dose-response studies

The sources of the fresh powder compounds use for dose-response confirmation studies were obtained from Aldrich Market Select which contains 8 million searchable unique structures. Purity of compounds ranged from 90-92%, and they were synthesized by AMS suppliers including: Princeton BioMolecular Research (1 compound), Vitas-M Laboratory, Ltd. (7 compounds), InterBioScreen Ltd. (1 compound), and ChemDiv, Inc (6 compounds).

Bibliography

1. Grimley, E., et al., *Inhibition of Pax2 Transcription Activation with a Small Molecule that Targets the DNA Binding Domain*. ACS Chem Biol, 2017. **12**(3): p. 724-734.
2. Grimley, E., *Thesis: Toward Molecularly Targeted Therapies for Renal Disease*. 2017, University of Michigan, Horace H. Rackham School of Graduate Studies.
3. Ibraghimov-Beskrovnya, O. and N. Bukanov, *Polycystic kidney diseases: From molecular discoveries to targeted therapeutic strategies*. Cellular and Molecular Life Sciences, 2008. **65**(4): p. 605-619.
4. Miyazaki, T., et al., *Tolvaptan, an orally active vasopressin V(2)-receptor antagonist - pharmacology and clinical trials*. Cardiovasc Drug Rev, 2007. **25**(1): p. 1-13.
5. Blair, H.A., *Tolvaptan: A Review in Autosomal Dominant Polycystic Kidney Disease*. Drugs, 2019.
6. Schrier, R.W., et al., *Tolvaptan, a selective oral vasopressin V2-receptor antagonist, for hyponatremia*. N Engl J Med, 2006. **355**(20): p. 2099-112.
7. Hanaoka, K. and W.B. Guggino, *cAMP regulates cell proliferation and cyst formation in autosomal polycystic kidney disease cells*. J Am Soc Nephrol, 2000. **11**(7): p. 1179-87.
8. Yamaguchi, T., et al., *cAMP stimulates the in vitro proliferation of renal cyst epithelial cells by activating the extracellular signal-regulated kinase pathway*. Kidney Int, 2000. **57**(4): p. 1460-71.
9. Belibi, F.A., et al., *Cyclic AMP promotes growth and secretion in human polycystic kidney epithelial cells*. Kidney Int, 2004. **66**(3): p. 964-73.
10. Gattone, V.H., 2nd, et al., *Inhibition of renal cystic disease development and progression by a vasopressin V2 receptor antagonist*. Nat Med, 2003. **9**(10): p. 1323-6.
11. Wang, X., et al., *Vasopressin directly regulates cyst growth in polycystic kidney disease*. J Am Soc Nephrol, 2008. **19**(1): p. 102-8.

12. Chebib, F.T., et al., *A Practical Guide for Treatment of Rapidly Progressive ADPKD with Tolvaptan*. J Am Soc Nephrol, 2018. **29**(10): p. 2458-2470.
13. Stayner, C., et al., *Pax2 gene dosage influences cystogenesis in autosomal dominant polycystic kidney disease*. Hum Mol Genet, 2006. **15**(24): p. 3520-8.
14. Rothenpieler, U.W. and G.R. Dressler, *Pax-2 is required for mesenchyme-to-epithelium conversion during kidney development*. Development, 1993. **119**(3): p. 711-20.
15. Patel, S.R., E. Ranghini, and G.R. Dressler, *Mechanisms of gene activation and repression by Pax proteins in the developing kidney*. Pediatr Nephrol, 2014. **29**(4): p. 589-95.
16. Dressler, G.R., et al., *Deregulation of Pax-2 expression in transgenic mice generates severe kidney abnormalities*. Nature, 1993. **362**(6415): p. 65-7.
17. Ostrom, L., et al., *Reduced Pax2 gene dosage increases apoptosis and slows the progression of renal cystic disease*. Dev Biol, 2000. **219**(2): p. 250-8.
18. Nickerson, M.L., et al., *Improved identification of von Hippel-Lindau gene alterations in clear cell renal tumors*. Clin Cancer Res, 2008. **14**(15): p. 4726-34.
19. Hsieh, J.J., et al., *Renal cell carcinoma*. Nat Rev Dis Primers, 2017. **3**: p. 17009.
20. Motzer, R.J., N.H. Bander, and D.M. Nanus, *Renal-cell carcinoma*. N Engl J Med, 1996. **335**(12): p. 865-75.
21. Escudier, B., et al., *Sorafenib in advanced clear-cell renal-cell carcinoma*. N Engl J Med, 2007. **356**(2): p. 125-34.
22. Motzer, R.J., et al., *Activity of SU11248, a multitargeted inhibitor of vascular endothelial growth factor receptor and platelet-derived growth factor receptor, in patients with metastatic renal cell carcinoma*. J Clin Oncol, 2006. **24**(1): p. 16-24.
23. Schmelzle, T. and M.N. Hall, *TOR, a central controller of cell growth*. Cell, 2000. **103**(2): p. 253-62.
24. Hudes, G., et al., *Temsirolimus, interferon alfa, or both for advanced renal-cell carcinoma*. N Engl J Med, 2007. **356**(22): p. 2271-81.

25. Motzer, R.J., et al., *Efficacy of everolimus in advanced renal cell carcinoma: a double-blind, randomised, placebo-controlled phase III trial*. *Lancet*, 2008. **372**(9637): p. 449-56.
26. Ozcan, A., et al., *PAX2 and PAX8 expression in primary and metastatic renal tumors: a comprehensive comparison*. *Arch Pathol Lab Med*, 2012. **136**(12): p. 1541-51.
27. Luu, V.D., et al., *Loss of VHL and hypoxia provokes PAX2 up-regulation in clear cell renal cell carcinoma*. *Clin Cancer Res*, 2009. **15**(10): p. 3297-304.
28. Gnarra, J.R. and G.R. Dressler, *Expression of Pax-2 in human renal cell carcinoma and growth inhibition by antisense oligonucleotides*. *Cancer Res*, 1995. **55**(18): p. 4092-8.
29. Hueber, P.A., et al., *PAX2 inactivation enhances cisplatin-induced apoptosis in renal carcinoma cells*. *Kidney Int*, 2006. **69**(7): p. 1139-45.
30. Hueber, P.A., et al., *In vivo validation of PAX2 as a target for renal cancer therapy*. *Cancer Lett*, 2008. **265**(1): p. 148-55.
31. *DataWarrior*. Available from: <http://www.openmolecules.org/datawarrior/>.
32. Lechner, M.S., I. Levitan, and G.R. Dressler, *PTIP, a novel BRCT domain-containing protein interacts with Pax2 and is associated with active chromatin*. *Nucleic Acids Res*, 2000. **28**(14): p. 2741-51.
33. Patel, S.R., et al., *The BRCT-domain containing protein PTIP links PAX2 to a histone H3, lysine 4 methyltransferase complex*. *Dev Cell*, 2007. **13**(4): p. 580-92.
34. Eberhard, D., et al., *Transcriptional repression by Pax5 (BSAP) through interaction with corepressors of the Groucho family*. *EMBO J*, 2000. **19**(10): p. 2292-303.
35. Cai, Y., et al., *Groucho suppresses Pax2 transactivation by inhibition of JNK-mediated phosphorylation*. *EMBO J*, 2003. **22**(20): p. 5522-9.
36. Lipinski, C.A., et al., *Experimental and computational approaches to estimate solubility and permeability in drug discovery and development settings*. *Advanced Drug Delivery Reviews*, 1997. **23**(1-3): p. 3-25.

Acknowledgements

We are grateful to the HTS team at Center for Chemical Genomics at the University of Michigan for assisting with the initial HTS campaign which was led and carried out by E. Grimley. We would also like to thank Dr. Lee for conducting the Cheminformatics analysis used for chemical re-mining efforts. Dr. Lee also conducted the SAR analysis reported in this Chapter which we are grateful for. Finally, we'd like to thank Dr. Nikolovska-Coleska for advice on compound selection for purchasing and testing

Chapter 5 – Conclusion and Future Directions

TGF- β and BMP signaling are implicated in the progression and reversal of CKD

Patients with Chronic Kidney Disease whether of the fibrotic or proliferative subtypes have limited therapeutic options once end-stage kidney disease is reached. Chronic kidney dialysis or kidney transplantation are the only therapies available. Chronic kidney dialysis is costly and does not restore full kidney function, while donor kidneys for transplantation are a scarce medical resource. Therefore, alternative strategies to treat kidney diseases are desperately needed. Several targets implicated in the progression or reversal of CKD (kidney fibrosis or proliferative kidney diseases) can be targeted for treatment. As demonstrated in this dissertation, high-throughput screening technologies can be applied towards the identification of drug/lead-like molecules that can potentially modulate signaling pathways and targets involved in kidney disease.

Longstanding studies have underscored persistent TGF- β activity as the principle driver of fibrogenesis in the kidney. TGF- β is a signaling cytokine and growth factor that helps orchestrate organ development, as well as, tissue repair and regeneration. However, overexpression or exogenous administration of TGF- β leads to the development of fibrotic lesions in the kidney and other organs. For instance, transgenic animals expressing high levels of TGF- β 1 selectively in hepatocytes develop liver fibrosis [1]. In addition, although these animals selectively express TGF- β 1 in hepatocytes, they also exhibit high circulating levels of TGF- β 1, which leads to the development of chronic glomerulonephritis [1] and progressive glomerulosclerosis [2].

Exogenous administration of TGF- β 2 in animals leads to the development of renal fibrosis [3]. Similarly, in an eleven participant phase I clinical study of systemic administration of TGF-

β 2 to multiple sclerosis patients, three participants experienced a decline in GFR of $> 25\%$ of the baseline value [4]. Notably, two participants from this clinical study developed hypertension under TGF- β 2 trial therapy [4]. Hypertension is the second leading cause of end-stage renal disease and TGF- β 1 has also been reported to be overexpressed in hypertensive patients compared to normotensive controls [5]. Even more, TGF- β 1 is hyperexpressed in hypertensive patients that are Americans of African descent compared to Americans of European descent [5].

In animal models of kidney disease, neutralizing TGF- β activity reduces renal damage caused by excessive TGF- β activity. For example, anti-TGF- β 1 treatment administered at the same time as the induction of glomerulonephritis causes evident suppression of extracellular matrix accumulation and fibrotic lesions [6]. On the other hand, genetic ablation of TGF- β in animals leads to uncontrolled inflammation and animal death within a couple of weeks [7, 8]. These observations underscore the benefits of suppressing TGF- β in renal disease, however, suppression or excessive suppression of TGF- β could lead to inflammatory lesions and other unwanted side effects. The mechanisms regulating elevated and prolonged TGF- β activity in chronic kidney disease are unclear. However, pathological levels of TGF- β could be activated in renal fibrosis by a plethora of aberrant mechanisms ranging from overactive integrin- $\alpha\beta$ receptors to suppression of negative regulators of TGF- β .

Therefore, numerous drug discovery programs for the treatment of chronic kidney disease have been designed around suppressing the pathological activity TGF- β . For example, a humanized monoclonal TGF- β 1 anti-body was developed by Eli Lilly and Company and tested for efficacy in diabetic nephropathy patients under renin-angiotensin system inhibitor therapy [9]. This clinical trial, however, was terminated early due to a lack of efficacy (no change in baseline

serum creatinine). Several explanations were proposed for the lack of efficacy including: 1) inadequate enrollment of American patients of African descent and type I diabetic patients 2) serum creatinine as a final efficacy marker was not sensitive enough to detect a beneficial effect 3) potentially higher doses of TGF- β or more frequent administration were needed. However, lack of success from this clinical trial may also suggest that in order to achieve a long term and full therapeutic effect other key pathways involved in the reversal of chronic kidney disease may need to be activated in combination with safe TGF- β suppression, i.e. avoiding excessive suppression which may be systemically toxic.

In contrast to work establishing TGF- β as the principle driver of renal fibrogenesis, seminal studies conducted over two decades ago were the first to provide evidence of renoprotection by BMPs. BMPs are a major branch of the TGF- β superfamily of signaling cytokines and growth factors. BMPs have important roles in the development, homeostasis, and disease processes of an array of tissue types. Particularly, BMPs are critical in the development of healthy kidneys [10]. In animal models of renal disease/fibrosis, however, BMP signaling is suppressed and reestablishment of BMP signaling reverses renal injury [11-16]. The direct molecular mechanisms underlying the beneficial actions of BMPs in the fibrotic kidney, however, remain elusive [17, 18]. Although, it is speculated that BMPs reactivate similar programs that it uses during kidney development to also repair injured renal tissues [14].

As there are many mechanisms that can activate TGF- β signaling in fibrotic kidneys, there are several ways in which BMP signaling can become dysregulated in fibrotic kidneys. For example, negative regulators of BMP signaling such as USAG-1, Gremlin, and CTGF may be aberrantly expressed in fibrotic kidneys [19-21]. Interestingly, in contrast to animal models with suppressed BMP signaling, early stage kidney disease patients with proteinuria have elevated

levels of BMP expression [22] along with elevated levels of the negative regulators of BMP signaling Gremlin [23, 24] and Connective Tissue Growth Factor (CTGF) [25]. Certain pathological conditions may cause low BMP receptor expression, which is another dynamic to consider that may contribute to dysregulated BMP signaling [17, 26].

Pre-clinical animal studies conducted to test the efficacy of THR-123, a cyclized peptide agonist of the type I BMP receptor, Alk3, demonstrated the ability to reverse established kidney fibrosis [27]. The investigators conducting this study reported that THR-123 reversed kidney fibrosis by suppressing inflammation, apoptosis, and epithelial-to-mesenchymal transition even though Alk3 receptors were depleted during end-stage kidney disease [27]. However, similar to the clinical trial assessing the efficacy of anti-TGF- β therapy in patients with diabetic nephropathy [9], perioperative use of THR-184 (THR-123 analog) in patients with cardiac surgery induced acute kidney injury yielded futile results [28]. THR-184 did not reduce the incidence of acute kidney injury within seven days of cardiac surgery [28]. Lack of efficacy of THR-184 was attributed to an insufficient dosing strategy which included inadequate administration of the frequency and duration of THR-184 [28].

Lack of efficacy of THR-184 in patients with cardiac surgery may also suggest the need for combination treatments. Ideally, combination treatments would work to safely repress pathological levels of TGF- β activity and simultaneously activate repressed BMP signaling which are detected in chronic kidney disease. To improve effectiveness further, these combination treatments would also ideally possess mechanisms that bypass negative regulators of BMP signaling such as Gremlin as well as act independently of BMP receptor status. Overall, it would be important clinically to reduce destructive ECM deposition driven by TGF- β and promote

regeneration of damage cellular constituents of the kidney, which are suggested to be encouraged by BMP signaling.

Future investigations to further develop the identified BMP signaling agonists

The first aim of the work described in this dissertation was to identify small-molecules that activate the BMP signaling pathway. Using HTS methods, several small-molecules were identified that activated a BRE-Luc reporter construct in a dose-dependent manner. Half maximal effective concentrations were calculated and ranged from approximately 74 nM to 1249 nM. In the presence of some of these small-molecule BMP signaling agonists, levels of p-SMAD-1/5/9 were significantly increased. For instance, after treatment with the BMP signaling agonists, sb4, levels of p-SMAD-1/5/9 were significantly increased 2.61-fold over baseline levels of p-SMAD-1/5/9 in DMSO treated samples. This finding and the fact that sb4 had the lowest EC_{50} prompted selection of sb4 as the first of the top twelve BMP signaling agonists to be interrogated further in mechanistic assays.

Notably, after treatment with the other BMP signaling agonists such as sb7 ($EC_{50} = 118.2$ nM) and sb8 ($EC_{50} = 129.1$) levels of p-SMAD-1/5/9 were also significantly increased by 3.15- and 2.96-fold respectively. Significantly increased levels of p-SMAD-1/5/9 were also detected after treatment with sb5 ($EC_{50} = 549.5$ nM) and sb6 ($EC_{50} = 983.2$ nM) by 3.13- and 3.73-fold respectively over DMSO treated samples. Given these findings, it is important to conduct follow-up studies with these additional BMP signaling agonists to determine if they act in a similar or different manner in comparison to sb4. For example, sb4 was shown to have modest effects on the endogenous BMP target genes ID1 and ID3. However, it is possible that some of the other BMP signaling agonists identified might increase the magnitude of activation of BMP target genes beyond what as detected with sb4. Although, it is important to consider that the modest effects of

sb4 may be advantageous because they may produce less side effects than rh-BMPs, which are very potent under optimal conditions. This could also be a beneficial feature of a drug that needs to be used long term in chronic diseases such as CKD.

Expansion of the initial/catalog-based SAR studies conducted on sb4 will also be necessary. Although the initial SAR highlighted that substitution at benzene ring for R₂ is important for the activity of sb4 and sb4-like compounds, the SAR data was very tight (narrow SAR). In order to conduct a more in-depth SAR analysis, sb4 will first need to be resynthesized (to ensure sb4 is still active and has the same potency in assays utilized) and many more compounds with similar structures to sb4 will need to be tested to better assess the relationship between structure and activity.

The procedure outlined above will also be necessary to conduct for the additional BMP signaling agonists identified that have promising activities such as compounds sb5, sb6, sb7, and sb8. It will be ideal to first determine if after treatment with these compounds endogenous BMP signaling target genes are increased. Once this is established, these small-molecules should also be resynthesized and tested alongside compounds with similar structures to aid in-depth SAR analysis. It is possible that testing structures with similar structures to sb5, sb6, sb7, and sb8 might yield even more potent and/or efficacious compounds. Furthermore, information gained from these future SAR studies could also aid in the development of assays to determine the direct binding target(s) of these BMP signaling agonists.

As mentioned above, sb4 was selected as the first of the top twelve BMP signaling agonists to be studied in further detail. Work conducted in this dissertation found that sb4 stimulates BMP signaling by stabilizing p-SMAD-1/5/9. The increased levels of p-SMAD-1/5/9 therefore resulted in increased expression of direct BMP targets genes, ID1 and ID3. Work from this dissertation

also found that sb4 is resistance to both Noggin and type I BMP receptor inhibition. The mechanism of BMP signaling activation such as that demonstrated by sb4, which bypasses negative regulation by Noggin and potentially similar negative regulators of BMP signaling, could be beneficial in specific clinical situations where these negative regulators are elevated. Further, the ability to activate BMP signaling when type I BMP receptors are inhibited could also be a useful mechanism in the event receptor status is low due to diseased states [17, 26, 27]. Moreover, compounds like sb4 could synergize with endogenous levels of BMPs and potentially abrogate the need for harmful doses of exogenous BMPs that lead to unwanted side effects [29-31].

Compounds with a benzoxazole moiety similar to sb4, have been reported to have important clinical applications. Pharmacological activities include working as anti-inflammatory [32] and anti-diabetic agents [33]. Studies in this dissertation suggest that these agents could also possess anti-fibrotic pharmacological activity due to their ability (sb4 and its analogs) to both activate and enhance BMP signaling. Therefore, future studies could test the effects of sb4 in combination with current therapies used to treat chronic kidney disease. For example, studies have been already been conducted to test the effects of anti-TGF- β therapy combined with RAAS inhibitors, as well as, BMPs combined with RAAS inhibitors [27, 34]. These studies have shown an increased therapeutic benefit that results in further disease reduction than these agents administered alone. Hence, future studies to assess the effects of anti-TGF- β therapy in combination with sb4, or sb4 in combination with RASS inhibitors in animal models of chronic kidney disease are warranted. RAAS inhibitors would be expected to slow the progression of disease while sb4 may simultaneously reverse the disease by stimulating BMP signaling to regenerate damaged renal cells.

As discussed in this dissertation, BMPs play a crucial role in kidney development [10]. Therefore, future studies to evaluate the potential capacity of sb4 to induce nephron progenitor cell proliferation similar to BMPs in embryonic renal organoid cultures will provide further insight into the mechanism of action of sb4. It will also strengthen the rationale of testing sb4 in animal models of chronic kidney disease. Specifically, if future studies find that sb4 stimulates the proliferation of nephron progenitor cells, such findings could imply that sb4 may also have the potential to stimulate the proliferation of damaged tubular epithelial cells of the nephron after injury similar to BMPs. Several of the other small-molecules that activate BMP signaling identified in this dissertation could also possess similar effects. Further experimentation will be required to determine how these BMP signaling agonists effect various cell types of the kidneys.

Prior to conducting pre-clinical animal studies, pharmacokinetic studies will be necessary. In particular, carrying out mouse liver microsomal assays will allow for assessment of the stability of sb4 *in vivo*. These future studies will help identify metabolic liabilities and support SAR studies. It should be considered too that even if these BMP signaling agonists are successful in pre-clinical animal models of chronic kidney disease limitations exist in utilizing these therapeutic approaches clinically. For instance, a potential therapy like sb4 would likely be most effective during the early stages of kidney disease. However, most CKD patients are unaware that they have kidney disease as it can progress for decades without noticeable symptoms. Therefore, it is critical to develop novel small-molecules that encourage the regeneration and repair of damage kidney tissues, as well as, identify biomarkers for early kidney disease and patients at risk for disease progression.

Future investigations to further develop the identified Pax2 inhibitors

As discussed in Chapters 1 and 4, Pax2 plays a role in the progression of proliferative diseases of the kidney such as polycystic kidney disease (PKD) and clear cell renal cell carcinoma (ccRCC). Appropriately, Pax2 is a potential therapeutic target in these diseases. The second aim of the work described in this dissertation was to identify small-molecules that inhibit Pax2 activity. Re-mining screens of over 300 compounds detailed in this dissertation identified 122 more Pax2 inhibitors which grouped into many clusters. Several Pax2 inhibitors from the top clusters were fresh powder tested. An emerging lead series of Pax2 inhibitors were found from the fresh powder dose-response experiments. The lead series contains compound EG-H26 which is an inhibitor of Pax2 activity first identified and reported by Grimley [35]. Since the original inhibitors from the re-mining screen were confirmed by fresh powder, initial SAR analysis for the original 122 CCG inhibitors was conducted. Initial SAR analysis was performed on 34 compounds with similar structures to EG-H26.

Future studies will include a more detailed SAR analysis after resynthesizing the compound with the best potency and efficacy from the lead series. Synthesis and testing of novel analogs similar to the most potent and efficacious compound may also be necessary to aid a more in-depth SAR analysis. Determination of the best compound will be assessed by testing in secondary assays. These secondary experiments will employ embryonic kidney organoids which will be assessed for 1) disturbed ureter tip bud branching morphogenesis and 2) defects in Pax2⁺ cell aggregation at ureter tip buds after Pax2 inhibitor treatment. Assessment of suppressed Pax2 activity in renal cancer cell lines after treatment with Pax2 inhibitors will also be conducted. Isothermal Titration Calorimetry (ITC) assays will too be of great importance. ITC assays will

help distinguish which compounds in the emerging lead series bind to Pax2. Data from ITC assays may also support in-depth SAR studies and help design improved Pax2 inhibitors.

Given that these Pax2 inhibitors were identified using HTS methodologies, it is possible that they could exert their inhibitory effects in numerous and novel ways. Some possible mechanism that may inhibit Pax2 activity include interference with the protein-protein interaction between Pax2 and PTIP (adaptor protein linking Pax2 to activating gene epigenetic complexes [36-38]). Alternatively, even if the interaction between Pax2 and PTIP remains intact with Pax2 inhibitor treatment, these Pax2 inhibitors could prevent the ability of PTIP to recruit activating epigenetic complexes to Pax2. Future experiments would then include the assessment of the ability of these Pax2 inhibitors to interfere with Pax2 activity not only at the level of DNA binding but also at the epigenetic level. For instance, studies can be conducted to determine if the proteins in the activating epigenetic complex ChIP to the Pax2 binding DNA element in a Pax2 dependent manner. Hence, experiments to determine which of the proteins in the epigenetic complex still ChIP to the Pax2 binding DNA element in the presence of these Pax2 inhibitors will provide further insight into their mechanisms of inhibition.

Determining the mechanism of action of the compounds in the emerging lead series of Pax2 inhibitors will ultimately help design future compounds that are optimal in potency, selectivity, and efficacy. However, prior to testing these Pax2 inhibitors in animal models of PKD or ccRCC it will be essential to conduct pharmacokinetic assays to assess for *in vivo* stability of these compounds. If optimized Pax2 inhibitors are successful in pre-clinical studies translation to clinical settings could be promising. However, clinical success will depend on many factors. In particular, early detection and proper characterization of PKD and ccRCC will be key in reducing cystogenesis in PKD and slowing the progression of ccRCC with Pax2 inhibitors.

Bibliography

1. Sanderson, N., et al., *Hepatic expression of mature transforming growth factor beta 1 in transgenic mice results in multiple tissue lesions*. Proc Natl Acad Sci U S A, 1995. **92**(7): p. 2572-6.
2. Kopp, J.B., et al., *Transgenic mice with increased plasma levels of TGF-beta 1 develop progressive renal disease*. Lab Invest, 1996. **74**(6): p. 991-1003.
3. Ledbetter, S., et al., *Renal fibrosis in mice treated with human recombinant transforming growth factor-beta2*. Kidney Int, 2000. **58**(6): p. 2367-76.
4. Calabresi, P.A., et al., *Phase 1 trial of transforming growth factor beta 2 in chronic progressive MS*. Neurology, 1998. **51**(1): p. 289-92.
5. Suthanthiran, M., et al., *Transforming growth factor-beta 1 hyperexpression in African-American hypertensives: A novel mediator of hypertension and/or target organ damage*. Proc Natl Acad Sci U S A, 2000. **97**(7): p. 3479-84.
6. Border, W.A., et al., *Suppression of experimental glomerulonephritis by antiserum against transforming growth factor beta 1*. Nature, 1990. **346**(6282): p. 371-4.
7. Shull, M.M., et al., *Targeted disruption of the mouse transforming growth factor-beta 1 gene results in multifocal inflammatory disease*. Nature, 1992. **359**(6397): p. 693-9.
8. Kulkarni, A.B., et al., *Transforming growth factor beta 1 null mutation in mice causes excessive inflammatory response and early death*. Proc Natl Acad Sci U S A, 1993. **90**(2): p. 770-4.
9. Voelker, J., et al., *Anti-TGF-beta1 Antibody Therapy in Patients with Diabetic Nephropathy*. J Am Soc Nephrol, 2017. **28**(3): p. 953-962.
10. Luo, G., et al., *BMP-7 is an inducer of nephrogenesis, and is also required for eye development and skeletal patterning*. Genes Dev, 1995. **9**(22): p. 2808-20.
11. Vukicevic, S., et al., *Osteogenic protein-1 (bone morphogenetic protein-7) reduces severity of injury after ischemic acute renal failure in rat*. J Clin Invest, 1998. **102**(1): p. 202-14.

12. Hruska, K.A., et al., *Osteogenic protein-1 prevents renal fibrogenesis associated with ureteral obstruction*. Am J Physiol Renal Physiol, 2000. **279**(1): p. F130-43.
13. Zeisberg, M., et al., *Bone morphogenic protein-7 inhibits progression of chronic renal fibrosis associated with two genetic mouse models*. Am J Physiol Renal Physiol, 2003. **285**(6): p. F1060-7.
14. Wang, S., et al., *Bone morphogenic protein-7 (BMP-7), a novel therapy for diabetic nephropathy*. Kidney Int, 2003. **63**(6): p. 2037-49.
15. Morrissey, J., et al., *Bone morphogenetic protein-7 improves renal fibrosis and accelerates the return of renal function*. J Am Soc Nephrol, 2002. **13 Suppl 1**: p. S14-21.
16. Zeisberg, M., et al., *BMP-7 counteracts TGF-beta1-induced epithelial-to-mesenchymal transition and reverses chronic renal injury*. Nat Med, 2003. **9**(7): p. 964-8.
17. Zeisberg, M., *Bone morphogenic protein-7 and the kidney: current concepts and open questions*. Nephrol Dial Transplant, 2006. **21**(3): p. 568-73.
18. Nakamura, J. and M. Yanagita, *Bmp modulators in kidney disease*. Discov Med, 2012. **13**(68): p. 57-63.
19. Yanagita, M., et al., *USAG-1: a bone morphogenetic protein antagonist abundantly expressed in the kidney*. Biochem Biophys Res Commun, 2004. **316**(2): p. 490-500.
20. Hsu, D.R., et al., *The Xenopus dorsalizing factor Gremlin identifies a novel family of secreted proteins that antagonize BMP activities*. Mol Cell, 1998. **1**(5): p. 673-83.
21. Zeisberg, M. and R. Kalluri, *Reversal of experimental renal fibrosis by BMP7 provides insights into novel therapeutic strategies for chronic kidney disease*. Pediatr Nephrol, 2008. **23**(9): p. 1395-8.
22. Rudnicki, M., et al., *Gene expression profiles of human proximal tubular epithelial cells in proteinuric nephropathies*. Kidney Int, 2007. **71**(4): p. 325-35.
23. Mezzano, S., et al., *Expression of gremlin, a bone morphogenetic protein antagonist, in glomerular crescents of pauci-immune glomerulonephritis*. Nephrology Dialysis Transplantation, 2007. **22**(7): p. 1882-1890.

24. Dolan, V., et al., *Expression of gremlin, a bone morphogenetic protein antagonist, in human diabetic nephropathy*. Am J Kidney Dis, 2005. **45**(6): p. 1034-9.
25. Turk, T., et al., *BMP Signaling and Podocyte Markers Are Decreased in Human Diabetic Nephropathy in Association With CTGF Overexpression*. Journal of Histochemistry & Cytochemistry, 2009. **57**(7): p. 623-631.
26. Bosukonda, D., et al., *Characterization of receptors for osteogenic protein-1/bone morphogenetic protein-7 (OP-1/BMP-7) in rat kidneys*. Kidney Int, 2000. **58**(5): p. 1902-11.
27. Sugimoto, H., et al., *Activin-like kinase 3 is important for kidney regeneration and reversal of fibrosis*. Nat Med, 2012. **18**(3): p. 396-404.
28. Himmelfarb, J., et al., *Perioperative THR-184 and AKI after Cardiac Surgery*. J Am Soc Nephrol, 2018. **29**(2): p. 670-679.
29. Carragee, E.J., E.L. Hurwitz, and B.K. Weiner, *A critical review of recombinant human bone morphogenetic protein-2 trials in spinal surgery: emerging safety concerns and lessons learned*. Spine J, 2011. **11**(6): p. 471-91.
30. Muchow, R.D., W.K. Hsu, and P.A. Anderson, *Histopathologic inflammatory response induced by recombinant bone morphogenetic protein-2 causing radiculopathy after transforaminal lumbar interbody fusion*. Spine J, 2010. **10**(9): p. e1-6.
31. Chen, N.F., et al., *Symptomatic ectopic bone formation after off-label use of recombinant human bone morphogenetic protein-2 in transforaminal lumbar interbody fusion Report of 4 cases*. Journal of Neurosurgery-Spine, 2010. **12**(1): p. 40-46.
32. Seth, K., et al., *2-(2-Arylphenyl)benzoxazole As a Novel Anti-Inflammatory Scaffold: Synthesis and Biological Evaluation*. Acs Medicinal Chemistry Letters, 2014. **5**(5): p. 512-516.
33. Kim, M.J., et al., *Novel SIRT1 activator MHY2233 improves glucose tolerance and reduces hepatic lipid accumulation in db/db mice*. Bioorg Med Chem Lett, 2018. **28**(4): p. 684-688.
34. Yu, L., et al., *Combining TGF-beta inhibition and angiotensin II blockade results in enhanced antifibrotic effect*. Kidney Int, 2004. **66**(5): p. 1774-84.

35. Grimley, E., *Thesis: Toward Molecularly Targeted Therapies for Renal Disease*. 2017, University of Michigan, Horace H. Rackham School of Graduate Studies.
36. Grimley, E. and G.R. Dressler, *Are Pax proteins potential therapeutic targets in kidney disease and cancer?* *Kidney Int*, 2018. **94**(2): p. 259-267.
37. Lechner, M.S., I. Levitan, and G.R. Dressler, *PTIP, a novel BRCT domain-containing protein interacts with Pax2 and is associated with active chromatin*. *Nucleic Acids Res*, 2000. **28**(14): p. 2741-51.
38. Patel, S.R., et al., *The BRCT-domain containing protein PTIP links PAX2 to a histone H3, lysine 4 methyltransferase complex*. *Dev Cell*, 2007. **13**(4): p. 580-92.